Novel Signaling Pathways in *Plasmodium falciparum*

Thesis submitted to

JAWAHARLAL NEHRU UNIVERSITY

In partial fulfillment of the requirements for the award of the degree

of

Doctor of Philosophy

Ankush Vaid

Eukaryotic Gene Expression Laboratory
National Institute of Immunology
New Delhi

June 2007

राष्ट्रीय प्रतिरक्षाविज्ञान संस्थान
NATIONAL INSTITUTE OF IMMUNOLOGY

CERTIFICATE

This is to certify that this thesis entitled **"Novel signaling pathways in *Plasmodium falciparum*"** embodies the work done by ***Ankush Vaid*** in partial fulfillment of the Ph.D. degree of the **Jawaharlal Nehru University** under my guidance at the **National Institute of Immunology**. This work is original and has not been submitted in part or full for any other degree or diploma of any university.

Dr. Pushkar Sharma
Thesis supervisor

अरूणा आसफ अली मार्ग, नई दिल्ली - 110067 फैक्स : 91-11-26162125, 26177626 तार : IMMUNOLOGY
Aruna Asaf Ali Marg, New Delhi - 110067 Fax : 91-11-26162125, 26177626 Grams : IMMUNOLOGY
दूरभाष (Telephones) EPABX : 26717121 - 45 & 26717010 - 19

AKNOWLEDGEMENTS

I would like to thank

to The Almighty.

to my family for everything

to my friends, labmates for tolerating me

to NII community from the Director to the technical staff.

and my mentor and supervisor Dr. Pushkar Sharma. Words cannot substitute my gratitude towards you.
Hat's off to you, Sir.

Ankush Varid
ankush

to Shani P. Joseph...

TABLE OF CONTENTS

ABBREVIATIONS

%	Percent
aa	amino acid
Ab	Antibody
AGC kinases	A family of kinases belonging to the same class as protein kinase A,G, C
Amp	Ampicillin
APS	Ammonium per sulphate
Bapta-AM	1,2-bis(2-amino-phenoxy)ethane-N,N,N',N'-tetraacetic acid tetrakis(acetoxymethyl)ester
BLAST	Basic Local Alignment Search Tool
bps	Base pairs
BSA	Bovine Serum Albumin
Ca^{2+}/CaM	Calcium/Calmodulin
CaM	Calmodulin
CBD	Calmodulin Binding Domain
ΔCBD	deletion of PfPKB lacking the CBD
cDNA	Complementary DNA
C- terminal	Carboxy terminal
cpm	Counts per minute
DAG	Diacyl glycerol
DAPI	6- Diamidino-2- phenylindone
dsRNA	Double stranded RNA
DMSO	Dimethylsulphoxide
DNA	Deoxyribose nucleic acid

DTT	Dithiothreiotol
E.coli	*Escherichia coli*
EDTA	Ethylenediamine tetraacetic acid
g	Gram
GST	Glutathione-S-Transferase
h	Hour
6x-His	hexa-histidine tag
HRPO	Horse radish peroxidase
HS	Human serum
IFA	Immunofluorescence assay
I(1,4,5)P_3	Inositol-1,4,5- tri phosphate
IPTG	Isoppropyl β-D-thio-galactopyranoside
kDa	Kilo Dalton
kb	Kilo base pairs
LB	Luria broth
M	Molarity
mAb	Monoclonal antibody
min	Minutes
mg	Milligrams
ml	Millilitres
mM	Millimolar
µg	Microgram
mRNA	Messenger RNA
MSP1	Merozoite Surface protein 1
N-terminal	Amino terminal
NTR	N-terminal region of PfPKB
ng	Nanogram
nm	nanometer
O/N	Overnight
^{0}C	Degree centigrade

O.D.	Optical Density
ORF	Open reading frame
PAGE	Polyacrylamide gel electrophoresis
PBS	Phosphate buffer saline
PCR	Polymerase chain reaction
PDK1	PI3 dependent kinase
PKB	Protein kinase B
PfPKB	PKB homologue in *P.falciparum*
ΔPfPKB	deletion of PfPKB lacking the NTR
PfPKB-IP	PfPKB immunoprecipitate
PKA	c-AMP dependent protein kinase A
PKC	Protein kinase C
PKG	c-GMP dependent protein kinase G
PlasmoDB	Plasmodium genome database
PIs	Phosphoinositides
PI 3K	Phosphatidylinositol 3-kinase
PI(3)P	Phosphatidylinositol-3-phosphate
$PI(4,5)P_2$	Phosphatidylinositol-4,5- bisphosphate
$PI(3,4)P_2$	Phosphatidylinositol-3,4- bisphosphate
$PI(3,4,5)P_3$	Phosphatidylinositol-3,4,5- trisphosphate
PH	Plecstrin Homology
PLC	Phospholipase C
PfPLC	Phospholipase C homologue in *P.falciparum*
pg	pictogram
pmol	Pico mole
PVM	Parasitophorous vacuolar membrane
TVM	Tubo vesicular membrane
RBCs	Red blood cells
RNA	Ribo nucleic acid
RNAi	RNA interference

rpm	Revolution per minute
scr	scrambled
siRNA	Small interfering RNA
SDS	Sodium dodecyl sulphate
sec	Seconds
SDS-PAGE	Sodim dodecyl sulpahte polyacrylamide gel electrophoresis
TEMED	N, N, N', N'-Tetramethylethylenediamine
WHO	World Health Organization
X-GAL	5-bromo-4-chloro-3-indoyl-b-D-galactopyranoside
βME	Beta mercaptoethanol
µg	Microgram
µl	Microlitre
µM	Micromolar

Chapter - One

Introduction

CHAPTER ONE

INTRODUCTION

Malaria, one of the deadliest and dreadful parasitic diseases has shown resurgence in causing close to a million human deaths annually. The menace of malaria is especially severe in tropical and sub tropical countries. The parasite that causes malaria is an apicomplexan protozoan called *Plasmodium*. *Plasmodium falciparum* is responsible for most cases of human malaria worldwide. This parasite invades both hepatocytes as well as erythrocytes in human host but it is the erythrocytic phase of its life cycle that causes severe pathogenesis of malaria.

After the anopheles mosquito bite, sporozoites are released into the blood stream where they invade hepatocytes and undergo rapid multiplication to form merozoites. Released merozoites invade erythrocytes and divide asexually inside these cells in a synchronized manner. At first, it has a ring-like morphology which subsequently changes to irregular shaped structures termed as trophozoites. Subsequently, the parasite undergoes nuclear division to form 24-32 merozoites in the schizont stages. These merozoites are released as a result of erythrocyte membrane rupture and invade fresh erythrocytes. Some merozoites arrest their cell division and differentiate into gametocytes (Inselburg, 1983), which undergo sexual development in the anopheles midgut.

Drug resistance and lack of a successful vaccine against this parasite has hampered efforts to eradicate this disease. The lack of in-depth understanding of the basic molecular mechanisms that regulate the development of this parasite has hampered the endeavor to eradicate malaria.

Given the importance of cell signaling cascades in proliferation and differentiation of eukaryotic cells, dissection of signal transduction mechanisms may provide useful insights into the development of this protozoan parasite. Sequencing of *Plasmodium falciparum* genome (Gardner et al., 2002) indicated that several putative signaling proteins like protein/lipid kinases are present in this parasite. At present, there is very limited information about the manner in which *Plasmodium* signal transduction pathways regulate complex signaling networks inside the parasite. Detailed insights into the signal transduction pathways in the malarial parasite may enhance our understanding of the molecular mechanisms that control the development of this parasite.

Phosphoinositides (PIs) are a group of differentially phosphorylated phospholipids which act as potent second messengers in most eukaryotic cells (Vanhaesebroeck et al., 2001). PIs interact with specific domains present in proteins and regulate their functions. One of the major PI-regulated signaling pathway in mammalian cells is the PI 3-kinase - Protein kinase B pathway, which is crucial for several important functions of mammalian cells (Marte and Downward, 1997; Vanhaesebroeck et al., 1997). Our laboratory has keen interest in understanding the role of PI 3-kinase and Protein kinase B mediated signaling in *Plasmodium falciparum*.

A PI 3-kinase homologue (PfPI3K) and a Protein kinase B homologue (PfPKB) in *P.falciparum* were identified in our laboratory. The manner in which these enzymes operate and direct signaling events in this parasite had remained largely unknown. The major objective of this thesis work was to understand the regulation and role of PfPKB in *Plasmodium falciparum*.

Following studies were pursued to elucidate the function of PfPKB in *Plasmodium falciparum*:

1. Biochemical and molecular characterization of PfPKB.

2. Identification of PfPKB regulators in *Plasmodium falciparum*.

3. Dissection of signaling pathways regulating PfPKB.

4. Elucidation of the role of PfPKB in *Plasmodium falciparum* lifecycle.

During the course of this work it became evident that Phospholipase C like enzyme may be involved in PfPKB regulation. Therefore, preliminary studies on PfPLC, the PLC homologue in *P.falciparum* were also performed.

Chapter - Two

Review of Literature

CHAPTER TWO

REVIEW OF LITERATURE

2.1 History of Malaria.

Malaria has been one of the major causes of human suffering for hundreds of years and still remains one of the major causes of serious illness and mortality in the world. Malaria is caused by a protist belonging to the genus *Plasmodium*. Human malaria is as old as mankind. In 400 B.C., Hippocrates gave first clinical descriptions of malarial fever. Pelletier and Cavention, in 1820 isolated an active ingredient from the bark of chinchona and called it as quinine, which had an anti-malarial effect. In 1880, Lavern, a French army surgeon in Algeria, for the first time observed and described malaria parasites in the red blood cells of man. Machiafava and Celli in 1884 studied the morphological aspects of blood schizogony of the parasite. Sir Ronald Ross, in 1887 described sporogony of *Plasmodium relictum* in anopheles mosquitoes and also demonstrated that the *P. falciparum* was transmitted to humans through the bite of mosquitoes.

Four species of *Plasmodium* are known to infect humans, namely, *P. vivax, P. falciparum, P. ovale and P. malariae*. The four species differ morphologically, in geographical distribution, relapse pattern and drug response. Of the four human malaria species, *P. falciparum* causes cerebral malaria, which is fatal. It is highly prevalent in Africa and is responsible for widespread death especially of children. In India, *P. vivax* and *P. falciparum* are widely prevalent.

WHO launched malaria eradication programme during 1955-56 in many countries, which achieved unprecedented success. However, in some areas the disease re-emerged mainly due to multiple drug resistance of the parasite and emergence of insecticide resistant mosquito vector. Therefore, an effective vaccine or more robust control measures is the need of the hour to save people dying of malaria.

2.2 Life Cycle of Malaria Parasite.

Plasmodium, the causative agent of malaria is a digenetic parasite with humans and mosquito being its hosts. In humans it undergoes asexual cycle whereas in mosquito it goes through sexual cycle called sporogony (Figure. 2.1).

Figure 2.1 Life cycle of *Plasmodium falciparum*.

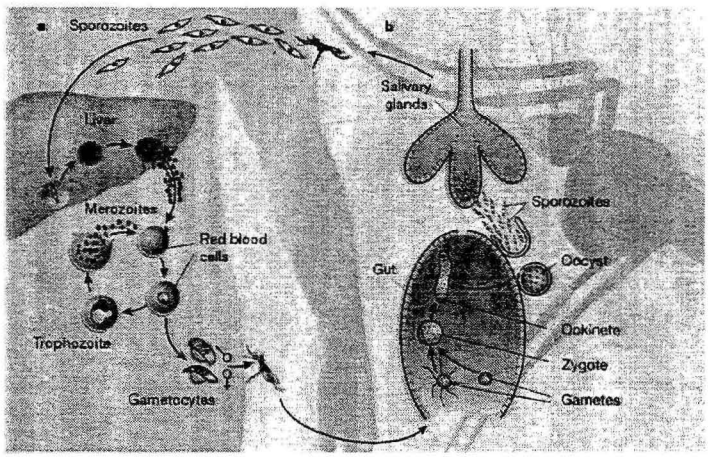

Plasmodium falciparum **life cycle showing its passage from the mosquito to the human host. The different stages of its development in both the hosts have been illustrated (Illustration courtesy malaria.org).**

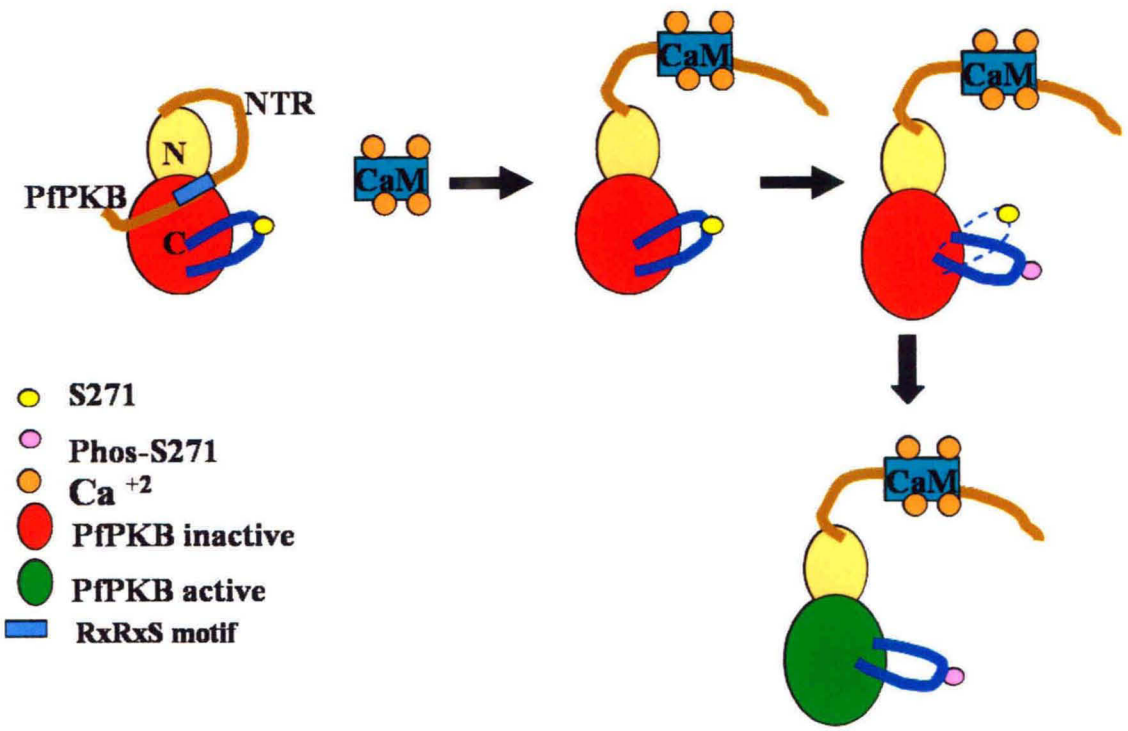

Figure. 4.12 **A model for PfPKB activation by Ca^{2+}/CaM.**

PfPKB is locked in an inactive state as a pseudosubstrate region in the NTR occupies its catalytic cleft. Ca^{2+}/CaM binding to CBD, which spans the pseudosubstrate motif, causes a conformational change resulting in the dissociation of NTR from the catalytic cleft thereby facilitating the autophosphorylation of Ser-271 of the activation loop. These events result in catalytic activation of PfPKB.

TABLE 4.1

Summary of the results of a BLAST search of *P. falciparum*-predicted gene database using human PK Bβ sequence as a query.

Plasmodium gene	Homology %	Experimental Identification
Ch12.glm521	71	*PfPKB* (this work)
Ch9.glm401	56	*PfPKA*
Ch14.glm391	56	*PfPKG*

% Homology represents the percent similarity in amino acids that are identical and belong to a similar chemical class. It is indicated as % similarity in the output of the BLAST program.

TABLE 4.2

Homology between PfPKB and other mammalian AGC kinases.

Kinase	Homology %
PKB	71
PKCα, -β, -γ	64
cAMP-dependent protein kinase	58
cGMP-dependent protein kinase	53

Chapter - Five

Regulation of PfPKB in *Plasmodium falciparum*

Chapter - 5

Regulation of PfPKB in *Plasmodium falciparum*

Ca^{2+}/CaM was identified as the activator of PfPKB. Using information from the biochemical results described in the previous chapter, studies directed at understanding the regulation of PfPKB in *Plasmodium falciparum* were performed.

5.1 PfPKB is expressed in schizonts and merozoites.

Western blotting, immunofluorescence, and RT-PCR techniques were used to examine the expression pattern of PfPKB during *P. falciparum* blood stage development. For this purpose, polyclonal antisera was raised against a synthetic peptide derived from the C terminus of PfPKB. PfPKB expression was predominantly observed in the schizont stages of the parasite as indicated by a band of ~52 kDa, which is consistent with the predicted molecular mass of 50 kDa(Figure. 5.1A). RT-PCR analysis indicated that PfPKB transcripts were mainly present in the schizont stages and were observed in the trophozoites only at very low levels (Figure. 5.1B). Immunofluorescence studies also revealed that PfPKB was present mainly in the mid-late schizont stages of the parasite; other mono-nucleated stages did not show any detectable PfPKB expression (Figure. 5.1C). These observations indicated that PfPKB is expressed mainly in schizonts/merozoites. Further experiments were performed to investigate if PfPKB was active in schizonts. PfPKB was immunoprecipitated from schizont lysates, PfPKB-IP was able to phosphorylate crosstide, indicating that it is active in parasite (Figure. 5.1D).

5.2 Regulation of PfPKB activity by CaM in *P. falciparum.*

Given the activation of recombinant PfPKB by Ca^{2+}/CaM, it was important to study the role of calcium and calmodulin in regulating PfPKB in the parasite. While PfPKB is specifically expressed in schizonts/merozoites (Figure. 5.1), CaM is present in all intra-erythrocytic stages (Cowman and Galatis, 1991; Rojas and Wasserman, 1995). Immunofluorescence studies revealed that CaM and PfPKB co-localize in schizonts and free merozoites (Figure. 5.2) indicating their presence in similar cellular compartments. Importantly, western blots revealed that CaM co-immunoprecipitates with PfPKB (Figure. 5.3A) indicating that these proteins associate in the parasite. In contrast, mock immunoprecipitation experiments performed with RBC lysates did not show the presence of CaM in PfPKB-IP (Figure. 5.3B). The ability of calmodulin to activate PfPKB in *P. falciparum* was tested by using W7, a CaM inhibitor, which has been used earlier to demonstrate its role in erythrocyte invasion (Matsumoto et al., 1987). Incubation of merozoites with W7 resulted in a significant loss of PfPKB activity indicating that CaM is indeed a PfPKB regulator *in vivo*. These results were confirmed when addition of Ca^{2+}/CaM to the PfPKB-IP from W7 treated parasites lead to a significant recovery of PfPKB activity (Figure. 5.3C). When PfPKB was immunoprecipitated in absence of calcium, it resulted in significant loss of CaM binding which suggested that calcium is essential for CaM-PfPKB interaction in the parasite (Figure. 5.3D). Collectively, these observations establish that CaM is a regulator of PfPKB in *Plasmodium falciparum.*

5.3 Phospholipase C mediated calcium release controls PfPKB activity.

Intracellular calcium levels are tightly regulated in *Plasmodium* (Garcia, 1999; Gazarini et al., 2003) and inhibitors of Phospholipase C (PLC), which blocks IP(1,4,5)P3 formation, prevent release of free calcium from intracellular parasite stores (Gazarini et al., 2003; Hotta et al., 2000). Since biochemical studies indicated that CaM regulates PfPKB in a calcium dependent manner, the role of PLC mediated calcium release was evaluated. For this purpose, schizonts were incubated either with U73122, a specific inhibitor of PLC, or its less potent analogue U73322 and PfPKB activity was assayed. U73122 treatment of merozoites resulted in a significant attenuation of PfPKB activity, while U73322 only had a marginal effect (Figure. 5.4A). The loss of PfPKB activity was accompanied by a reduction in amount of CaM associated with PfPKB in U73122 treated parasites (Figure. 5.4B).

It was important to determine whether PLC-mediated regulation of PfPKB was due to its ability to control intracellular calcium levels. To probe this, parasites were treated with U73122 in the presence of ionomycin, a calcium ionophore that can mobilize intracellular calcium. Recovery of PfPKB activity, which was lost due to PLC inhibition (Figure. 5.4C), was observed suggesting that PLC controls PfPKB activity by regulating calcium levels inside the parasite. Cell-permeable intracellular calcium chelator, BAPTA-AM also attenuated PfPKB activity, providing direct evidence that PfPKB is regulated by intracellular calcium (Figure. 5.4C). It is important to indicate that *P. falciparum* has a PLC homologue that shares significant similarity with the catalytic domain of mammalian PLC (Chapter-7).

In summary, a novel signaling pathway was identified in the malarial parasite that involves activation of PfPKB by CaM, and PLC serves as an upstream activator of this pathway as it provides the release of calcium necessary for PfPKB activation (Figure. 5.5). This is one of the first multi-component pathway to be identified in *Plasmodium falciparum*.

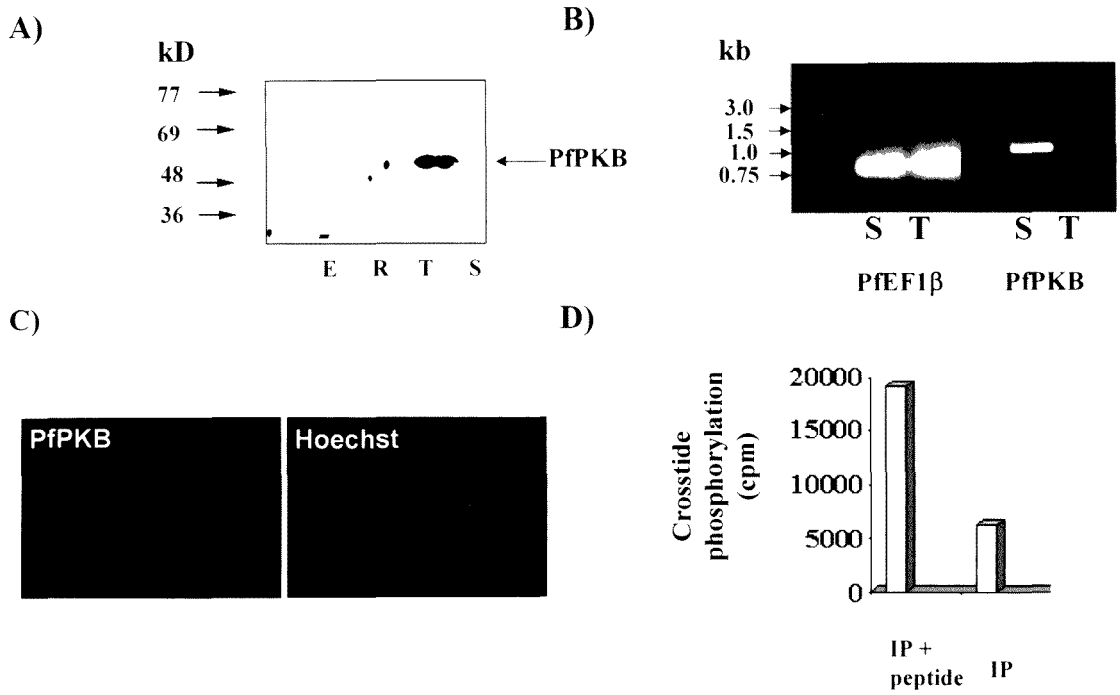

Figure. 5.1 **PfPKB is expressed mainly in schizont stage of *P. falciparum* life cycle.**
(A) Equal amount of cell lysate prepared from either uninfected erythrocytes (E), schizonts (S), trophozoites (T) or rings (R) was used for western blot analysis with anti-PfPKB antisera. (B) Equal amount of RNA isolated from either schizont (S) or trophozoite (T) stages of *P. falciparum* was used for RT-PCR analysis using primers specific for PfPKB. *P. falciparum* elongation factor 1beta (PfEF1β) was used as control. Equal amount of PCR product was electrophoresed on 1% agarose gel. (C) Immunofluorescence was performed on *P.falciparum* thin smears to study PfPKB expression. PfPKB staining was seen only in multi-nucleated schizonts, no other intra-erythrocytic asexual stages (Hoechst stained) exhibited PfPKB expression. (D) PfPKB immunoprecipitate (IP) from schizont-rich parasite lysates was used in kinase assays. PfPKB-IP could phosphorylate crosstide suggesting that it is active in schizonts.

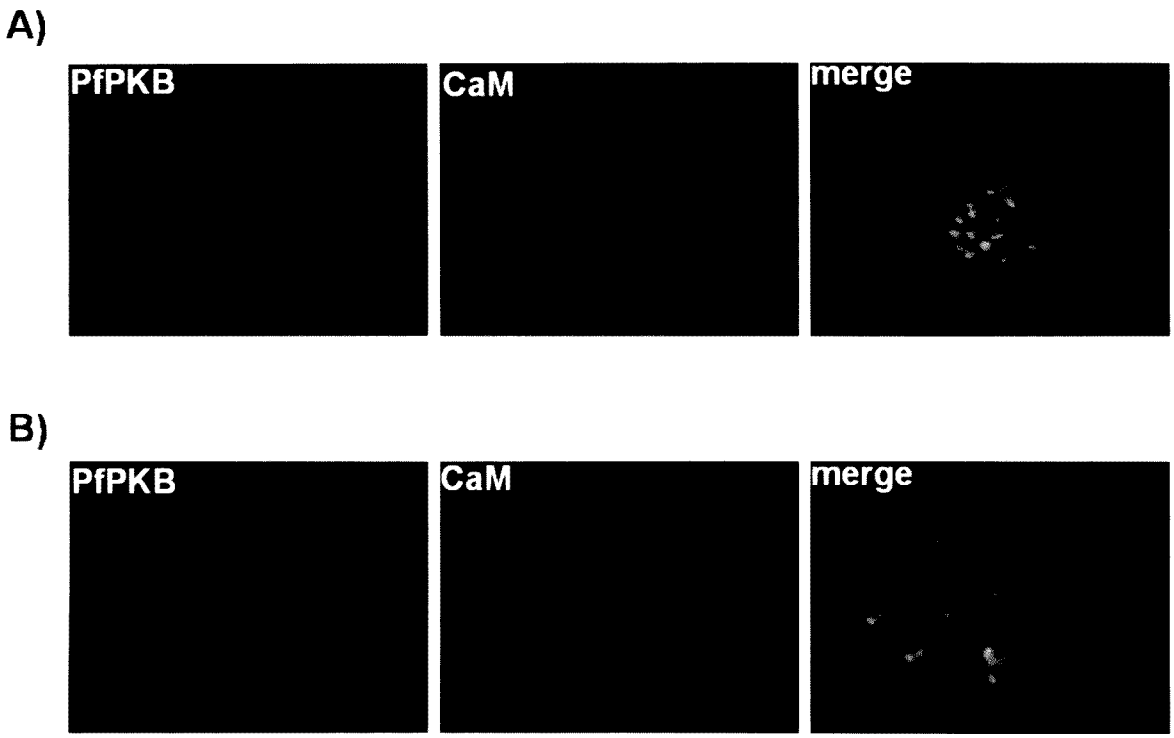

Figure. 5.2 **PfPKB and CaM co-localize in the late schizont stage.**

Immunofluorescence assay was performed on thin smears of schizont/merozoite rich parasite cultures using anti-PfPKB (red) or anti-CaM (green) antibodies. PfPKB and CaM co-localized in schizonts (A) and free merozoites (B).

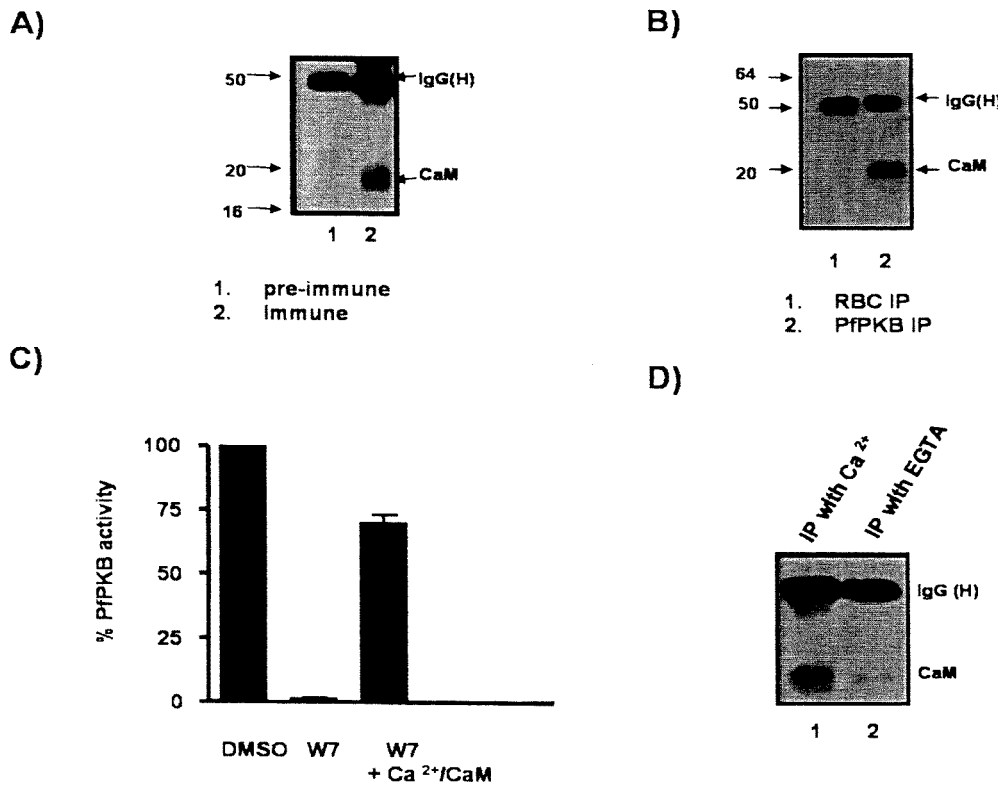

Figure. 5.3 **CaM regulates PfPKB activity in *P. falciparum* cultures.**

PfPKB was immunoprecipitated from schizont (*A,B*) or red blood cell (B) lysates, and immunoprecipitate (*IP*) was electrophoresed on an SDS-PAGE gel followed by Western blot analysis using anti-CaM antibody. Detection of CaM in the immunoprecipitate of PfPKB suggested that these proteins interact in the parasite (panel A and B, lane 2). Mock immunoprecipitation experiments were performed by using preimmune antisera (A, *lane 1*) or red blood cell lysate (B, *lane 1*). C) CaM inhibitor W7 inhibits PfPKB activation in *P. falciparum* cultures. Schizont-rich *P. falciparum* cultures were treated with 50 µM W7and PfPKB was immunoprecipitated from parasite protein lysates. PfPKB-IP-associated activity was assayed using crosstide. A significant loss in PfPKB activity was observed upon W7 treatment. Addition of 0.1 mM $CaCl_2$ and 5 µM CaM to PfPKB-IP from W7-treated parasites resulted in a significant recovery of PfPKB activity. (D) PfPKB was immunoprecipitated from schizonts in a buffer containing either 1 mM $CaCl_2$ or 1 mM EGTA, and immunoblotting was performed to detect the associated CaM.

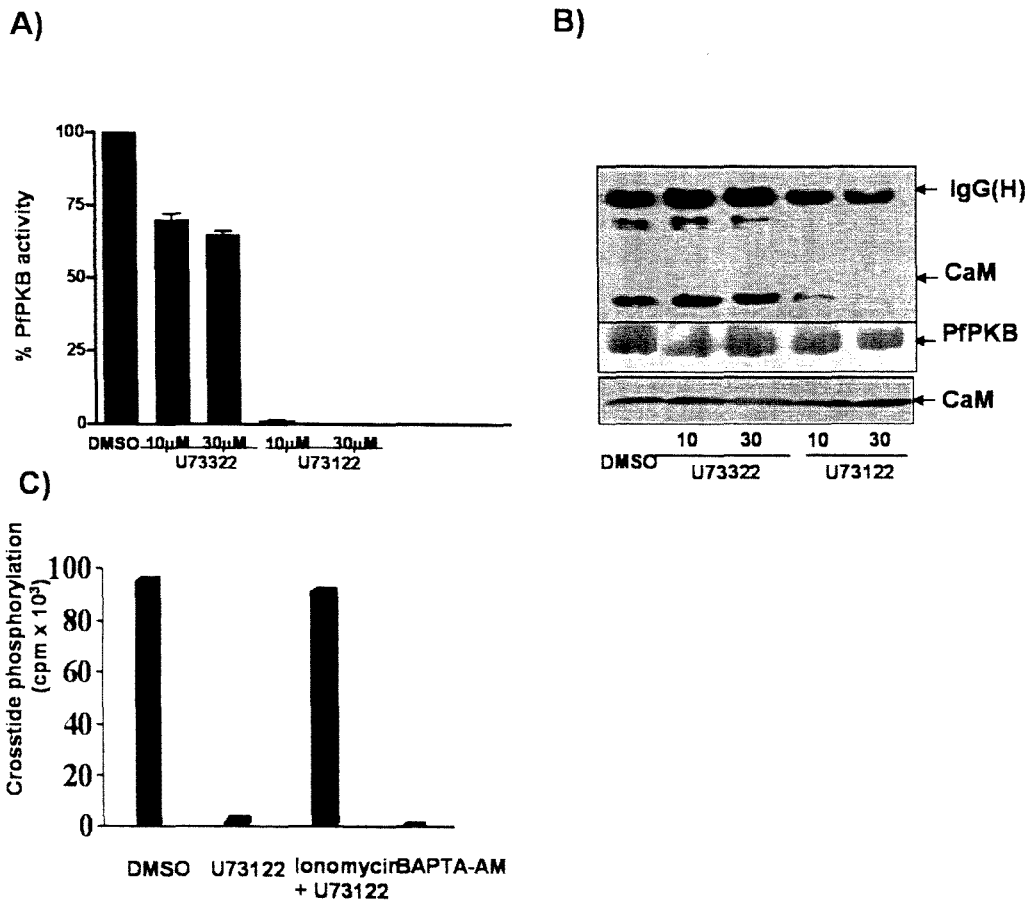

Figure 5.4 **Phospholipase C is an upstream regulator of PfPKB signaling pathway.**

(A) P. falciparum schizonts were incubated with the indicated concentrations of either phospholipase C inhibitor U73122 or its analogue U73322 for 30 min, and PfPKB-IP activity was determined. U73122 treatment caused a significant decrease in PfPKB activity. The activity of PfPKB in DMSO treated parasites was considered as 100%. *B)* PfPKB-IP (*top panel*) or whole cell lysates (*bottom panel*) were subjected to Western blotting for CaM and PfPKB. A significant decrease in the amount of CaM co-immunoprecipitated with PfPKB was observed only in U73122-treated parasite without altering levels of PfPKB and CaM in whole parasite lysates (*bottom panels*). C) Schizont stage parasites were treated with U73122 (30 μM) or BAPTA-AM (100 μM) alone or with a combination of U73122 (30 μM) and ionomycin (10 μM), and PfPKB-IP-associated activity was assayed using crosstide as substrate.

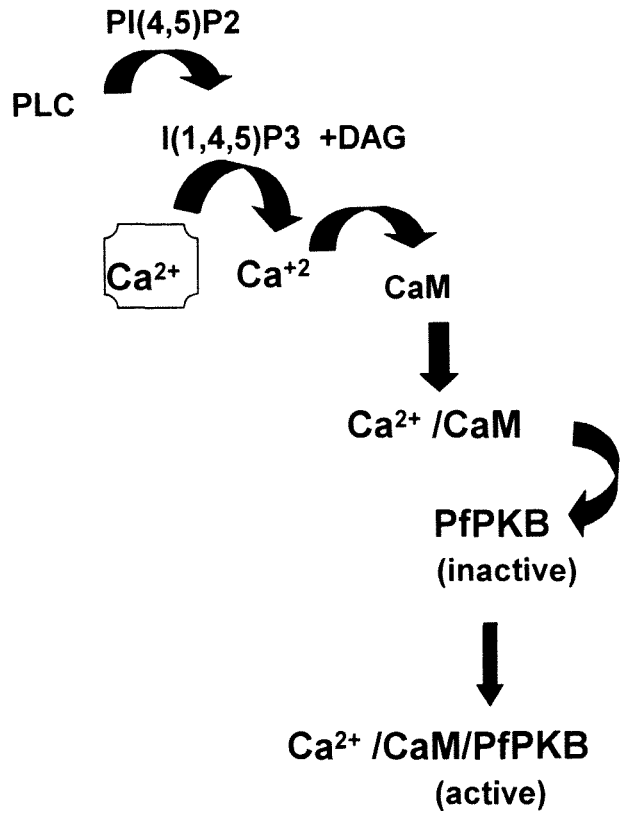

Figure. 5.5 **A novel-signaling pathway in *P. falciparum*.**

Studies described suggest that CaM activates PfPKB in a calcium dependent manner by interacting with a CBD in its N-terminus (Figure. 4.7; 4.8, 5.3). Phospholipase C, the enzyme involved in generation of $I(1,4,5)P_3$, acts as an upstream regulator of this pathway (Figure. 5.4) as IP_3 may facilitate the release of calcium needed for PfPKB activation.

Chapter - Six

Role of PfPKB signaling pathway in parasite life cycle

Chapter Six

Role of PfPKB signaling pathway in parasite life cycle

As described in chapters 4 and 5, the mechanism of PfPKB activation was worked out which led to the identification of a novel parasite signaling pathway in *P.falciparum*. However, the function of this signaling pathway and PfPKB in parasite development still remained unknown. The PfPKB pathway (Figure. 5.5) was modulated at different steps by using several molecular tools to gain insights into its role in parasite development.

6.1 PfPKB is localized at the apical end of merozoites.

PfPKB is expressed mainly in the schizont/merozoite stage of the parasite life cycle (Figure. 5.1). .To gain insights into its function, immunofluorescence studies were performed for localizing this enzyme in merozoites. These studies revealed that it may be present at the apical end of the merozoite (Figure. 6.1A). Recently, components of the actin-myosin motor in *Plasmodium* sporozoite and merozoites have been identified (Bergman et al., 2003a; Green et al., 2006; Menard, 2001) and are considered to be important for invasion (Baum et al., 2006; Jones et al., 2006). This motor complex mainly resides in the Inner Membranal Complex (IMC) and concentrates at the apical end of the merozoite which probably facilitates its role in invasion. One of the components of this protein complex, GAP45 (Rees-Channer et al., 2006) is a peripheral membrane protein, PfPKB exhibited significant co-localization with GAP45 (Figure. 6.1B). Moreover, co-immunoprecipitation experiments revealed that PfPKB was associated with Myosin tail interacting protein (MTIP), a myosin light chain homologue, in the parasite (Figure.

6.1C) and other components of IMC (not shown here). Localization of PfPKB in these compartments and interaction with IMC proteins of the parasite was suggestive of a possible role in invasion.

6.2 Inhibition of PfPKB upstream activators block invasion.

The pathway described in the previous chapter suggested that PfPKB is regulated by CaM, calcium and Phospholipase C as inhibition of CaM and PLC resulted in down regulation of PfPKB activity. To evaluate the role of PfPKB pathway in parasite development, effect of CaM and PLC inhibitors on parasite life cycle was monitored. When CaM inhibitor W7 was added to the schizont stage parasites, the formation of rings in the next cycle was blocked (Figure. 6.2A). Free merozoites were successfully isolated to perform direct invasion assays (Fig. 6.6). Since addition of this inhibitor to free merozoites also inhibited ring formation (Figure. 6.2B), it is reasonable to suggest that W7 blocks invasion. These findings were consistent with previous observations made by Aikawa and co-workers (Matsumoto et al., 1987; Scheibel et al., 1987). When the upstream activator of this pathway PLC was inhibited, similar inhibition of invasion was observed (discussed in Chapter-7) further supporting the role of this pathway in this important parasitic process.

6.3 PfPKB may play an important role in RBC invasion by the parasite.

Inhibition of CaM and PLC resulted in inhibition of invasion (Chapter-7 and section 6.2). It is likely that these proteins may have several targets via which they may control this important

parasitic process. Since PfPKB was identified as one of the targets of this pathway, its contribution to invasion was worth studying. Various approaches were used to either inhibit PfPKB activity or suppress its expression to understand its function in *P.falciparum*.

6.3.1 A443654 is an effective inhibitor of PfPKB which blocks invasion.

There were no specific inhibitors available against PKB-like enzymes when these studies were initiated. Recently, Abbott laboratories developed pharmacological inhibitors which have IC_{50} in nano molar range against mammalian PKB and exhibit at least 40 fold less affinity for AGC family kinases like PKA, PKC, RSK6 (Han et al., 2007; Luo et al., 2005). These inhibitors were obtained from Abbott laboratories under an MTA agreement and were tested against PfPKB. One of these compounds, A443654, successfully inhibited PfPKB activity with IC_{50} ~200 nM (Figure. 6.3A). These inhibitors were then added to parasite cultures to inhibit parasite PfPKB. Reduced activity of PfPKB-IP from A443654 treated parasites suggested that this inhibitor can effectively block PfPKB in the parasite (Figure. 6.3B). When A443654 was added to synchronized parasite cultures at the ring stage, the development of parasites was normal till 44 h. Subsequently, the number of rings formed in the next cycle was significantly reduced in comparison to DMSO treated cultures (Figure. 6.4).The inhibition in ring formation could have been a result of impaired invasion. When A443654 was added to schizonts the formation of rings was significantly reduced without altering the number of schizonts (Figure. 6.5A). To further establish if these inhibitors block invasion, experiments with free merozoites were performed (Freeman and Holder, 1983; Mohrle et al., 1997). For this purpose, free merozoites were isolated from parasite cultures. These merozoites retained their ability to invade RBCs till

~ 30 min after isolation (Figure. 6.6). When A443654 was added to merozoites, it impaired their ability to invade RBCs as the number of rings formed was significantly less (Figure. 6.5B). These data suggested that PfPKB may be involved in the process of invasion.

6.3.2 Go6983 inhibits PfPKB and blocks parasite growth.

Before PKB inhibitor A443654 was available for studies, Go 6893 was identified as an effective inhibitor of PfPKB activity. Rationale for using Go6983 (a specific PKC inhibitor) as PfPKB inhibitor was 1) *in silico* analysis had suggested that catalytic domain of PfPKB was most closely related to PKC in comparison to other AGC kinases (Table 4.I;4.2) and 2) *Plasmodium falciparum* appears to lack a PKC homologue which will rule out the possibility of cross-reactivity of PKC inhibitors. Go 6983 and Go6976 are isoform-specific PKC inhibitors which target the ATP binding site (Gschwendt et al., 1996) and inhibition of any other AGC kinases by these compounds has not yet been reported. Go6983 inhibited ΔPfPKB activity as judged by its ability to phosphorylate crosstide (Figure. 6.7A) with IC_{50} of ~1 μM. In contrast, Go 6976 was unable to inhibit the ΔPfPKB activity even at 10 μM concentration (Figure. 6.7B). Synchronized *P. falciparum* cultures were incubated with Go 6983 and parasite growth was monitored at different time points. There were no apparent effects of this drug till the rings were formed in the next cycle. In Go6983 treated cultures, the number of rings in the following cycle was markedly less compared to the control cultures (Figure. 6.7C). This observation correlates well with the expression profile of PfPKB in the schizont/merozoite stages of the life cycle. To further establish the effect of this inhibitor, *P. falciparum* schizonts were incubated with Go 6983 and development of the parasite was monitored. While untreated cells formed rings within four-

six hours, Go 6983 treatment resulted in almost 60% decrease in formation of new rings (Figure. 6.7D). These results corroborate well with A443654 inhibition data (Figure.6.3-6.5) and suggest a role of PfPKB in invasion.

6.3.3 Design of peptide inhibitors of PfPKB to demonstrate its role in invasion.

Even though pharmacological inhibitors A443654 and Go6983 were used to demonstrate a role of PfPKB in invasion, it was worth extending these studies using an independent approach. Biochemical studies suggested that CBD-peptide could act as a specific tool to elucidate the function of PfPKB as it possesses "two-pronged" ability to inhibit PfPKB activity: its pseudosubstrate nature via which it competes for the active site of the kinase and its ability to compete with CaM for PfPKB. In order to generate a peptide inhibitor that blocks PfPKB activity exclusively by interacting with its active site and not by competing with CaM, a peptide with only 15 residues of CBD was synthesized (Figure. 6.8A). This peptide, CBD_{1-15}, did not interact with CaM in mobility shift assays (Figure.6.8B). However, it inhibited ΔPfPKB activity by pseudosubstrate mechanism (Figure. 6.8C). Addition of both CBD and CBD_{1-15} peptides to parasites resulted in a significant reduction in PfPKB activity suggesting that these peptides can act as inhibitors of PfPKB in parasites, scrambled CBD peptide (scr-CBD) did not alter PfPKB activity (Figure. 6.8D).

When CBD peptides were added to segmenters/mature schizonts, a significant decrease in formation of new rings was observed in the next cycle suggesting that erythrocyte invasion may

have been impaired by these peptides. The number of schizonts remained almost unaffected and the control scrambled CBD peptide (scr-CBD) did not alter parasite growth (Figure. 6.9A). To further establish the role of PfPKB in invasion, experiments were performed with free merozoites as described earlier (Figure. 6.5B). When added to merozoites, both CBD and CBD_{1-15} peptides caused severe defects in formation of rings indicating that the impairment of inavsion (Figure. 6.9B). These peptides when added to synchronized ring stage *P.falciparum* cultures did not cause any detectable changes to the other parasitic stages as the parasitemia was almost unaltered till 46 h time point. Subsequently, in the next cycle after invasion, the number of rings formed in peptide treated cultures was markedly reduced (Figure. 6.10).

It was important to demonstrate if these inhibitor peptides worked intracellularly. For this purpose, CBD peptides were tagged with fluorescein iso-thiocyanate (FITC) at the N-terminus and added to parasite cultures. The peptide associated fluorescence was seen inside the merozoite (Figure. 6.11) and also schizonts (not shown here). The localization of the peptides was at the apical end as observed for PfPKB (Figure. 5.2). These data provided additional support to pharmacological inhibitor data and suggested that PfPKB may play an important role in invasion.

6.3.4 siRNA mediated silencing of PfPKB impairs invasion.

Gene silencing by RNA interference (RNAi) is a potent tool to explore gene function in eukaryotes. The existence and the mechanism of a RNAi pathway in the malaria parasite has

been questioned (Aravind et al., 2003). Failure of genome mining approaches to identify classical RNAi pathway components in *Plasmodium* has rightly contributed to these speculations (Ullu et al., 2004). Despite the lack of information about the mechanism of RNAi pathway in *Plasmodium*, several groups have reported the successful use of dsRNA as well as 21 nucleotide siRNA for functional analysis of several genes in *Plasmodium* (Gissot et al., 2005; Kumar et al., 2002; Malhotra et al., 2002; McRobert and McConkey, 2002). It is possible that the RNAi-pathway components in *Plasmodium* do not share significant homology with their counterparts from other species which has resulted in failure to identify them by *in silico* analysis and/or this pathway in the parasite is very different from other organisms. Since 20-26nt siRNA are at the business-end of RNAi-pathway, two sets of 21nt siRNA duplexes designed against different regions of PfPKB were used (see Materials and Methods). PfPKB is first expressed at mid-late schizont stage, therefore, *P.falciparum* late-trophozoites were treated with siRNA duplexes. RT-PCR revealed a significant decrease (~ 80%) in PfPKB transcript levels (Figure. 6.12A), which was accompanied by a concomitant decrease in PfPKB protein levels (~ 90%) in siRNA treated parasites (Figure. 6.12B). Importantly, there was no significant change in the levels of schizont/merozoite specific antigens MSP1 (Figure. 6.12A), EBA-175 (Figure. 6.12A,B) and a control siRNA with scrambled nucleotide sequence did not alter PfPKB expression (Figure. 6.12A,B).

Examination of siRNA treated parasite cultures revealed a marked reduction in the number of rings in siRNA treated parasites (Figure. 6.13, right panel). Since no significant change in schizonts was observed (Figure. 6.13, left panel), it is reasonable to conclude that defects in

invasion by PfPKB-siRNA causes defects in ring formation. Importantly, no non-specific effects of these siRNA were observed on growth and development of other intra-erythrocytic stages (Figure. 6.14). The siRNA results corroborate well with the pharmacological inhibitor (Figure. 6.5-6.7) as well as peptide inhibitor data (Figure. 6.8-6.10).

Collectively, these studies suggest that PfPKB may play an important role in early stage of the parasite lifecycle by regulating invasion of erythrocytes.

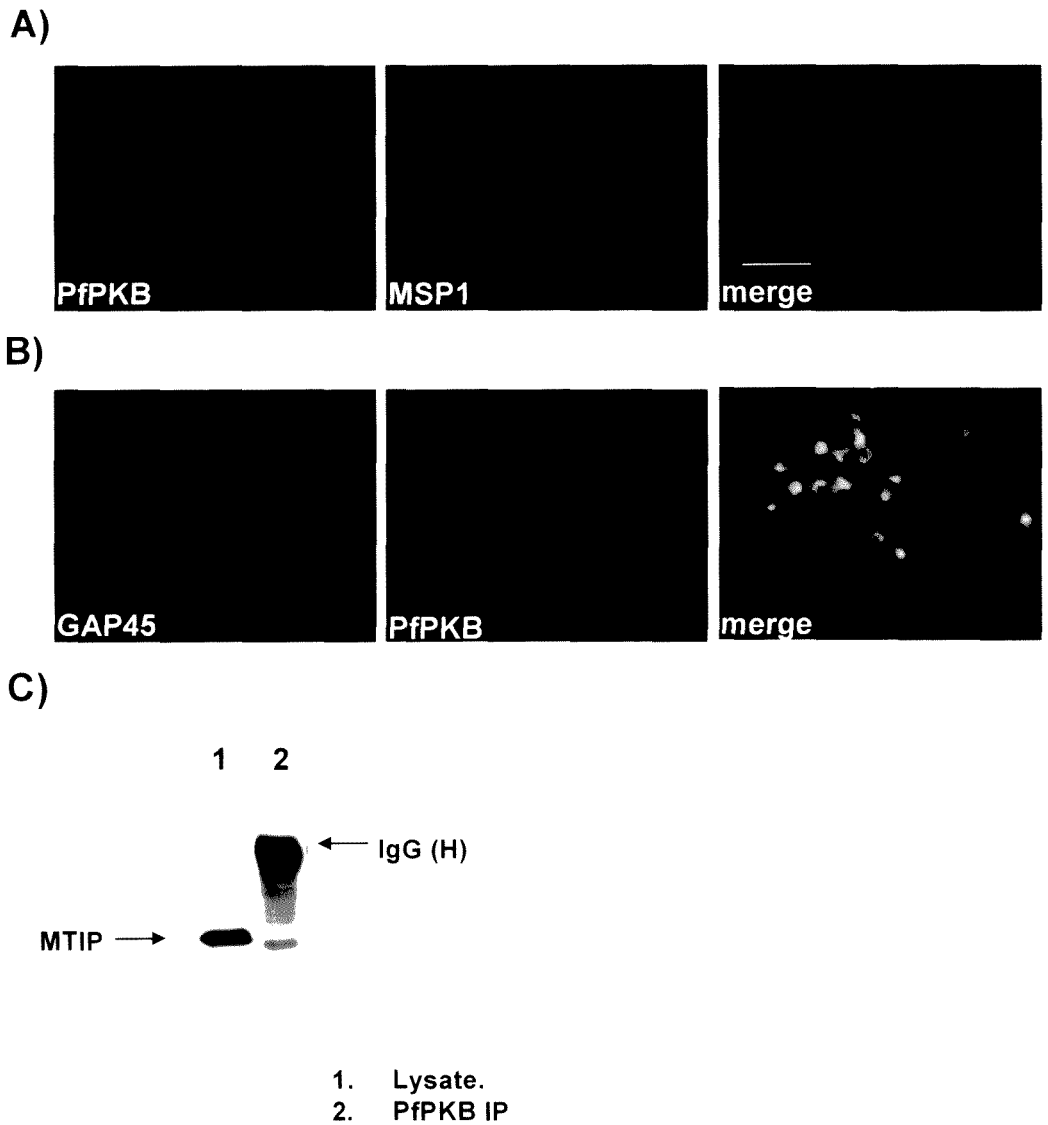

Figure. 6.1 **PfPKB localizes to the apical end of the merozoite.**

(A) Immunofluorescence was performed on thin blood smears of schizont rich parasites to localize PfPKB. (A) PfPKB (Green) localizes at the apical end of the parasite, the surface of merozoite was identified by MSP1 staining (Red). (B) GAP45 (Green), a component of actin-myosin motor co-localizes with PfPKB (Red). (C) PfPKB was immunoprecipitated from schizonts and PfPKB-IP was subjected to western blot using antisera against MTIP, a component of actin-myosin motor. MTIP was found associated with PfPKB immunoprecipitate further confirming that PfPKB interacts with components of actin-myosin motor complex.

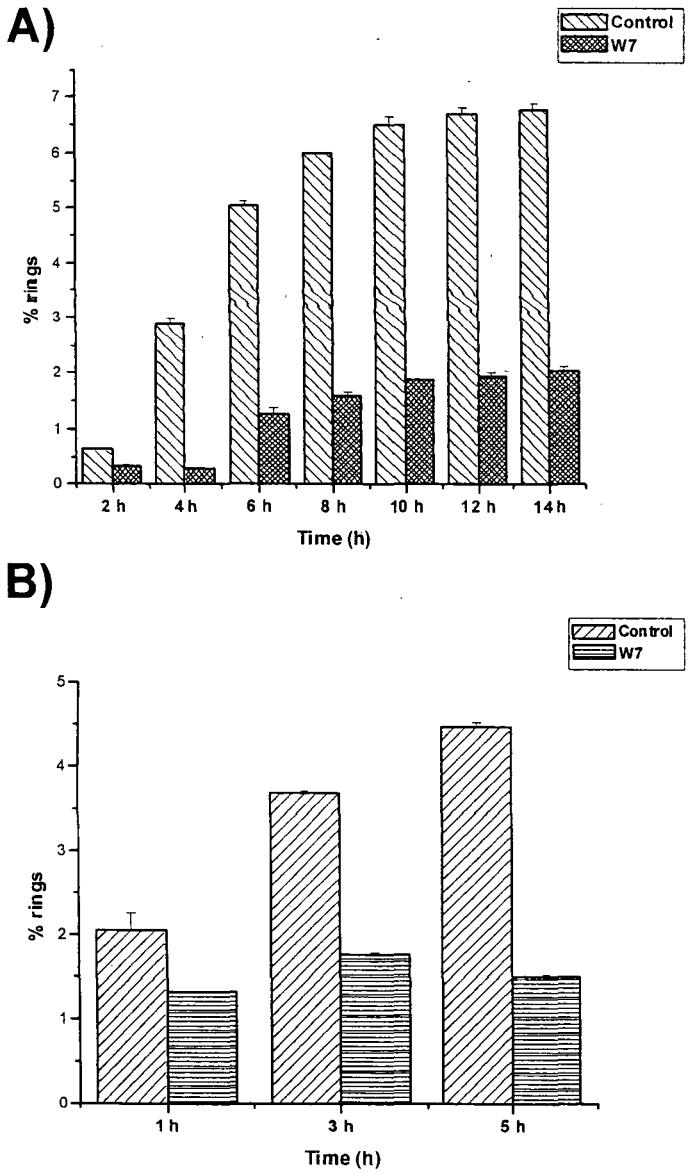

Figure. 6.2 **Calmodulin inhibitor W7 inhibits invasion.**

(A) 50 μM Calmodulin inhibitor W7 was added to schizont stage parasites and number of rings formed was monitored by giemsa staining of thin blood smears from parasite cultures at indicated time points. Formation of new rings in the next cycle of the parasite growth was inhibited by W7. (B) Free merozoites were isolated and incubated with 50 μM W7 or medium alone for 10 min at 37^{0}C before addition of RBCs. While untreated merozoites successfully invaded RBCs and formed rings, invasion was significantly blocked in W7 treated merozoites. % rings in the graph refers to the RBCs that were infected with ring stage parasites.

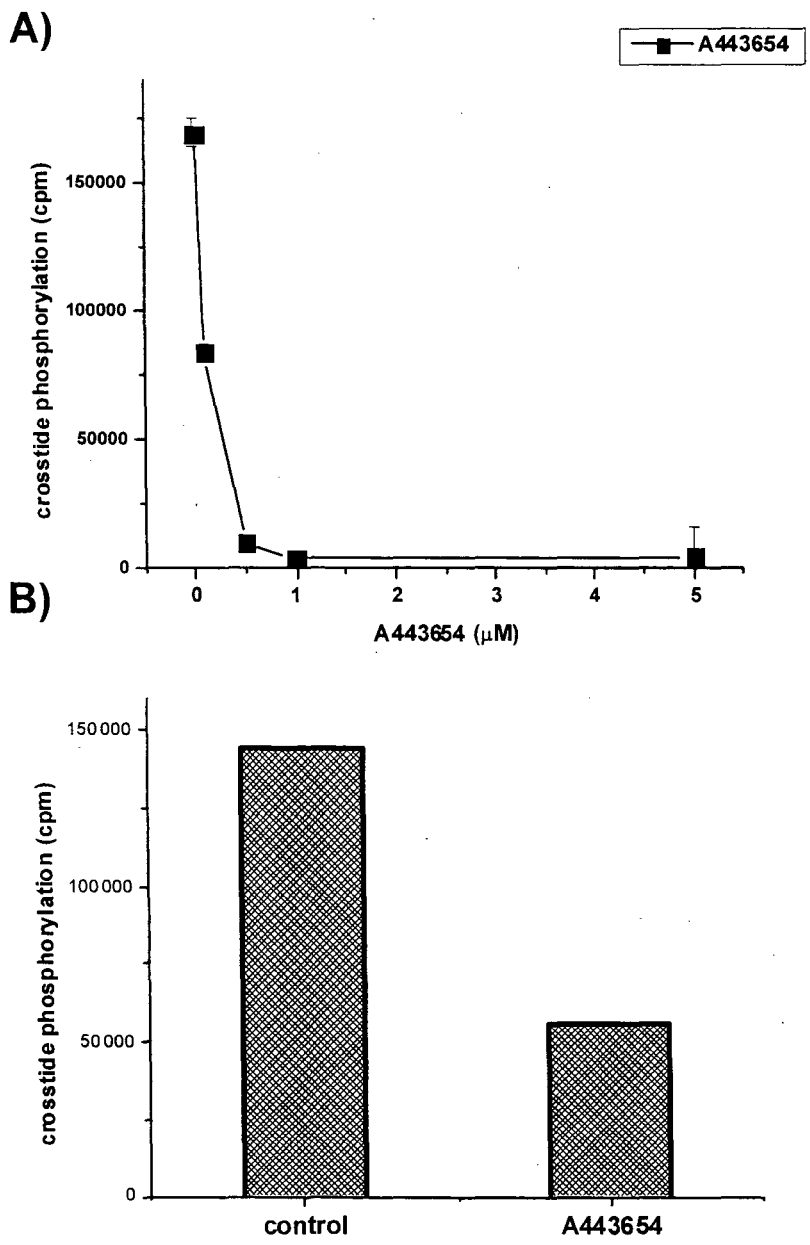

Figure 6.3 **A443654 inhibits PfPKB activity.**

(A) A443654 was used in kinase assays with recombinant ΔPfPKB, it inhibited PfPKB activity with IC_{50} of ~200 nM. (B) Schizont rich cultures were treated with A443654 (500 nM) or with DMSO (control) for 2 h and PfPKB was immunoprecipitated. PfPKB- IP associated kinase activity was significantly reduced in the presence of A443654. Kinase activity was assayed using crosstide (~100 μM) as substrate (see Materials and Methods).

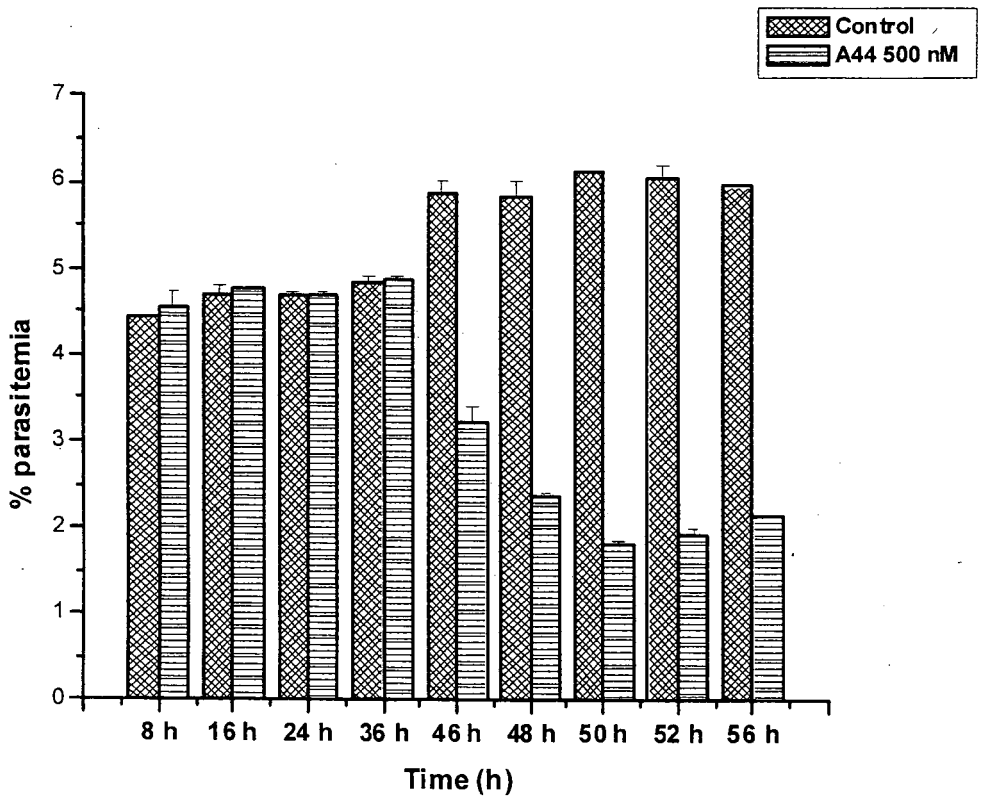

Figure. 6.4 **PfPKB inhibitor A443654 inhibits *P.falciparum* growth.**

500 nM A443654 or DMSO (control) alone was added to synchronized ring stage parasites and parasite maturation was followed at indicated time points. Microscopic examination and quantitation of various parasitic stages suggested that there was no significant change in intra-erythrocytic parasitic stages until 44 h. Decrease in the formation of rings in the next cycle was observed in inhibitor treated cultures. Following parasitic stages were present at the indicated time points: 8 h, rings; 16-36 h trophozoites: 36-46 h, schizonts; 46 h-56 h, rings.

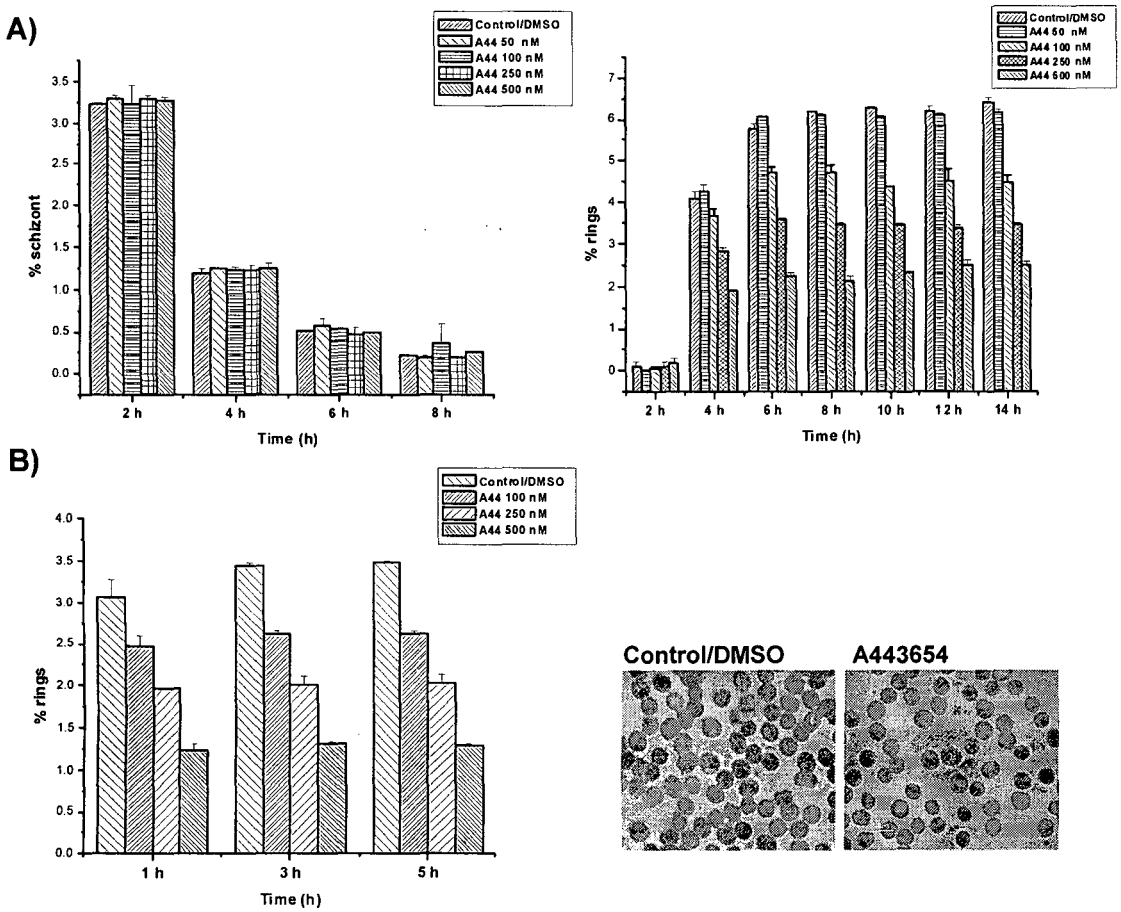

Figure. 6.5 **A443654 inhibits RBC invasion by the parasite.**

(A) To schizonts harvested from synchronized cultures, 500 nM A443654 or DMSO (control) was added. At indicated time post-addition of the inhibitor, number of schizonts and rings were individually scored. Formation of new rings (right panel) was inhibited significantly but the schizont number did not change significantly (left panel). (B) Free merozoites were isolated (Materials and Methods and Figure. 6.6) and were treated with 500 nM A443654 for 10 min at 37^{0}C before addition to RBCs in culture. The number of rings were scored at indicated time points to assess invasion. These data are representative of three independent experiments and error bars represent S.E. within replicates from a single experiment.

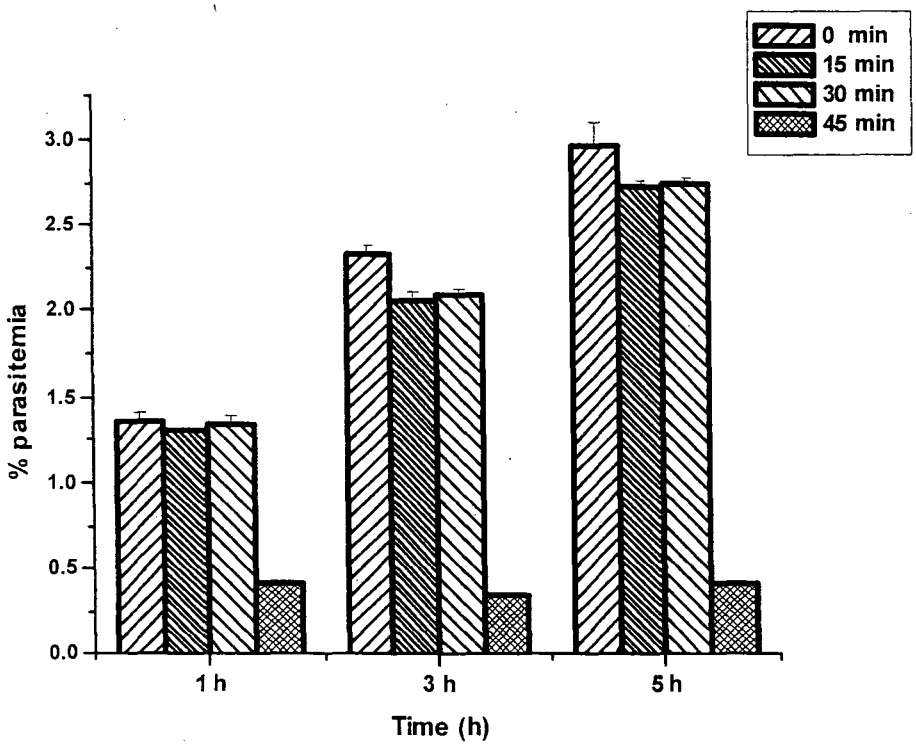

Figure. 6.6 **Isolation of merozoites for invasion assays.**

Merozoites were isolated from parasite cultures and the effect of pre-incubation (before addition to RBCs) on invasion was studied. After isolating the merozoites were resuspended in complete medium and were incubated for 0 min, 15 min, 30 min, 45 min at 37^{0}C and ring formation was monitored at indicated time points by giemsa staining of thin blood smears.

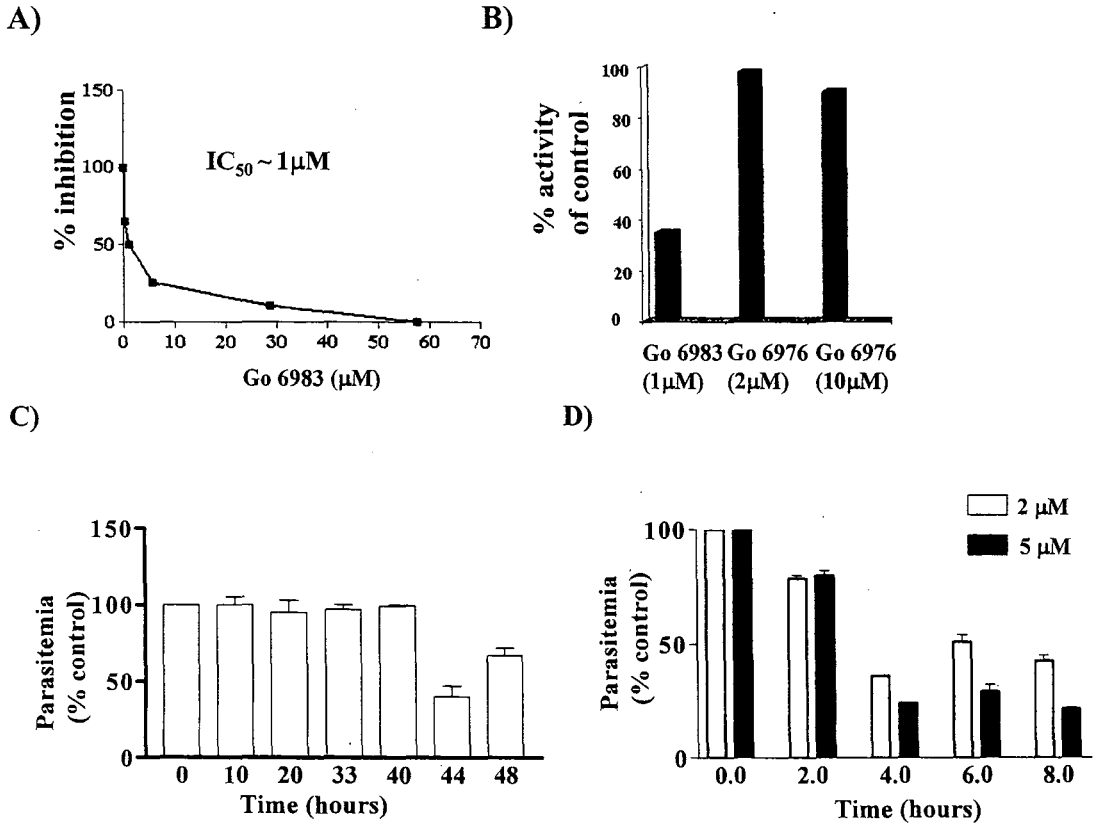

Figure. 6.7 **Go 6983 inhibits PfPKB activity and affects parasite growth.**

Various concentrations of Go 6983 (A and B) or Go 6976 (B) were used to inhibit peptide substrate phosphorylation by GST-ΔPfPKB. Enzyme activity in the absence of the inhibitor is considered as 100%. Go6983 inhibited recombinant ΔPfPKB activity with IC_{50} ~1 μM. C) Either 5 μM Go 6983 or 0.1% DMSO was added to synchronized *P. falciparum* cultures (1% parasitemia) and parasite growth was monitored at indicated times. (C). *P. falciparum* schizonts (~ 3% parasitemia) were treated with indicated concentrations of Go 6983 or 0.1% DMSO. Formation of new rings was monitored at indicated times (D). Number of parasites were counted at indicated times by microscopic examination of Giemsa-stained thin blood smears (C and D). Y -axis is the ratio of percentage of parasitemia of drug treated cultures to that of DMSO treated cultures. Error bars reflect ±S.E. from three experiments.

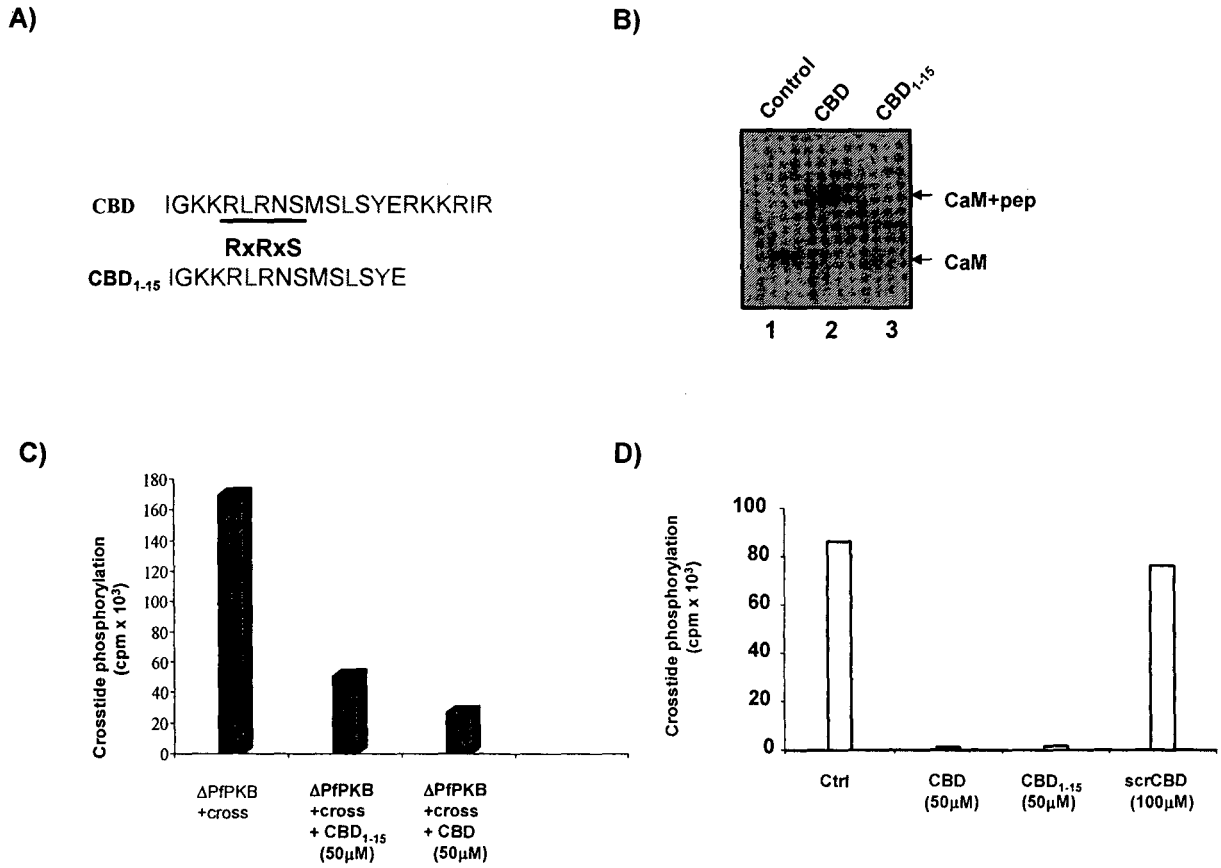

Figure. 6.8 **CBD peptides inhibit PfPKB activity from the parasites.**

(A) Sequences of CBD peptides with the RxRxS motif are highlighted. (B) CaM (10 μM) was incubated with 10 μM CBD (lane 2) or CBD_{1-15} (lane 3) or alone (lane 1) in a buffer containing 1 mM $CaCl_2$. The mixture was separated on NATIVE-PAGE as described for figure. 4.9. Coomassie stained gel shows that CBD but not CBD_{1-15} causes a changes the mobility of CaM. (C) Recombinant ΔPfPKB was incubated in kinase assay buffer containing 1 mM phosphoacceptor substrate crosstide in presence or absence of indicated peptides. Phosphate incorporation in crosstide was determined as described in Materials and Methods. Both CBD and CBD_{1-15} inhibit ΔPfPKB activity. (D) *P. falciparum* merozoites were incubated with CBD, CBD_{1-15} or scr-CBD peptides for 10 min. Subsequently, activity of PfPKB immunoprecipitated from parasite lysates was assayed. PfPKB- IP activity was significantly attenuated in the presence of the CBD peptides.

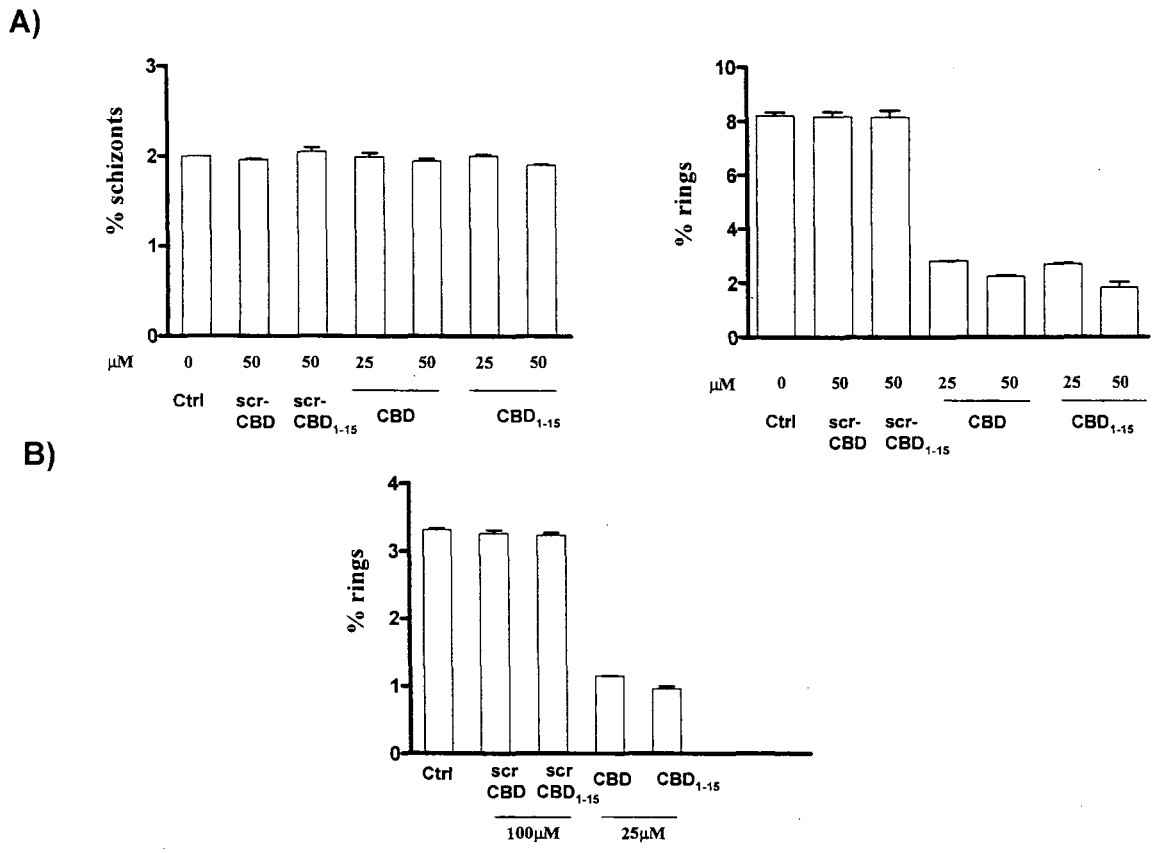

Figure. 6.9 **CBD-peptide inhibitors block invasion**

(A) CBD peptides prevent invasion of erythrocytes by *P. falciparum*. Indicated amount of CBD-peptides or scr-CBD was added to cultures containing mature schizonts/segmenters and formation of new rings was monitored microscopically after 6h. Rings and schizonts were individually scored and data represents % RBCs infected with these stages. (B) Free merozoites isolated from *P. falciparum* cultures were incubated either with 25 µM CBD peptides or 100 µM of scr-peptides for 10 min at 37°C and were subsequently added to uninfected erythrocytes. Thin blood smears were made after 5h and numbers of rings were counted by giemsa staining. Merozoite invasion was severely compromised in the presence of CBD peptides.

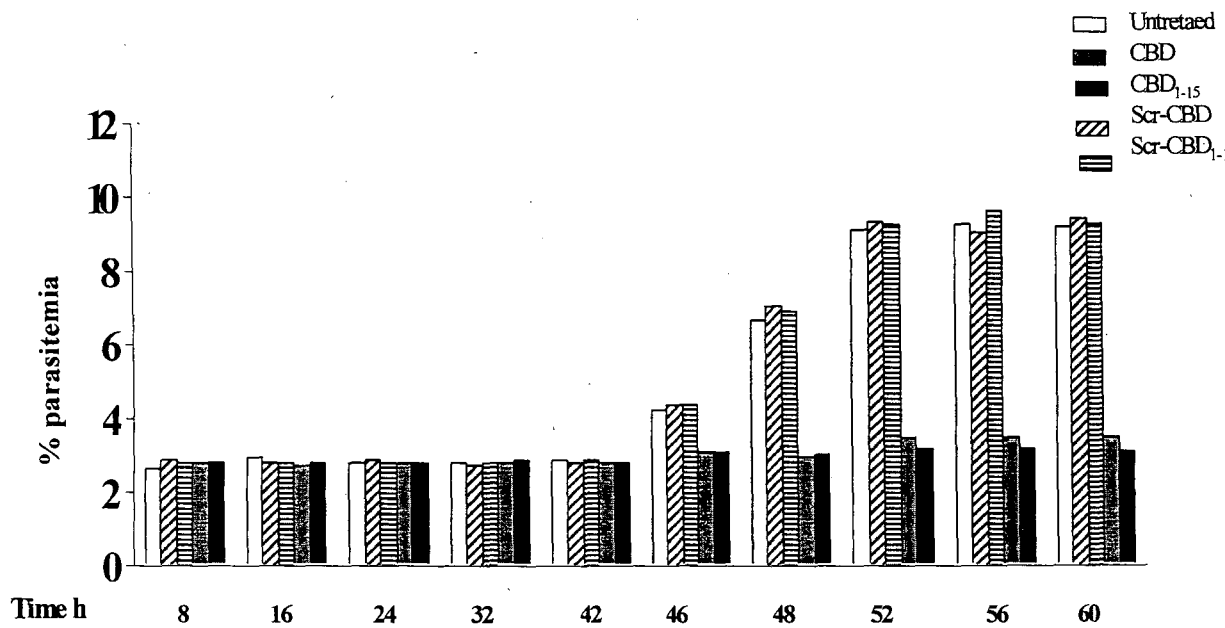

Figure. 6.10 **CBD peptides act specifically during invasion and have no effect on other parasitic stages.**

25 μM CBD peptides or 100 μM scr-CBD peptides were added to ring stage parasite culture and development of parasites was counted at different time points as described for figure.6.4. Peptides were replaced after 24 h when the medium was changed. Effect of peptides could be seen only on the formation of rings in the next cycle of parasite growth (after ~46 h) when new rings were formed. Data are average of replicates from one experiment and is representative of three independent determinations.

Figure. 6.11 **Localization of CBD peptides in *P.falciparum* merozoites.**

CBD (A) or CBD_{1-15} (B) peptides conjugated with FITC at their N-terminus were added to *P.falciparum* cultures at late schizont stage for 2 h and indirect immunofluorescence was performed using antisera against merozoite surface protein-1 (MSP1). FITC-CBD associated fluorescence can be seen concentrated at a "spot" on the merozoite.

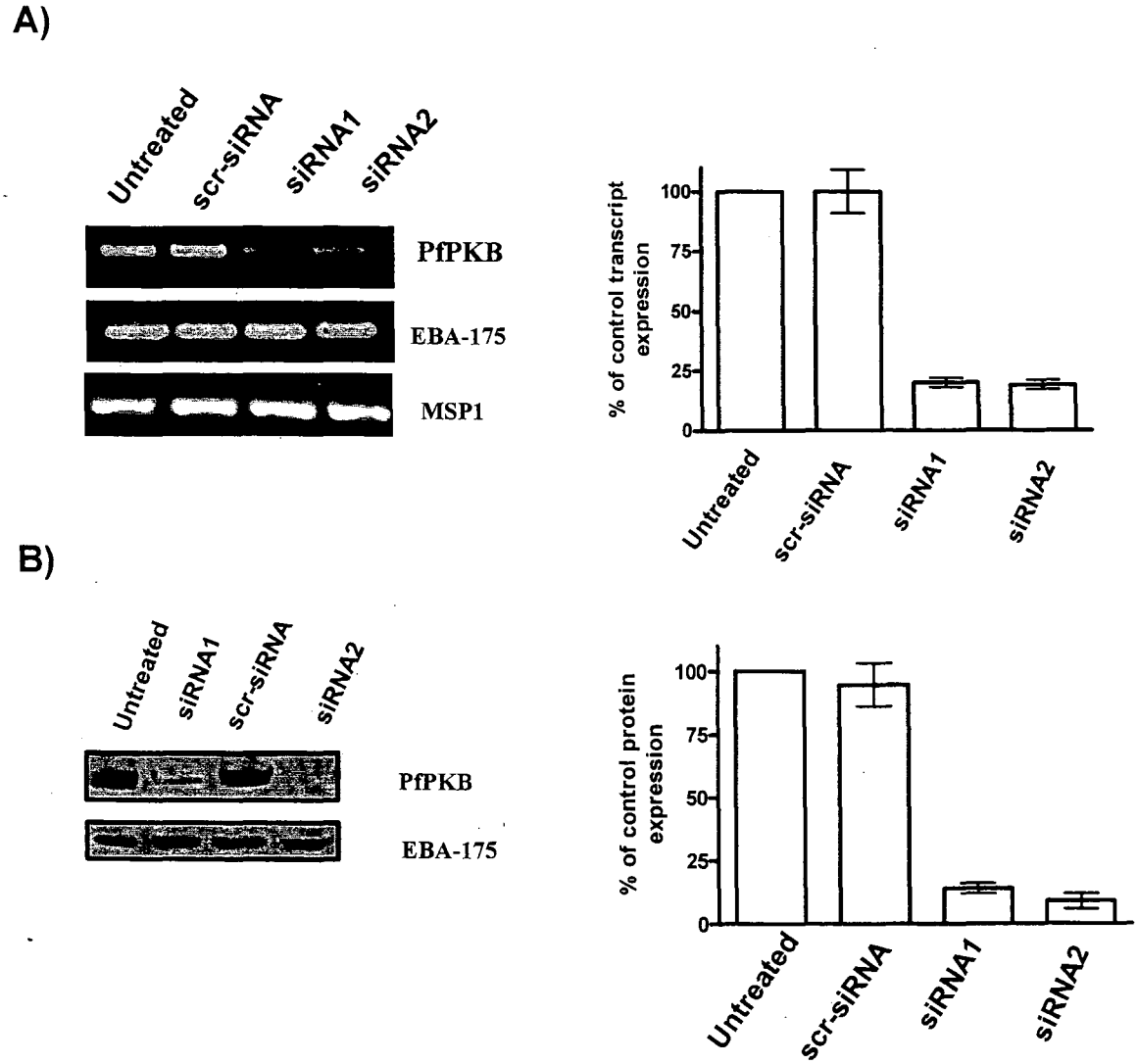

Figure. 6.12 **siRNA mediated PfPKB gene silencing in *P.falciparum*.**

siRNA against PfPKB inhibits its expression. Late-trophozoite stage parasites were treated either with two sets of siRNA duplexes complementary to two different regions of PfPKB or a control scrambled siRNA duplex. RT-PCR (A) or western blot analysis (B) were performed after isolating RNA or protein 8h after addition of siRNA. Quantitation of PfPKB bands in RT-PCR and western blot experiments was done by densitometric analysis and data are represented as percentage of intensities of signal in the control samples (right panels). A significant reduction in PfPKB transcripts and protein levels was observed only in siRNA treated cultures. MSP-1 and EBA-175 were used as controls for RT-PCR and western blots. Left panels indicate S.E.M from three independent experiments and error bars represent S.E.

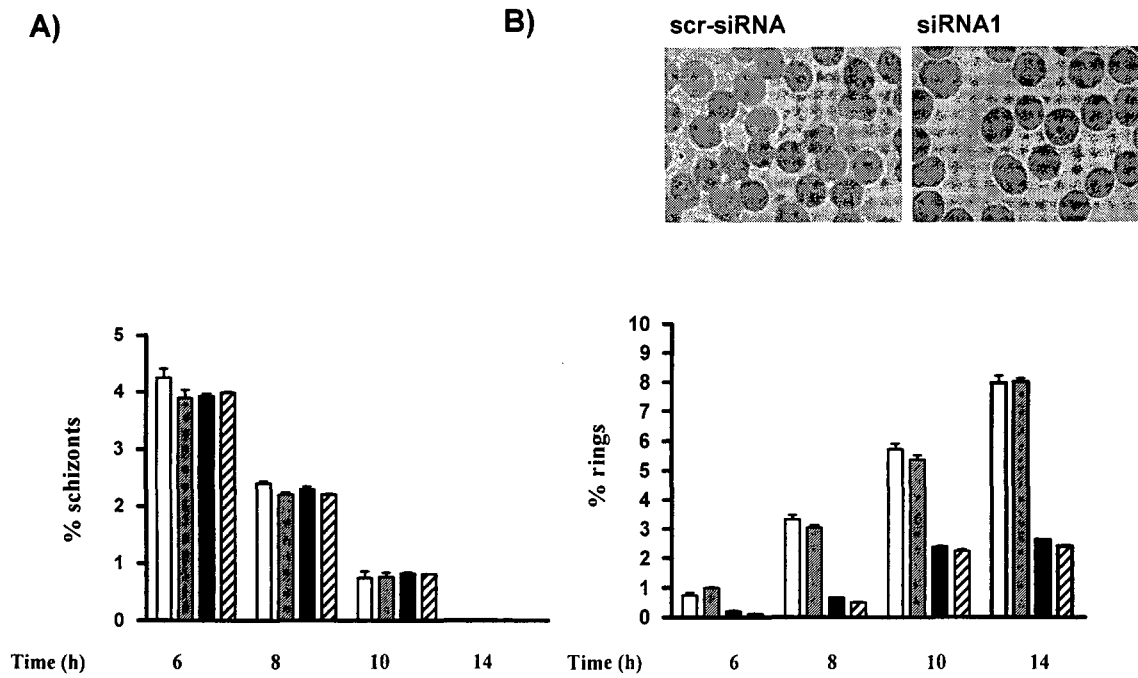

Figure. 6.13 **siRNA against PfPKB impairs merozoite invasion.**

Late-trophozoites were treated with only buffer (white), control scr-siRNA (grey) or PfPKB-siRNA1 (black) and PfPKB-siRNA2 (hatched) and schizonts (A) and rings (B) were counted at indicated time after addition of siRNA. PfPKB-siRNA treated cultures exhibited a significant decrease in formation of rings without significantly changing the schizont number. % ring or schizont infected erythrocytes are indicated. Inset shows a representative giemsa stained blood smear of scr-siRNA or siRNA1. Data are the average of replicates from a single experiment and error bars indicate ± S.E. from replicates. A representative of more than three independent experiments is shown.

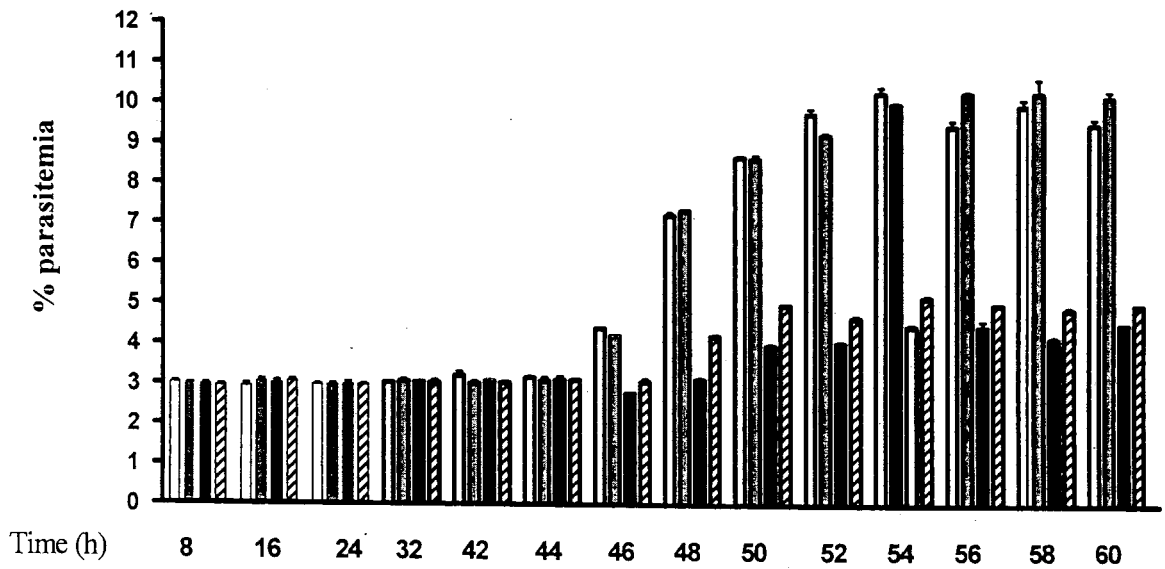

Figure. 6. 14 **siRNA against PfPKB does not affect any other intra-erythrocytic stage except merozoite invasion.**

Synchronized P. falciparum cultures were treated with only buffer (white), a scrambled siRNA (grey) or PfPKB-siRNA1 (black) and PfPKB-siRNA 2 (hatched) first at ring stages (6 h) and again 24h later when parasites were mid-late trophozoites (30 h). Total number of infected erythrocytes with various parasitic stages was counted at indicated time points post-invasion. Microscopic examination and quantitation of various parasitic stages suggested that there was no significant change in intra-erythrocytic parasitic stages from 6-44 h. Following parasitic stages were present at indicated time points: 8 h, rings; 18-34 h trophozoites; 42 and 44 h, schizonts; 46 h, schizonts and rings; 48-54 h rings. The increase in parasitemia caused due to invasion of erythrocytes after schizont rupture (46-50 h) was markedly reduced in PfPKB-siRNA treated cultures.

Chapter – Seven

Identification and stage specific expression of PfPLC

Chapter Seven

Identification and stage specific expression of PfPLC

Studies described in the previous chapters highlight the important role played by calcium in regulation of PfPKB activity. Phospholipase C (PLC) is the enzyme responsible for generation of I(1,4,5)P_3 which facilitates release of calcium from the intracellular stores. PfPLC, a PLC homologue in *P.falciparum* was identified in the laboratory.

7.1 Identification and molecular cloning of PfPLC.

During the course of this work, a putative PI-PLC gene was annotated in PlasmoDB (PF10_0132), which was named, PfPLC (Fig. 7.1A,C). It exists as a ~ 4.5 kB gene on chromosome 10. PlasmoDB predicted gene has one large exon followed by three small exons at the 3'end of the gene (Fig. 7.1A). Based on the sequence of annotated PF10_0132 gene, PCR primers were designed to amplify the PfPLC gene and to confirm intron exon boundaries. For this purpose Reverse Transcription (RT) was done using parasite RNA and random hexamer primers and the cDNA was used to amplify PfPLC gene (see Materials and Methods). The nucleotide sequence of the first exon was almost identical to PF10_0132. However, there were slight differences in predicted intonic sequences and experimentally determined sequence. The intron-exon boundaries were reconfirmed by amplifying the ~1.1 kb region spanning these introns (Figure. 7.1B) and DNA sequencing. Bioinformatic analysis of PfPLC sequence revealed that it has ~ 32% similarity with the mammalian PLC γ. The similarity in the catalytic X and Y sub domains with PLC γ is higher (~ 40%). PfPLC also has a putative PH

domain at its N-Terminal region which may help in its membrane recruitment and an EF-hand motif to facilitate its interactions with calcium (Figure. 7.1C).

7.2 PfPLC is expressed in trophozoites and schizonts.

Specific antibody was needed to study the expression of PfPLC in parasite life cycle. For this purpose, the catalytic Y sub domain of PfPLC (531 bp) was cloned in pQE30UA expression vector and was expressed as a 6x-His fusion protein in *E.coli.* (Figure. 7.2A). This recombinant protein was used to raise antisera in rabbits (see Materials and Methods). Parasite lysate prepared different stages was used to determine the expression profile of PfPLC. Western blots revealed that PfPLC is predominantly expressed during the trophozoite and schizont (Figure. 7.2B) stage of the parasite life cycle, the expression was very low in ring stage. Expression of PfPLC during the schizont stage fits well with results described in chapters 5 and 6 wherein phospholipase C mediated calcium release in combination with CaM controls activation of PfPKB in the schizont stage.

7.3 PLC inhibitors cause impaired parasite growth.

PLC inhibitor U73122 when used in malarial parasite blocks intracellular calcium release (Gazarini et al., 2003), which suggests that this inhibitor may be effective against PfPLC. PfPKB signaling pathway which is regulated by Ca^{2+}/CaM is involved in invasion and PLC inhibitors block its activity (Figure. 5.4). The role of PfPLC in invasion was adjudged directly by performing invasion assays in presence of U73122 or its inactive analogue U73322. When added to schizonts, U73122 blocked the formation of rings subsequent to merozoite release

and invasion (Figure. 7.3A). When added to free merozoites, U73122 caused a marked decrease in invasion (Figure. 7.3B). In contrast, U73322 did not alter parasite growth (Figure. 7.3A, B). These results suggested that PLC plays a major role in regulating invasion, which is in good agreement with its expression in schizont stages. Moreover, these data also fit in well with the proposed role of PfPKB pathway in RBC invasion where PfPLC is an upstream regulator.

A) **Gene Structure of PfPLC**

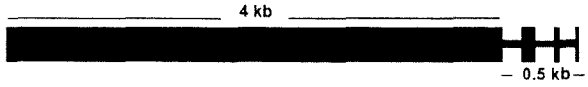

B)

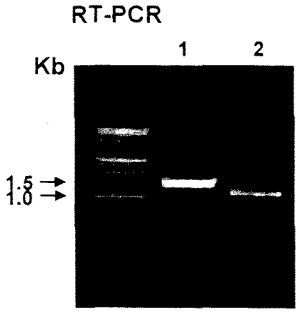

ATGAATATTCCTGCTTAAAAGGATATGTATTTCGAAATTTTTATGAAACCAGAAATTATAATGAAATATGTTCCATTAGTGAAAATA
AATTTATTAAATTAATTAAAAAAAACGAAAACGAAATTATTAAATATAATCAAAAAACCCTAACAAGGGTTTATCCATCAGGAACA
CGACTAGCATCTACCAATTTCAATCCTTTAATATTTTGGAATGCAGGTATACAAGTTGTAGCATTAAATTATCAATATAATGGATT
AAGTATGTTGTTAAATAAAGGAAGGTTTTTAGAAAATGGTGGAAAACACTCAGGCTATATTTTAAAACCTGAATTATTAAGATTTA
ATGAAAAACAAGATTATAATACCTTATTATTAGATTTACAAATATTGTCATTACATCAAATAAATTTACTATTTTCAATAAAAAATAA
ATATCATGAAAAAAAACTAAAAAAGAAATTATTTCAAATGGATATGATTCAAAGAATTCAAACACATAAAAAAATAAAAAAGAAAAT
CAAAAACTGGAAAGATCTACAAAATTAGAAAAAAGAGAAGAAAAATATACTTTTTTCAGATGTTCAGTCAGATGATAATAAAAATAA
ACATATTAGTTATGAATTACTTCTTAACAAAATTAATGATAATGATGATGTTAATTATATACATAATAAATGTTTAAATGTAGAAAA
GAAATATGAAGACATGTTAACAGAATATAAATCGTTCTTATTATGTTCTTCATCCTTATCACATAGTAGTAGCTTCAATAGTTGTA
GTAGTAACACAACTACATCAAATGATGGAAATAAAACACATTCCAATAAAAATAATTCATCCAAATATAAAAACAAAAATTTTTATC
AAACATTTGAAGAATTAAAAAAAGCAAATAATTTATTTTTTTATCTCTATCTTACTATATCCATTCATGGATATAATGAGAACAAAT
ATTACTTTAAAACTGAAATTGCAAAAGTTAATTTTTTATGACATTAATTATTGGTATGTAACAAAATATCTTAAATACATTATACAAA
AAGAAAAAATAAATAAAATAATAAAAACATTAATAATAATAATAAATATGTGTATATTTATTTATTTATTCATATATATATTTATTGTT
TATTTTATTTTATTTTTGTAGTTGGTCAAAACCATCCACTTTCCAAATGAAAATATCTTATCCTTCCTTGGCTCTTATAGTATTTGA
ATTAAAGGCATATGTAAGTTTAAAATATTGTATTTATATTTTTTTTTTATAAAATTAATGATTTAGTATATGTGATCATATAAATAAA
TGTATAGATCCATGTGATATACAAAGTACCATAGAATAGAAGTTATATATACCATGTGATTATATGTACATTATATATATAATATAT
ATGTATTTATTTATTTATATTTTATATAGGATACTGTAAAAAGTGAAATAATAGCTTGCGCCTGCTTTCCAGTTAAATGCTTAAG
AGAAGGGTAATTATAAAAATATACATAAAACTTGTTGTATCCATATTTATTACTTAAATATCATTTTATCTATAATAATATTTTTTC
CTATTTATTTTTTTTTTTTTTTAATTTCTAATAGATTACGATTTGTACCATTGTGCGATAA

C) **Domain organization of PfPLC**

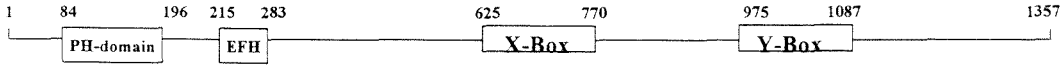

Figure. 7.1 **Domain architecture and RT-PCR cloning of PfPLC gene structure.**

(A) PfPLC predicted as gene PF10_0132 by PlasmoDB has four exons, first is ~4 kb size followed by three small exons at 3'-end. The three introns span the last 500 bps of the gene. (B) RT-PCR analysis of PfPLC gene, ~1.1 kb upstream 3' end of predicted PfPLC gene was amplified from genomic as well as cDNA to confirm the presence of introns. Presence of introns was reflected by the larger size of genomic PCR product, which was confirmed by DNA sequencing. Sequence of 3' 1.1 kb is shown with the three introns underlined. (C) Bioinformatics analysis of PfPLC sequence revealed a PH domain and an EF hand motif in addition to the catalytic X and Y sub domains.

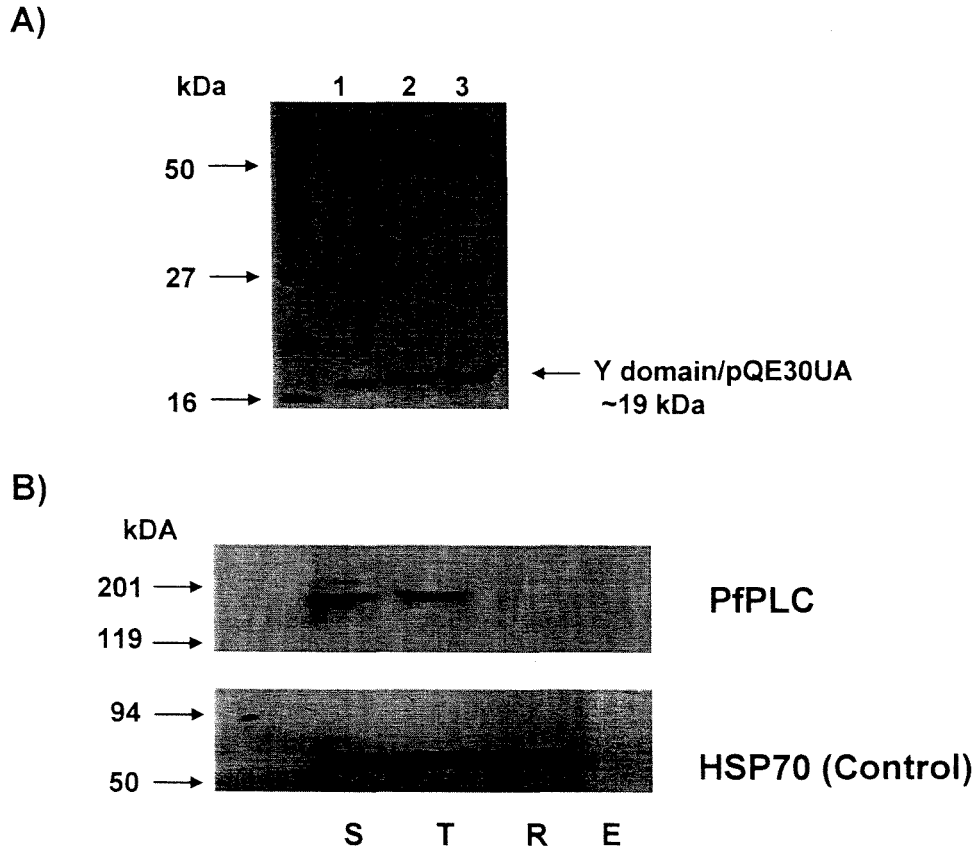

S – Schizont
T – Trophozoite
R – Ring
E – Erythrocyte

Figure. 7.2 **Stage specific expression of PfPLC.**

(A) Y-domain of PfPLC (531 bp) was cloned in pQE30UA vector and expressed in *E.coli* as 6x-His fusion protein. Coomassie stained gel shows the expressed protein which was used to raise antisera in rabbits. (B) Stage specific protein lysates were made from synchronized parasite cultures and western blotting was performed using anti-PfPLC or HSP-70 (control) antisera. PfPLC, ~160 kDa was expressed mainly in the trophozoite and schizont stage.

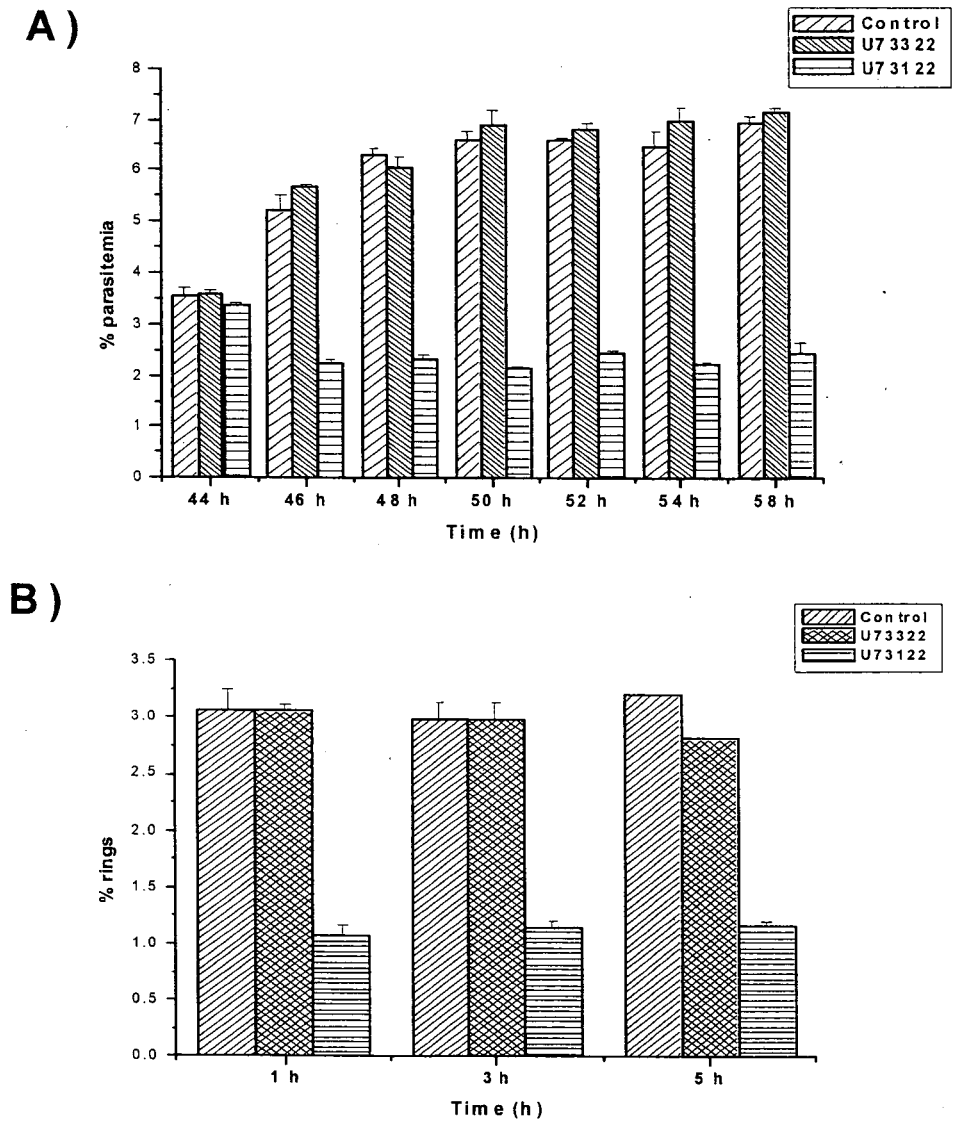

Figure. 7.3 **PLC inhibitor impairs RBC invasion by *P. falciparum*.**

The effect of PLC inhibitors on invasion was tested using schizonts (A) or free merozoites (B) as described earlier in chapter 6. (A) When 30 µM U73122 or U73322 was added to synchronized schizont cultures, new ring formation was hampered in presence of U73122 without altering the number of schizonts. (B) Isolated free merozoites were incubated with 30 µM U73122 or U73322 for 10 min and invasion was assessed by counting rings at indicated time points. Merozoites were severely compromised in their invasive capacity in the presence of PLC inhibitor U73122.

Chapter - Eight

Discussion

Chapter Eight

Discussion

One of the highlights of *Plasmodium falciparum* genome sequencing (Gardner et al., 2002) was the presence of several putative signaling molecules like protein kinases in the parasite (Ward et al., 2004). Despite this information, the role of signal transduction events in the development of malaria parasite was very limited. Especially, information about molecular machinery involved in carrying out signaling events was scarce. Our laboratory had identified a PI3K homologue and a PKB homologue (described here) in *P. falciparum*, which suggested that signaling pathways regulated by these enzymes might be important for the parasite. The major goal of this thesis was to understand the regulation and function of PfPKB, the PKB like protein kinase in *P. falciparum*.

PfPKB shows significant sequence homology to catalytic domain of protein kinase B in higher eukaryotes. In addition, it also shares almost 65% sequence homology with the catalytic domain of protein kinase C, another AGC class Ser/Thr kinase. It is likely that *P. falciparum* lacks a PKC homologue (Ward et al., 2004). Bioinformatic analysis suggested that PfPKB is closest to, besides PKB, mammalian PKC α,β,γ at the sequence level. PfPKB does not have a PH domain, which plays an important role in sub cellular localization and activation of PKB by binding to 3'-phosphorylated phosphoinositides, a product of PI-3 kinase in mammalian cells (Andjelkovic et al., 1996; Vanhaesebroeck and Alessi, 2000). It is interesting to note that yeast and *T.cruzi* homologues also do not have a PH domain (Fujita and Yamamoto, 1998; Pascuccelli et al.,

1999; Toda et al., 1988) suggesting that PKB in these unicellular eukaryotes may not be directly regulated by phosphoinositides. Interestingly, the N-terminal region of PfPKB did not share any significant similarity to any protein in various databases.

In contrast to mammalian PKB which is activated by PDK1, PfPKB was regulated by autophosphorylation of S271 (Figure. 4.7). This serine residue is complementary to T308 of PKB and phosphorylation of this site by PDK1 is crucial for PKB activation. Despite sequence conservation in the vicinity of S271, human PDK1 was unable to activate PfPKB (data not shown). Several AGC kinases (e.g. cPKC isoforms and S6K1) are regulated by autophosphorylation and do not appear to require PDK1 (Biondi et al., 2000; Parekh et al., 2000). It was interesting to note that the PKB homologue from another protozoan parasite *T. cruzi* was also regulated by autophosphorylation (Pascuccelli et al., 1999).

The PI3-kinase-PKB pathway is a major player in a wide variety of cellular processes in mammalian cells (Scheid and Woodgett, 2003; Vanhaesebroeck and Alessi, 2000). *Plasmodium* has only one PI3K homologue (Sharma *et.al.*, unpublished results) and PfPKB, a protein kinase B like enzyme in *P.falciparum* (Kumar et al., 2004). PfPKB is not likely to be regulated by phosphoinositides as it lacks the N-terminal PH domain present in PKB, which is needed for interaction with 3'-phosphorylated phosphoinositides (Alessi and Cohen, 1998). Results reported here suggest that PfPKB is directly regulated by Ca^{2+}/CaM and therefore is independent of the PI-3 kinase regulation.

Free calcium levels in the parasite are controlled by phospholipase C (PLC) as it generates IP_3 which releases calcium from the intracellular stores (Garcia, 1999). PLC inhibitor, U73122, has been successively used in *Plasmodium* to block calcium release (Hotta et al., 2003). Studies performed using this inhibitor suggested that PLC is the upstream regulator of PfPKB as calcium release mediated by it was crucial for PfPKB activation. These data provided a link between PfPKB and PLC mediated calcium signaling (Figure. 5.4). Both calcium (Wasserman, 1990) and calmodulin (Matsumoto et al., 1987; Scheibel et al., 1987) have been implicated in invasion of erythrocytes by malaria parasite. However, the identity of the signaling pathways via which they may control invasion had remained elusive. Present studies resulted in identification of one of the first targets of CaM in malaria parasite and a multi-component signaling pathway (Figure. 5.5).

In order to decipher the role and importance of PfPKB in *P. falciparum,* pharmacological inhibitors against PfPKB were used. One of the major problems in performing these studies early on was unavailability of effective mammalian PKB inhibitors. Subsequently, Abbott laboratories released information about a series of compounds which were specific inhibitors of mammalian PKB. One of these indazole-pyridine based inhibitors (A443654) was especially specific to PKB in comparison to other kinases. Its second best target was PKA with almost 40 fold lower affinity (Han et al., 2007; Luo et al., 2005). Given the high similarity between PfPKB and PKB in the catalytic region, A443654 was selected and used against PfPKB, It turned out be a reasonably good inhibitor of PfPKB (IC_{50} ~ 200nM). Experiments using this compound suggested a role of PfPKB in invasion (Figure. 6.4; 6.5), which was supported by the expression

of PfPKB in merozoites and its localization at the apical end (Figure. 6.1;6.2). Importantly, this compound did not affect the development of any other parasitic stage, which would have suggested its cross-affinity with kinases in other parasitic stages (Figure. 6.4).

Extensive biochemical studies were performed to work out the mechanism of regulation of PfPKB by Ca^{2+}/CaM (Figure. 4.7; 4.8). CaM interacts with segments on proteins that are rich in basic and hydrophobic residues and have the propensity of forming α-helices. The hydrophobic residues in CBDs of target proteins are critical for anchoring them to hydrophobic pockets present in CaM. Typically, these residues may be separated by 10, 14, or 16 residues (Hoeflich and Ikura, 2002; Yamauchi et al., 2003). The number of CBDs which do not strictly follow these rules has grown, moreover, there are CBDs which use only one of these residues for interaction (Rhoads and Friedberg, 1997; Yamauchi et al., 2003). These studies reflect the diversity in interaction of CaM with its targets. PfPKB-CBD has a L6 and I20 that are spaced by 15 residues and may anchor binding to CaM, which is a minor diversion from standard examples (Figure. 4.8). Mapping of the CBD was followed by the identification of a **RxRxS** pseudosubstrate motif in the NTR which helped in elucidating the mechanism of PfPKB activation by CaM.

Biochemical studies not only provided insights into PfPKB regulation, they also lead to the identification of peptide inhibitors for PfPKB. Even though CBD-peptide inhibited PfPKB in parasites, there was a possibility that the interaction of CaM with other targets contributed to these effects. Since CBD_{1-15} acts mainly as a pseudosubstrate inhibitor of PfPKB (Figure. 6.8), it turned out to be a useful and a more specific tool to overcome this problem. This peptide also

blocked the ability of parasite to invade RBCs (Figure. 6.9). Clearly, these studies were aided by the ability of these peptides to enter parasites. Several groups have shown uptake of peptides/ proteins to the parasite including a recent report which shows that peptides of ~2400 Da can enter the parasites efficiently (Farias et al., 2005), although, the mechanism for the transport is not clear. Using FITC labeled CBD peptides, we were able to demonstrate that both CBD and CBD_{1-15} peptide enter the parasites (Figure. 6.11) and therefore may work intracellularly. With the intention of using an independent approach to suppress PfPKB function, siRNA mediated knockdown of PfPKB expression was performed (Figure. 6.12; 6.13). The results of these experiments were remarkably similar to that of peptide and pharmacological inhibitor data (Figure. 6.5; 6.7; 6.9) and suggested that PfPKB may be involved in early stage of parasite infection or invasion. Importantly, pharmacological inhibitor, siRNA as well as peptide inhibitor studies did not show any obvious defects in the development of other parasitic stages except impaired ability to form rings after invasion (Figure. 6.4; 6.10; 6.14). Experiments performed with free merozoites were very useful in suggesting the role of PfPKB in RBC invasion (Figure. 6.5; 6.9). The results obtained by various tools point towards a role of PfPKB in invasion.

The release of intracellular calcium is critical for various parasitic functions (Biagini et al., 2003). Importantly, it appears to be indispensable for successful erythrocytes invasion (Garcia et al., 1996; McCallum-Deighton and Holder, 1992). CaM is known to localize at strategic location in merozoites and controls invasion (Matsumoto et al., 1987; Scheibel et al., 1987). Using inhibitors of CaM, it was shown that to play a crucial role in merozoite invasion(Matsumoto et

al., 1987; Scheibel et al., 1987). Immuno-EM studies suggested that CaM is localized at the apical end of merozoites, which may allow it to control invasion (Scheibel et al., 1987). Since the identity of CaM targets in *Plasmodium* had remained elusive, the molecular basis for these effects had remained unclear. Identification of PfPKB as one of the first CaM targets (Figure. 5.3) via which it may control invasion certainly provides at least one of the clues to this query. CaM has been localized in apical organelles of merozoites in addition to other cellular locations. Immunofluorescence studies suggest that PfPKB may also be present in the apical region (Figure. 5.2), therefore, it is possible that PfPKB phosphorylates proteins present at these locations, which may be important for invasion. The identification of PfPKB targets will indeed provide further insight into the role of this signaling pathway in this crucial event in the life cycle of the malaria parasite. PfPKB was found to co-localize and interact with proteins of the actin-myosin motor complex (Figure. 6.1) which is suggestive of one of the ways via which it may participate in invasion by targeting proteins of this complex.

Chapter – Nine

Summary and Conclusion

Chapter Nine

SUMMARY and CONCLUSION

It is evident from the genome sequencing (Gardner et al., 2002) and bioinformatics (Aravind et al., 2003; Ward et al., 2004) that several signal transduction proteins like protein kinases may be present in the malaria parasite. There is little information about the molecular mechanisms via which the signaling events occur and guide the development of the parasite. The major goal of this thesis was to understand the regulation and function of PfPKB, the PKB like protein kinase in *P. falciparum*.

Biochemical studies directed at understanding the mechanism of PfPKB regulation revealed:

1. The NTR of PKB is inhibitory which keeps it inactive.
2. PfPKB activity is regulated by Ca^{2+}/CaM, which regulates its activity by promoting autophosphorylation of S271 in its activation loop. In the absence of calcium, CaM does not activate PfPKB.
3. The NTR has a Calmodulin binding domain (CBD) via which the interaction with CaM takes place.
4. A RxRxS pseudosubstrate motif is embedded in the CBD, which seems to be responsible for keeping PfPKB inhibited and binding of CaM causes release of this inhibition.

These studies resulted in identification of PfPKB as one of the first CaM targets in the malaria parasite and helped elucidate the mechanism for its catalytic activation (Figure. 4.12).

Biochemical studies were pivotal in understanding the regulation of PfPKB in the parasite. Taking clue from these studies, PfPKB regulation in the parasite was explored:

1. CaM was found to associate with PfPKB and regulate its activity in the parasite.
2. Availability of intracellular calcium was critical for CaM dependent PfPKB activation.
3. Phospholipase C was identified as the upstream regulator of PfPKB as it was responsible for calcium release which was necessary for PfPKB activation by CaM.

These findings resulted in identification of a novel multi-component signaling pathway in *P. falciparum* (Figure. 5.5).

To elucidate the function of PfPKB pathway in *P. falciparum*, this pathway was blocked at several steps and alteration of parasite growth was monitored. Following evidence suggested that PfPKB and this pathway may be involved erythrocyte invasion by the parasite:

1. PfPKB was localized at the apical end of the merozoites.
2. Both inhibitors of CaM and PLC, the upstream activators of PfPKB, attenuated the ability of parasites to invade RBCs indicating the involvement of these proteins in invasion.

3. A pharmacological inhibitor of mammalian PKB, A443654, was found to inhibit PfPKB with reasonable efficacy. This inhibitor blocked the ability of *P. falciparum* merozoites to invade RBCs.
4. Based on biochemical studies, peptide inhibitors were designed against PfPKB. Peptides with sequence similar to CBD or its truncated version, which lacked last six amino acids (CBD_{1-15}), successfully inhibited PfPKB activity in the parasite. Like pharmacological inhibitors, these peptides also blocked RBC invasion.
5. siRNA against PfPKB was used to inhibit its expression in the parasite. PfPKB-siRNA treated parasites also demonstrated impaired ability to form rings suggesting a role of PfPKB in invasion.

It had been demonstrated previously that both CaM (Matsumoto et al., 1987; Scheibel et al., 1987) and calcium (Scheibel et al., 1987; Wasserman, 1990) are crucial for the malaria parasite to successfully invade RBCs. However, the molecular events via which this may happen were not clear. Present studies suggest that regulation of PfPKB may be one of the ways via which invasion may be regulated by calcium signaling.

References

References

Adams,J.H., Blair,P.L., Kaneko,O., and Peterson,D.S. (2001). An expanding ebl family of Plasmodium falciparum. Trends in Parasitology *17*, 297-299.

Aikawa,M., Hepler,P.K., Huff,C.G., and Sprinz,H. (1966). The feeding mechanism of avian malarial parasites. J Cell Biol *28*, 355-373.

Aikawa,M., Miller,L.H., Rabbege,J.R., and Epstein,N. (1981). Freeze-fracture study on the erythrocyte membrane during malarial parasite invasion. J. Cell Biol *91*, 55-62.

Alessi,D.R., Andjelkovic,M., Caudwell,B., Cron,P., Morrice,N., Cohen,P., and Hemmings,B.A. (1996). Mechanism of activation of protein kinase B by insulin and IGF-1. EMBO J *15*, 6541-6551.

Alessi,D.R. and Cohen,P. (1998). Mechanism of activation and function of protein kinase B. Curr. Opin. Genet. Dev. *8*, 55-62.

Alleva,L.M. and Kirk,K. (2001). Calcium regulation in the intraerythrocytic malaria parasite Plasmodium falciparum. Mol Biochem. Parasitol. *117*, 121-128.

Anamika, Srinivasan,N., and Krupa,A. (2005). A genomic perspective of protein kinases in Plasmodium falciparum. Proteins *58*, 180-189.

Anderson,R.A., Boronenkov,I.V., Doughman,S.D., Kunz,J., and Loijens,J.C. (1999). Phosphatidylinositol phosphate kinases, a multifaceted family of signaling enzymes. J. Biol Chem. *274*, 9907-9910.

Andjelkovic,M., Jakubowicz,T., Cron,P., Ming,X.F., Han,J.W., and Hemmings,B.A. (1996). Activation and phosphorylation of a pleckstrin homology domain containing protein kinase (RAC-PK/PKB) promoted by serum and protein phosphatase inhibitors. Proc. Natl. Acad. Sci U. S. A *93*, 5699-5704.

Apiyo,D., Zhao,L., Tsai,M.D., and Selby,T.L. (2005). X-ray structure of the R69D phosphatidylinositol-specific phospholipase C enzyme: insight into the role of calcium and surrounding amino acids in active site geometry and catalysis. Biochemistry *44*, 9980-9989.

Aravind,L., Iyer,L.M., Wellems,T.E., and Miller,L.H. (2003). Plasmodium Biology: Genomic Gleanings. Cell *115*, 771-785.

Bahl,A., Brunk,B., Coppel,R.L., Crabtree,J., Diskin,S.J., Fraunholz,M.J., Grant,G.R., Gupta,D., Huestis,R.L., Kissinger,J.C., Labo,P., Li,L., McWeeney,S.K., Milgram,A.J., Roos,D.S., Schug,J.,

and Stoeckert,C.J., Jr. (2002). PlasmoDB: the Plasmodium genome resource. An integrated database providing tools for accessing, analyzing and mapping expression and sequence data (both finished and unfinished). Nucl. Acids Res. *30*, 87-90.

Balla,T. (2005). Inositol-lipid binding motifs: signal integrators through protein-lipid and protein-protein interactions. J. Cell Sci. *118*, 2093-2104.

Bannister,L.H. (1977). Structural aspects of Plasmodium relevant to vaccination against malaria. Trans. R. Soc. Trop. Med. Hyg. *71*, 275-276.

Baum,J., Richard,D., Healer,J., Rug,M., Krnajski,Z., Gilberger,T.W., Green,J.L., Holder,A.A., and Cowman,A.F. (2006). A Conserved Molecular Motor Drives Cell Invasion and Gliding Motility across Malaria Life Cycle Stages and Other Apicomplexan Parasites. J. Biol. Chem. *281*, 5197-5208.

Belham,C., Wu,S., and Avruch,J. (1999). Intracellular signalling: PDK1--a kinase at the hub of things. Curr. Biol. *9*, R93-R96.

Bergman,L.W., Kaiser,K., Fujioka,H., Coppens,I., Daly,T.M., Fox,S., Matuschewski,K., Nussenzweig,V., and Kappe,S.H. (2003a). Myosin A tail domain interacting protein (MTIP) localizes to the inner membrane complex of Plasmodium sporozoites. J. Cell Sci. *116*, 39-49.

Bergman,L.W., Kaiser,K., Fujioka,H., Coppens,I., Daly,T.M., Fox,S., Matuschewski,K., Nussenzweig,V., and Kappe,S.H.I. (2003b). Myosin A tail domain interacting protein (MTIP) localizes to the inner membrane complex of Plasmodium sporozoites. J Cell Sci *116*, 39-49.

Berridge,M.J. (1993). Inositol trisphosphate and calcium signalling. Nature *361*, 315-325.

Berridge,M.J. and Irvine,R.F. (1989). Inositol phosphates and cell signalling. Nature *341*, 197-205.

Biagini,G.A., Bray,P.G., Spiller,D.G., White,M.R., and Ward,S.A. (2003). The digestive food vacuole of the malaria parasite is a dynamic intracellular Ca2+ store. J. Biol. Chem. *278*, 27910-27915.

Biondi,R.M., Cheung,P.C., Casamayor,A., Deak,M., Currie,R.A., and Alessi,D.R. (2000). Identification of a pocket in the PDK1 kinase domain that interacts with PIF and the C-terminal residues of PKA. EMBO J. *19*, 979-988.

Bravo,J., Karathanassis,D., Pacold,C.M., Pacold,M.E., Ellson,C.D., Anderson,K.E., Butler,P.J., Lavenir,I., Perisic,O., Hawkins,P.T., Stephens,L., and Williams,R.L. (2001). The crystal structure of the PX domain from p40(phox) bound to phosphatidylinositol 3-phosphate. Mol Cell *8*, 829-839.

Brazil,D.P. and Hemmings,B.A. (2001). Ten years of protein kinase B signalling: a hard Akt to follow. Trends Biochem. Sci *26*, 657-664.

Brazil,D.P., Yang,Z.Z., and Hemmings,B.A. (2004). Advances in protein kinase B signalling: AKTion on multiple fronts. Trends Biochem Sci *29*, 233-242.

Brown,W.J., DeWald,D.B., Emr,S.D., Plutner,H., and Balch,W.E. (1995). Role for phosphatidylinositol 3-kinase in the sorting and transport of newly synthesized lysosomal enzymes in mammalian cells. J Cell Biol *130*, 781-796.

Carafoli,E. (2002). Calcium signaling: a tale for all seasons. Proc. Natl. Acad. Sci U. S. A *99*, 1115-1122.

Chen,W.S., Xu,P.Z., Gottlob,K., Chen,M.L., Sokol,K., Shiyanova,T., Roninson,I., Weng,W., Suzuki,R., Tobe,K., Kadowaki,T., and Hay,N. (2001). Growth retardation and increased apoptosis in mice with homozygous disruption of the Akt1 gene. Genes Dev. *15*, 2203-2208.

Cho,H., Mu,J., Kim,J.K., Thorvaldsen,J.L., Chu,Q., Crenshaw,E.B., III, Kaestner,K.H., Bartolomei,M.S., Shulman,G.I., and Birnbaum,M.J. (2001). Insulin resistance and a diabetes mellitus-like syndrome in mice lacking the protein kinase Akt2 (PKB beta). Science *292*, 1728-1731.

Coffer,P.J., Jin,J., and Woodgett,J.R. (1998). Protein kinase B (c-Akt): a multifunctional mediator of phosphatidylinositol 3-kinase activation. Biochem. J. *335 (Pt 1)*, 1-13.

Coffer,P.J. and Woodgett,J.R. (1991). Molecular cloning and characterisation of a novel putative protein-serine kinase related to the cAMP-dependent and protein kinase C families. Eur. J. Biochem. *201*, 475-481.

Cowman,A.F. and Crabb,B.S. (2006). Invasion of Red Blood Cells by Malaria Parasites. Cell *124*, 755-766.

Cowman,A.F. and Galatis,D. (1991). Plasmodium falciparum: The calmodulin gene is not amplified or overexpressed in chloroquine resistant or sensitive isolates. Experimental Parasitology *73*, 269-275.

Cross,D.A., Alessi,D.R., Cohen,P., Andjelkovich,M., and Hemmings,B.A. (1995). Inhibition of glycogen synthase kinase-3 by insulin mediated by protein kinase B. Nature *378*, 785-789.

Dekker,L.V., Palmer,R.H., and Parker,P.J. (1995). The protein kinase C and protein kinase C related gene families. Curr. Opin. Struct. Biol *5*, 396-402.

Delmas,P., Coste,B., Gamper,N., and Shapiro,M.S. (2005). Phosphoinositide Lipid Second Messengers: New Paradigms for Calcium Channel Modulation. Neuron *47*, 179-182.

Deng,W. and Baker,D.A. (2002). A novel cyclic GMP-dependent protein kinase is expressed in the ring stage of the Plasmodium falciparum life cycle. Mol Microbiol. *44*, 1141-1151.

Di Paolo,G. and De Camilli,P. (2006). Phosphoinositides in cell regulation and membrane dynamics. Nature *443*, 651-657.

DiNitto,J.P. and Lambright,D.G. (2006). Membrane and juxtamembrane targeting by PH and PTB domains. Biochim. Biophys. Acta *1761*, 850-867.

DiNitto, J. P. Cronin T. C. & Lambright D. G. Membrane recognition and targeting by lipid-binding domains. Sci.STKE , re16. 2003.
Ref Type: Generic

Dong,L.Q. and Liu,F. (2005). PDK2: the missing piece in the receptor tyrosine kinase signaling pathway puzzle. Am J Physiol Endocrinol Metab *289*, E187-E196.

Dumas,J.J., Merithew,E., Sudharshan,E., Rajamani,D., Hayes,S., Lawe,D., Corvera,S., and Lambright,D.G. (2001). Multivalent endosome targeting by homodimeric EEA1. Mol Cell *8*, 947-958.

Easton,R.M., Cho,H., Roovers,K., Shineman,D.W., Mizrahi,M., Forman,M.S., Lee,V.M., Szabolcs,M., de Jong,R., Oltersdorf,T., Ludwig,T., Efstratiadis,A., and Birnbaum,M.J. (2005). Role for Akt3/protein kinase Bgamma in attainment of normal brain size. Mol Cell Biol *25*, 1869-1878.

Eckstein-Ludwig,U., Webb,R.J., van Goethem,I.D.A., East,J.M., Lee,A.G., Kimura,M., O'Neill,P.M., Bray,P.G., Ward,S.A., and Krishna,S. (2003). Artemisinins target the SERCA of Plasmodium falciparum. Nature *424*, 957-961.

Engelman,J.A., Luo,J., and Cantley,L.C. (2006a). The evolution of phosphatidylinositol 3-kinases as regulators of growth and metabolism. Nat Rev. Genet. *7*, 606-619.

Engelman,J.A., Luo,J., and Cantley,L.C. (2006b). The evolution of phosphatidylinositol 3-kinases as regulators of growth and metabolism. Nat Rev. Genet. *7*, 606-619.

Farias,S.L., Gazarini,M.L., Melo,R.L., Hirata,I.Y., Juliano,M.A., Juliano,L., and Garcia,C.R. (2005). Cysteine-protease activity elicited by Ca2+ stimulus in Plasmodium. Mol. Biochem. Parasitol. *141*, 71-79.

FISCHER,E.H. and KREBS,E.G. (1955). Conversion of phosphorylase b to phosphorylase a in muscle extracts. J. Biol Chem. *216*, 121-132.

Ford,M.G., Mills,I.G., Peter,B.J., Vallis,Y., Praefcke,G.J., Evans,P.R., and McMahon,H.T. (2002). Curvature of clathrin-coated pits driven by epsin. Nature *419*, 361-366.

Ford,M.G., Pearse,B.M., Higgins,M.K., Vallis,Y., Owen,D.J., Gibson,A., Hopkins,C.R., Evans,P.R., and McMahon,H.T. (2001). Simultaneous binding of PtdIns(4,5)P2 and clathrin by AP180 in the nucleation of clathrin lattices on membranes. Science *291*, 1051-1055.

Freeman,R.R. and Holder,A.A. (1983). Surface antigens of malaria merozoites. A high molecular weight precursor is processed to an 83,000 mol wt form expressed on the surface of Plasmodium falciparum merozoites. J Exp. Med. *158*, 1647-1653.

Fujita,M. and Yamamoto,M. (1998). S. pombe sck2+, a second homologue of S. cerevisiae SCH9 in fission yeast, encodes a putative protein kinase closely related to PKA in function. Curr. Genet. *33*, 248-254.

Gao,T., Furnari,F., and Newton,A.C. (2005). PHLPP: a phosphatase that directly dephosphorylates Akt, promotes apoptosis, and suppresses tumor growth. Mol Cell *18*, 13-24.

Garcia,C.R., Dluzewski,A.R., Catalani,L.H., Burting,R., Hoyland,J., and Mason,W.T. (1996). Calcium homeostasis in intraerythrocytic malaria parasites. Eur. J. Cell Biol. *71*, 409-413.

Garcia,C.R.S. (1999). Calcium Homeostasis and Signaling in the Blood-stage Malaria Parasite. Parasitology Today *15*, 488-491.

Gardner,M.J., Shallom,S.J., Carlton,J.M., Salzberg,S.L., Nene,V., Shoaibi,A., Ciecko,A., Lynn,J., Rizzo,M., Weaver,B., Jarrahi,B., Brenner,M., Parvizi,B., Tallon,L., Moazzez,A., Granger,D., Fujii,C., Hansen,C., Pederson,J., Feldblyum,T., Peterson,J., Suh,B., Angiuoli,S., Pertea,M., Allen,J., Selengut,J., White,O., Cummings,L.M., Smith,H.O., Adams,M.D., Venter,J.C., Carucci,D.J., Hoffman,S.L., and Fraser,C.M. (2002). Sequence of Plasmodium falciparum chromosomes 2, 10, 11 and 14. Nature *419*, 531-534.

Gaur,D., Mayer,D.C., and Miller,L.H. (2004). Parasite ligand-host receptor interactions during invasion of erythrocytes by Plasmodium merozoites. Int. J. Parasitol. *34*, 1413-1429.

Gazarini,M.L., Thomas,A.P., Pozzan,T., and Garcia,C.R.S. (2003). Calcium signaling in a low calcium environment: how the intracellular malaria parasite solves the problem. J. Cell Biol. *161*, 103-110.

Gehrmann,T. and Heilmeyer,L.M., Jr. (1998). Phosphatidylinositol 4-kinases. Eur. J. Biochem. *253*, 357-370.

Gilberger,T.W., Thompson,J.K., Triglia,T., Good,R.T., Duraisingh,M.T., and Cowman,A.F. (2003). A novel erythrocyte binding antigen-175 paralogue from Plasmodium falciparum defines a new trypsin-resistant receptor on human erythrocytes. J. Biol Chem. *278*, 14480-14486.

Gissot,M., Briquet,S., Refour,P., Boschet,C., and Vaquero,C. (2005). PfMyb1, a Plasmodium falciparum transcription factor, is required for intra-erythrocytic growth and controls key genes for cell cycle regulation. J Mol Biol *346*, 29-42.

Green,J.L., Martin,S.R., Fielden,J., Ksagoni,A., Grainger,M., Yim Lim,B.Y.S., Molloy,J.E., and Holder,A.A. (2006). The MTIP-Myosin A Complex in Blood Stage Malaria Parasites. Journal of Molecular Biology *355*, 933-941.

Gschwendt,M., Dieterich,S., Rennecke,J., Kittstein,W., Mueller,H.J., and Johannes,F.J. (1996). Inhibition of protein kinase C mu by various inhibitors. Differentiation from protein kinase c isoenzymes. FEBS Lett. *392*, 77-80.

Han,E.K.H., Leverson,J.D., McGonigal,T., Shah,O.J., Woods,K.W., Hunter,T., Giranda,V.L., and Luo,Y. (2007). Akt inhibitor A-443654 induces rapid Akt Ser-473 phosphorylation independent of mTORC1 inhibition. Oncogene.

Hanks,S.K. and Hunter,T. (1995a). Protein kinases 6. The eukaryotic protein kinase superfamily: kinase (catalytic) domain structure and classification. FASEB J. *9*, 576-596.

Hanks,S.K. and Hunter,T. (1995b). Protein kinases 6. The eukaryotic protein kinase superfamily: kinase (catalytic) domain structure and classification. FASEB J *9*, 576-596.

Hannon,G.J. (2002). RNA interference. Nature *418*, 244-251.

Hoeflich,K.P. and Ikura,M. (2002). Calmodulin in action: diversity in target recognition and activation mechanisms. Cell *108*, 739-742.

Hondal,R.J., Zhao,Z., Kravchuk,A.V., Liao,H., Riddle,S.R., Yue,X., Bruzik,K.S., and Tsai,M.D. (1998). Mechanism of phosphatidylinositol-specific phospholipase C: a unified view of the mechanism of catalysis. Biochemistry *37*, 4568-4580.

Hotta,C.T., Markus,R.P., and Garcia,C.R. (2003). Melatonin and N-acetyl-serotonin cross the red blood cell membrane and evoke calcium mobilization in malarial parasites. Braz. J. Med. Biol. Res. *36*, 1583-1587.

Hotta,C.T., Gazarini,M.L., Beraldo,F.H., Varotti,F.P., Lopes,C., Markus,R.P., Pozzan,T., and Garcia,C.R.S. (2000). Calcium-dependent modulation by melatonin of the circadian rhythm in malarial parasites. Nat Cell Biol *2*, 466-468.

Hunter,T. (1987). A thousand and one protein kinases. Cell *50*, 823-829.

Inselburg,J. (1983). Gametocyte formation by the progeny of single Plasmodium falciparum schizonts. J Parasitol. *69*, 584-591.

Jacinto,E., Facchinetti,V., Liu,D., Soto,N., Wei,S., Jung,S.Y., Huang,Q., Qin,J., and Su,B. (2006). SIN1/MIP1 Maintains rictor-mTOR Complex Integrity and Regulates Akt Phosphorylation and Substrate Specificity. Cell *127*, 125-137.

Janse,C.J., van der Klooster,P.F., van der Kaay,H.J., van der,P.M., and Overdulve,J.P. (1986). DNA synthesis in Plasmodium berghei during asexual and sexual development. Mol Biochem Parasitol. *20*, 173-182.

Johnson,L.N., Noble,M.E., and Owen,D.J. (1996). Active and inactive protein kinases: structural basis for regulation. Cell *85*, 149-158.

Jones,M.L., Kitson,E.L., and Rayner,J.C. (2006). Plasmodium falciparum erythrocyte invasion: A conserved myosin associated complex. Molecular and Biochemical Parasitology *147*, 74-84.

Jones,P.F., Jakubowicz,T., and Hemmings,B.A. (1991). Molecular cloning of a second form of rac protein kinase. Cell Regul. *2*, 1001-1009.

Kaneko,O., Mu,J., Tsuboi,T., Su,X., and Torii,M. (2002). Gene structure and expression of a Plasmodium falciparum 220-kDa protein homologous to the Plasmodium vivax reticulocyte binding proteins. Mol Biochem. Parasitol. *121*, 275-278.

Kappe,S., Bruderer,T., Gantt,S., Fujioka,H., Nussenzweig,V., and Menard,R. (1999). Conservation of a gliding motility and cell invasion machinery in Apicomplexan parasites. J. Cell Biol *147*, 937-944.

Klemba,M., Beatty,W., Gluzman,I., and Goldberg,D.E. (2004). Trafficking of plasmepsin II to the food vacuole of the malaria parasite Plasmodium falciparum. J Cell Biol *164*, 47-56.

Konishi,H., Kuroda,S., Tanaka,M., Matsuzaki,H., Ono,Y., Kameyama,K., Haga,T., and Kikkawa,U. (1995). Molecular cloning and characterization of a new member of the RAC protein kinase family: association of the pleckstrin homology domain of three types of RAC protein kinase with protein kinase C subspecies and beta gamma subunits of G proteins. Biochem. Biophys. Res. Commun. *216*, 526-534.

Krauss,M. and Haucke,V. (2007). Phosphoinositides: Regulators of membrane traffic and protein function. FEBS Letters *581*, 2105-2111.

Kumar,A., Vaid,A., Syin,C., and Sharma,P. (2004). PfPKB, a Novel Protein Kinase B-like Enzyme from Plasmodium falciparum: I. IDENTIFICATION, CHARACTERIZATION, AND POSSIBLE ROLE IN PARASITE DEVELOPMENT. J. Biol. Chem. *279*, 24255-24264.

Kumar,R., Adams,B., Oldenburg,A., Musiyenko,A., and Barik,S. (2002). Characterisation and expression of a PP1 serine/threonine protein phosphatase (PfPP1) from the malaria parasite, Plasmodium falciparum: demonstration of its essential role using RNA interference. Malar. J *1*, 5.

Lambros,C. and Vanderberg,J.P. (1979). Synchronization of Plasmodium falciparum erythrocytic stages in culture. J Parasitol. *65*, 418-420.

Li,J., Yen,C., Liaw,D., Podsypanina,K., Bose,S., Wang,S.I., Puc,J., Miliaresis,C., Rodgers,L., McCombie,R., Bigner,S.H., Giovanella,B.C., Ittmann,M., Tycko,B., Hibshoosh,H., Wigler,M.H., and Parsons,R. (1997). PTEN, a putative protein tyrosine phosphatase gene mutated in human brain, breast, and prostate cancer. Science *275*, 1943-1947.

Lindberg,R.A., Quinn,A.M., and Hunter,T. (1992). Dual-specificity protein kinases: will any hydroxyl do? Trends Biochem. Sci *17*, 114-119.

Luo,Y., Shoemaker,A.R., Liu,X., Woods,K.W., Thomas,S.A., de Jong,R., Han,E.K., Li,T., Stoll,V.S., Powlas,J.A., Oleksijew,A., Mitten,M.J., Shi,Y., Guan,R., McGonigal,T.P., Klinghofer,V., Johnson,E.F., Leverson,J.D., Bouska,J.J., Mamo,M., Smith,R.A., Gramling-Evans,E.E., Zinker,B.A., Mika,A.K., Nguyen,P.T., Oltersdorf,T., Rosenberg,S.H., Li,Q., and Giranda,V.L. (2005). Potent and selective inhibitors of Akt kinases slow the progress of tumors in vivo. Mol Cancer Ther *4*, 977-986.

Maier,A.G., Duraisingh,M.T., Reeder,J.C., Patel,S.S., Kazura,J.W., Zimmerman,P.A., and Cowman,A.F. (2003). Plasmodium falciparum erythrocyte invasion through glycophorin C and selection for Gerbich negativity in human populations. Nat Med. *9*, 87-92.

Malhotra,P., Dasaradhi,P.V., Kumar,A., Mohmmed,A., Agrawal,N., Bhatnagar,R.K., and Chauhan,V.S. (2002). Double-stranded RNA-mediated gene silencing of cysteine proteases (falcipain-1 and -2) of Plasmodium falciparum. Mol Microbiol. *45*, 1245-1254.

Manning,G., Whyte,D.B., Martinez,R., Hunter,T., and Sudarsanam,S. (2002). The protein kinase complement of the human genome. Science *298*, 1912-1934.

Marte,B.M. and Downward,J. (1997). PKB/Akt: connecting phosphoinositide 3-kinase to cell survival and beyond. Trends Biochem. Sci *22*, 355-358.

Matsumoto,Y., Perry,G., Scheibel,L.W., and Aikawa,M. (1987). Role of calmodulin in Plasmodium falciparum: implications for erythrocyte invasion by the merozoite. Eur. J Cell Biol *45*, 36-43.

Mayer,D.C., Kaneko,O., Hudson-Taylor,D.E., Reid,M.E., and Miller,L.H. (2001). Characterization of a Plasmodium falciparum erythrocyte-binding protein paralogous to EBA-175. Proc. Natl. Acad. Sci. U. S. A *98*, 5222-5227.

McCallum-Deighton,N. and Holder,A.A. (1992). The role of calcium in the invasion of human erythrocytes by Plasmodium falciparum. Mol. Biochem. Parasitol. *50*, 317-323.

McRobert,L. and McConkey,G.A. (2002). RNA interference (RNAi) inhibits growth of Plasmodium falciparum. Mol Biochem Parasitol. *119*, 273-278.

Menard,R. (2001). Gliding motility and cell invasion by Apicomplexa: insights from the Plasmodium sporozoite. Cell Microbiol. *3*, 63-73.

Menard,R., Sultan,A.A., Cortes,C., Altszuler,R., van Dijk,M.R., Janse,C.J., Waters,A.P., Nussenzweig,R.S., and Nussenzweig,V. (1997). Circumsporozoite protein is required for development of malaria sporozoites in mosquitoes. Nature *385*, 336-340.

Milhavet,O., Gary,D.S., and Mattson,M.P. (2003). RNA interference in biology and medicine. Pharmacol. Rev. *55*, 629-648.

Misra,S. and Hurley,J.H. (1999). Crystal structure of a phosphatidylinositol 3-phosphate-specific membrane-targeting motif, the FYVE domain of Vps27p. Cell *97*, 657-666.

Mitchell,G.H. and Bannister,L.H. (1988). Malaria parasite invasion: interactions with the red cell membrane. Crit Rev. Oncol. Hematol. *8*, 225-310.

Mitchell,G.H., Thomas,A.W., Margos,G., Dluzewski,A.R., and Bannister,L.H. (2004). Apical membrane antigen 1, a major malaria vaccine candidate, mediates the close attachment of invasive merozoites to host red blood cells. Infect. Immun. *72*, 154-158.

Mohrle,J.J., Zhao,Y., Wernli,B., Franklin,R.M., and Kappes,B. (1997). Molecular cloning, characterization and localization of PfPK4, an eIF-2alpha kinase-related enzyme from the malarial parasite Plasmodium falciparum. Biochem J *328 (Pt 2)*, 677-687.

Morrissette,N.S. and Sibley,L.D. (2002). Cytoskeleton of apicomplexan parasites. Microbiol. Mol Biol Rev. *66*, 21-38.

Obata,T., Yaffe,M.B., Leparc,G.G., Piro,E.T., Maegawa,H., Kashiwagi,A., Kikkawa,R., and Cantley,L.C. (2000). Peptide and protein library screening defines optimal substrate motifs for AKT/PKB. J Biol Chem. *275*, 36108-36115.

Odorizzi,G., Babst,M., and Emr,S.D. (2000). Phosphoinositide signaling and the regulation of membrane trafficking in yeast. Trends Biochem. Sci. *25*, 229-235.

Parekh,D.B., Ziegler,W., and Parker,P.J. (2000). Multiple pathways control protein kinase C phosphorylation. EMBO J. *19*, 496-503.

Parsons,R. (2004). Human cancer, PTEN and the PI-3 kinase pathway. Semin. Cell Dev. Biol *15*, 171-176.

Pascuccelli,V., Labriola,C., Tellez-Inon,M.T., and Parodi,A.J. (1999). Molecular and biochemical characterization of a protein kinase B from Trypanosoma cruzi. Mol Biochem Parasitol. *102*, 21-33.

Pinder,J.C., Fowler,R.E., Dluzewski,A.R., Bannister,L.H., Lavin,F.M., Mitchell,G.H., Wilson,R.J., and Gratzer,W.B. (1998). Actomyosin motor in the merozoite of the malaria parasite, Plasmodium falciparum: implications for red cell invasion. J. Cell Sci. *111 (Pt 13)*, 1831-1839.

Rameh,L.E., Tolias,K.F., Duckworth,B.C., and Cantley,L.C. (1997). A new pathway for synthesis of phosphatidylinositol-4,5-bisphosphate. Nature *390*, 192-196.

Rees-Channer,R.R., Martin,S.R., Green,J.L., Bowyer,P.W., Grainger,M., Molloy,J.E., and Holder,A.A. (2006). Dual acylation of the 45 kDa gliding-associated protein (GAP45) in Plasmodium falciparum merozoites. Molecular and Biochemical Parasitology *149*, 113-116.

Rhee,S.G., Suh,P.G., Ryu,S.H., and Lee,S.Y. (1989). Studies of inositol phospholipid-specific phospholipase C. Science *244*, 546-550.

Rhoads,A.R. and Friedberg,F. (1997). Sequence motifs for calmodulin recognition. FASEB J. *11*, 331-340.

Robson,K.J., Gamble,Y., and Acharya,K.R. (1993). Molecular modelling of malaria calmodulin suggests that it is not a suitable target for novel antimalarials. Philos. Trans. R. Soc. Lond B Biol Sci *340*, 39-53.

Robson,K.J., Hall,J.R., Jennings,M.W., Harris,T.J., Marsh,K., Newbold,C.I., Tate,V.E., and Weatherall,D.J. (1988). A highly conserved amino-acid sequence in thrombospondin, properdin and in proteins from sporozoites and blood stages of a human malaria parasite. Nature *335*, 79-82.

Rojas,M.O. and Wasserman,M. (1995). State-Specific Expressions of the Calmodulin Gene in Plasmodium falciparum. J Biochem (Tokyo) *118*, 1118-1123.

Sanders,P.R., Gilson,P.R., Cantin,G.T., Greenbaum,D.C., Nebl,T., Carucci,D.J., McConville,M.J., Schofield,L., Hodder,A.N., Yates,J.R., III, and Crabb,B.S. (2005). Distinct protein classes including novel merozoite surface antigens in Raft-like membranes of Plasmodium falciparum. J. Biol Chem. *280*, 40169-40176.

Scheibel,L.W., Colombani,P.M., Hess,A.D., Aikawa,M., Atkinson,C.T., and Milhous,W.K. (1987). Calcium and calmodulin antagonists inhibit human malaria parasites (Plasmodium falciparum): implications for drug design. Proc. Natl. Acad. Sci. U. S. A *84*, 7310-7314.

Scheid,M.P. and Woodgett,J.R. (2003). Unravelling the activation mechanisms of protein kinase B/Akt. FEBS Lett. *546*, 108-112.

Sim,B.K., Chitnis,C.E., Wasniowska,K., Hadley,T.J., and Miller,L.H. (1994). Receptor and ligand domains for invasion of erythrocytes by Plasmodium falciparum. Science *264*, 1941-1944.

Soldati,D. and Meissner,M. (2004). Toxoplasma as a novel system for motility. Curr. Opin. Cell Biol *16*, 32-40.

Soldati,D., Foth,B.J., and Cowman,A.F. (2004). Molecular and functional aspects of parasite invasion. Trends in Parasitology *20*, 567-574.

Staal,S.P. (1987). Molecular cloning of the akt oncogene and its human homologues AKT1 and AKT2: amplification of AKT1 in a primary human gastric adenocarcinoma. Proc. Natl. Acad. Sci. U. S. A *84*, 5034-5037.

Staal,S.P., Hartley,J.W., and Rowe,W.P. (1977). Isolation of transforming murine leukemia viruses from mice with a high incidence of spontaneous lymphoma. Proc. Natl. Acad. Sci. U. S. A *74*, 3065-3067.

Stambolic,V., Suzuki,A., de la Pompa,J.L., Brothers,G.M., Mirtsos,C., Sasaki,T., Ruland,J., Penninger,J.M., Siderovski,D.P., and Mak,T.W. (1998). Negative regulation of PKB/Akt-dependent cell survival by the tumor suppressor PTEN. Cell *95*, 29-39.

Steck,P.A., Pershouse,M.A., Jasser,S.A., Yung,W.K., Lin,H., Ligon,A.H., Langford,L.A., Baumgard,M.L., Hattier,T., Davis,T., Frye,C., Hu,R., Swedlund,B., Teng,D.H., and Tavtigian,S.V. (1997). Identification of a candidate tumour suppressor gene, MMAC1, at chromosome 10q23.3 that is mutated in multiple advanced cancers. Nat Genet. *15*, 356-362.

Stenmark,H., Aasland,R., and Driscoll,P.C. (2002). The phosphatidylinositol 3-phosphate-binding FYVE finger. FEBS Letters *513*, 77-84.

Sultan,A.A., Thathy,V., Frevert,U., Robson,K.J., Crisanti,A., Nussenzweig,V., Nussenzweig,R.S., and Menard,R. (1997). TRAP is necessary for gliding motility and infectivity of plasmodium sporozoites. Cell *90*, 511-522.

Sun,X.T., Li,B., Zhou,G.M., Tang,W.Q., Bai,J., Sun,D.Y., and Zhou,R.G. (2000). Binding of the maize cytosolic Hsp70 to calmodulin, and identification of calmodulin-binding site in Hsp70. Plant Cell Physiol *41*, 804-810.

Syin,C., Parzy,D., Traincard,F., Boccaccio,I., Joshi,M.B., Lin,D.T., Yang,X.M., Assemat,K., Doerig,C., and Langsley,G. (2001a). The H89 cAMP-dependent protein kinase inhibitor blocks Plasmodium falciparum development in infected erythrocytes. Eur. J. Biochem. *268*, 4842-4849.

Syin,C., Parzy,D., Traincard,F., Boccaccio,I., Joshi,M.B., Lin,D.T., Yang,X.M., Assemat,K., Doerig,C., and Langsley,G. (2001b). The H89 cAMP-dependent protein kinase inhibitor blocks Plasmodium falciparum development in infected erythrocytes. Eur. J. Biochem. *268*, 4842-4849.

T.Sasaki, A.Suzuki, J.Sasaki, and J.M.Penninger. Phosphoinositide 3-Kinases in Immunity: Lessons from Knockout Mice. The Journal of Biochemistry 131[4], 495-501. 2002.
Ref Type: Generic

Tanabe,K., Izumo,A., Kato,M., Miki,A., and Doi,S. (1989). Stage-dependent inhibition of Plasmodium falciparum by potent Ca2+ and calmodulin modulators. J Protozool. *36*, 139-143.

Taniguchi,C.M., Emanuelli,B., and Kahn,C.R. (2006). Critical nodes in signalling pathways: insights into insulin action. Nat Rev. Mol Cell Biol *7*, 85-96.

Thompson,J.K., Triglia,T., Reed,M.B., and Cowman,A.F. (2001). A novel ligand from Plasmodium falciparum that binds to a sialic acid-containing receptor on the surface of human erythrocytes. Mol Microbiol. *41*, 47-58.

Thong,F.S., Dugani,C.B., and Klip,A. (2005). Turning signals on and off: GLUT4 traffic in the insulin-signaling highway. Physiology. (Bethesda.) *20*, 271-284.

Toda,T., Cameron,S., Sass,P., and Wigler,M. (1988). SCH9, a gene of Saccharomyces cerevisiae that encodes a protein distinct from, but functionally and structurally related to, cAMP-dependent protein kinase catalytic subunits. Genes Dev. *2*, 517-527.

Toker,A. (1998). The synthesis and cellular roles of phosphatidylinositol 4,5-bisphosphate. Curr. Opin. Cell Biol *10*, 254-261.

Trager,W. and Jensen,J.B. (1976). Human malaria parasites in continuous culture. Science *193*, 673-675.

Tschopp,O., Yang,Z.Z., Brodbeck,D., Dummler,B.A., Hemmings-Mieszczak,M., Watanabe,T., Michaelis,T., Frahm,J., and Hemmings,B.A. (2005). Essential role of protein kinase B gamma (PKB gamma/Akt3) in postnatal brain development but not in glucose homeostasis. Development *132*, 2943-2954.

Ullu,E., Tschudi,C., and Chakraborty,T. (2004). RNA interference in protozoan parasites. Cell Microbiol. *6*, 509-519.

Vanhaesebroeck,B. and Alessi,D.R. (2000). The PI3K-PDK1 connection: more than just a road to PKB. Biochem J *346 Pt 3*, 561-576.

Vanhaesebroeck,B., Leevers,S.J., Panayotou,G., and Waterfield,M.D. (1997). Phosphoinositide 3-kinases: a conserved family of signal transducers. Trends Biochem. Sci. *22*, 267-272.

Vanhaesebroeck,B., Leevers,S.J., Ahmadi,K., Timms,J., Katso,R., Driscoll,P.C., Woscholski,R., Parker,P.J., and Waterfield,M.D. (2001). SYNTHESIS AND FUNCTION OF 3-PHOSPHORYLATED INOSITOL LIPIDS. Annual Review of Biochemistry *70*, 535-602.

Ward,P., Equinet,L., Packer,J., and Doerig,C. (2004). Protein kinases of the human malaria parasite Plasmodium falciparum: the kinome of a divergent eukaryote. BMC. Genomics *5*, 79.

Wasserman,M. (1990). The role of calcium ions in the invasion of Plasmodium falciparum. Blood Cells *16*, 450-451.

Woodgett,J.R. (2005). Recent advances in the protein kinase B signaling pathway. Curr. Opin. Cell Biol *17*, 150-157.

Yamauchi,E., Nakatsu,T., Matsubara,M., Kato,H., and Taniguchi,H. (2003). Crystal structure of a MARCKS peptide containing the calmodulin-binding domain in complex with Ca2+-calmodulin. Nat Struct. Biol *10*, 226-231.

Yang,J., Cron,P., Good,V.M., Thompson,V., Hemmings,B.A., and Barford,D. (2002a). Crystal structure of an activated Akt/protein kinase B ternary complex with GSK3-peptide and AMP-PNP. Nat Struct. Biol *9*, 940-944.

Yang,J., Cron,P., Thompson,V., Good,V.M., Hess,D., Hemmings,B.A., and Barford,D. (2002b). Molecular Mechanism for the Regulation of Protein Kinase B/Akt by Hydrophobic Motif Phosphorylation. Molecular Cell *9*, 1227-1240.

Yoshida,N., Nussenzweig,R.S., Potocnjak,P., Nussenzweig,V., and Aikawa,M. (1980). Hybridoma produces protective antibodies directed against the sporozoite stage of malaria parasite. Science *207*, 71-73.

Yu,J.W. and Lemmon,M.A. (2003). Genome-wide analysis of signaling domain function. Curr. Opin. Chem. Biol *7*, 103-109.

Zhang,X., Loijens,J.C., Boronenkov,I.V., Parker,G.J., Norris,F.A., Chen,J., Thum,O., Prestwich,G.D., Majerus,P.W., and Anderson,R.A. (1997). Phosphatidylinositol-4-phosphate 5-kinase isozymes catalyze the synthesis of 3-phosphate-containing phosphatidylinositol signaling molecules. J. Biol Chem. *272*, 17756-17761.

THE JOURNAL OF BIOLOGICAL CHEMISTRY

Vol. 279, No. 23, Issue of June 4, pp. 24255–24264, 2004
Printed in U.S.A.

PfPKB, a Novel Protein Kinase B-like Enzyme from *Plasmodium falciparum*

I. IDENTIFICATION, CHARACTERIZATION, AND POSSIBLE ROLE IN PARASITE DEVELOPMENT*

Received for publication, November 25, 2003, and in revised form, March 8, 2004
Published, JBC Papers in Press, March 15, 2004, DOI 10.1074/jbc.M312855200

Amit Kumar‡, Ankush Vaid‡§, Chiang Syin¶, and Pushkar Sharma‖

From the Eukaryotic Gene Expression Laboratory, National Institute of Immunology, New Delhi 110067, India and ¶Center for Biologics Evaluation and Research, Food and Drug Administration, Rockville, Maryland 20852

Extracellular signals control various important functions of a eukaryotic cell, which is often achieved by regulating a battery of protein kinases and phosphatases. Protein Kinase B (PKB) is an important member of the phosphatidylinositol 3-kinase-dependent signaling pathways in several eukaryotes, but the role of PKB in protozoan parasites is not known. We have identified a protein kinase B homologue in *Plasmodium falciparum* (PfPKB) that is expressed mainly in the schizonts and merozoites. Even though PfPKB shares high sequence homology with PKB catalytic domain, it lacks a pleckstrin homology domain typically found at the N terminus of the mammalian enzyme. Biochemical studies performed to understand the mechanism of PfPKB catalytic activation suggested (i) its activation is dependent on autophosphorylation of a serine residue (Ser-271) in its activation loop region and (ii) PfPKB has an unusual N-terminal region that was found to negatively regulate its catalytic activity. We also identified an inhibitor of PfPKB activity that also inhibits *P. falciparum* growth, suggesting that this enzyme may be important for the development of the parasite.

Plasmodium falciparum, a unicellular protozoan responsible for the most lethal form of human malaria, has re-emerged as a leading cause of mortality in developing countries, especially in the population of young children age 5 and under. Widespread drug resistance exacerbates the problem and limits our options for effective malaria control. Current efforts to produce effective vaccines have not yet resulted in any significant success. Identification of drugs that interfere with parasite development could be a useful way to inhibit parasite growth in humans. Detailed knowledge of molecular mechanisms that control the life cycle of malaria parasite could provide crucial information needed to achieve this goal.

The life cycle of the malaria parasite is a complex but a well synchronized series of events. After invasion of the erythrocytes, the parasite can either propagate asexually or undergo sexual differentiation. The role of extracellular signals and molecular events in parasite life cycle are not well understood. It is well known that the fate of most eukaryotic cells is controlled by specific cell signaling pathways. Therefore, it is reasonable to assume that cell-signaling cascades may be very important for the development of *Plasmodium*. Systematic analysis of molecules involved in cell signaling events that occur during the course of *P. falciparum* development need to be pursued. A recently published genome sequence (1) and earlier studies suggest that several homologues of eukaryotic signaling proteins, such as protein kinases and phosphatases, are conserved in *P. falciparum* (2–13). The major challenge is to understand how these enzymes integrate in cellular machinery of *Plasmodium* and what roles they play in parasite development. The answer to these questions could lead to identification of important signaling pathways involved in the development of this parasite.

We are interested in understanding the role of phosphatidylinositol 3-kinase (PI3K)[1] and protein kinase B (PKB) in *P. falciparum*. The PI3K-PKB-mediated signaling is important for proliferation and survival of several eukaryotic cell types such as fibroblasts and neuronal cells (14). After PI3K activation, 3′-phosphorylated phosphoinositides (phosphatidylinositol 3,4-diphosphate or phosphatidylinositol 3,4,5-trisphosphate) are generated, and they bind to the PH domain present at the N terminus of PKB, resulting in its translocation to the cell surface and phosphorylation-dependent activation (15–17). This regulatory phosphorylation is carried out by phosphatidylinositol-dependent kinase 1 (PDK1), which also regulates other members of the AGC group of protein kinases like PKA and isoforms of PKC (18, 19). However, maximal catalytic activity is achieved only upon phosphorylation of a C-terminal site. PKB[2] targets a wide variety of cellular targets ranging from transcription factors, anti/pro-apoptotic proteins, enzymes involved in glycogen metabolism, etc. (15–17). Function of neither PI3K nor PKB in *Plasmodium* or any other protozoan parasite is understood.

* This work is supported by a Department of Biotechnology, Government of India core grant to the National Institute of Immunology and by a Wellcome Trust, UK, International Senior Research Fellowship (to P. S.). The costs of publication of this article were defrayed in part by the payment of page charges. This article must therefore be hereby marked "*advertisement*" in accordance with 18 U.S.C. Section 1734 solely to indicate this fact.

The nucleotide sequence(s) reported in this paper has been submitted to the GenBank™/EBI Data Bank with accession number(s) AY596821.

‡ These authors contributed equally to this work.

§ Supported by a Council for Scientific and Industrial Research, India, Junior Research Fellowship.

‖ To whom correspondence should be addressed. Tel.: 91-11-26717123 (ext. 491); Fax: 91-11-26162125; E-mail: pushkar@nii.res.in.

[1] The abbreviations used are: PI3K, phosphatidylinositol 3-kinase; PKA, cAMP-dependent protein kinase; PKB, protein kinase B; PKC, protein kinase C; PKG, cGMP-dependent kinase; PfPKB, *Plasmodium falciparum* homologue of protein kinase B; ΔPfPKB, catalytic domain of PfPKB with the C-terminal extension and without the N-terminal region; AGC kinases, a family of kinases belonging to the same class as protein kinase A, G, and C; BLAST, basic local alignment search tool; PH, Pleckstrin homology domain; PDK1, PI3-dependent kinase; GST, glutathione *S*-transferase; NTR, N-terminal region of PfPKB; PlasmoDB, sequence database of *Plasmodium*; MSP1, merozoite surface protein 1; ORF, open reading frame; contig, group of overlapping clones.

[2] PKB refers to mammalian PKB in general. For the purpose of sequence comparison and amino acid number assignment human PKBβ (accession number A46288) was used.

We report identification and biochemical characterization of a PKB homologue from *P. falciparum*, PfPKB. Although it shares significant homology with mammalian-PKB catalytic domain, PfPKB lacks a phosphoinositide interaction domain (PH domain). Biochemical studies suggested that PfPKB autophosphorylation is pivotal for its activation, unlike the mammalian enzyme, which needs phosphorylation by PDK1. PfPKB was expressed at highest levels during the schizont/merozoite stage of the parasite lifecycle. Studies using a pharmacological inhibitor suggested that PfPKB activity may be important for parasite development.

EXPERIMENTAL PROCEDURES

P. falciparum Cultures—P. falciparum 3D7 strain was cultured at 37 °C in RPMI 1640 medium using either AB^+ human serum or 10% Albumax II (Invitrogen) as previously described (20). Cultures were gassed with 7% CO_2, 5% O_2, and 88% N_2. Synchronization of the parasites in culture was achieved by sorbitol treatment (21).

Molecular Cloning and Mutagenesis of PfPKB cDNA—Human PKBβ sequence was used to BLAST search (in tBLASTN mode) the *Plasmodium* genome sequence at Sanger Center, The Institute of Genomic Research, and Stanford University (chromosome 12). A contig highly homologous to PKB was found on chromosome 12. The longest open reading frame (ORF) spanning this region was named PfPKB (described in detail under "Results"). PCR was performed using primers (sequences given below) based on the PfPKB ORF (Fig. 1). Total RNA was isolated from asynchronous *P. falciparum* 3D7 cultures, and reverse transcription was performed using random hexamers provided in the Thermoscript reverse transcription-PCR kit (Invitrogen). Complimentary or genomic DNA was used as the template in PCR reactions, which were performed using platinum *Taq* polymerase (Invitrogen) with the following cycling parameters: 94 °C for 2 min initial denaturation followed by 30 cycles at 94 °C for 30 s, 42 °C for 30 s, 72 °C for 2 min and final extension at 72 °C for 10 min. The following primer sets were used for cloning the full-length PfPKB gene (PfPKB_1 and PfPKB_3) and its catalytic domain, ΔPfPKB (PfPKB_2 and PfPKB_3): forward (PfPKB_1), 5′-ATGATCATATACATGTACCATATCTATGCCC-C-3′; forward, (PfPKB_2), 5′-CGTAACTCTATGTCCTTATCATATGAA-AGGAAA-3′; reverse, (PfPKB_3), 5′-TCATTTTTGTTGACCTGATTTT-TCTCATAATAGTTG-3′.

PCR products were cloned in pGEM-T easy vector (Promega), and several clones were sequenced by automated DNA sequencing. All site-directed mutagenesis studies were performed using the QuikChange kit (Stratagene) following the manufacturer's instructions and using primers 5′-GAAACCAATTTAACTAAAGCATTATGCGGAACTCC-3′ and 5′-GGGTTCCGCATAATGCTTTAGTTAAATTGGTCTT-3′ for mutant S271A, 5′-GAAACCATTTAACTAAAGACTTATGCGGAACTCC-3′ and 5′-GGAGTTCCGCATAAGTCTTTAGTTAAAATGGTTTC-3′ for mutant S271D, and 5′-AACTATTATGAATTTGACGGTCAACAAAAATGA-3′ and 5′-TCATTTTTGTTGACCGTCAAATTCATAATAGTT-3′ for the mutant S442D. Desired mutations were confirmed by automated DNA sequencing.

Expression and Purification of Recombinant PfPKB and Its Variants—PfPKB or ΔPfPKB was amplified using primers (described above) containing overhangs for BamHI and XhoI restriction enzymes to facilitate cloning into a GST fusion protein expression vector pGEX-4T1 (Amersham Biosciences). Recombinant expression vectors containing either the PfPKB gene or its variants were transformed in *Escherichia coli* BL21-RIL strain (Stratagene). Cultures were grown in LB media containing 100 μg/ml ampicillin and 25 μg/ml chloramphenicol. When cultures were in mid-logarithmic phase (A_{600} value of 0.6), expression of proteins was induced by 1 mM isopropyl-1-thio-β-D-galactopyranoside either at 37 °C for 4 h or at 18 °C for 14 h. Bacterial cells were harvested by centrifugation at 4000 × *g* for 30 min suspended in Buffer A (50 mM Tris, pH 7.4, 2 mM EDTA, 1 mM dithiothreitol, 1% Triton X-100, and protease inhibitor mixture (Roche Applied Science)) followed by sonication for 8 cycles of 1 min each on ice. Cell lysates were clarified by centrifugation at 20,000 × *g* for 30 min at 4 °C. Subsequently, the supernatant was incubated with glutathione-Sepharose resin (Amersham Biosciences) with end-to-end shaking for 6 h at 4 °C and was washed with Buffer A. The recombinant GST fusion proteins were eluted in 50 mM Tris, pH 8.0, containing 10 mM glutathione, dialyzed against 50 mM Tris, pH 7.5, 1 mM dithiothreitol, and 10% glycerol, concentrated using 10-kDa cutoff concentrator (Millipore), and analyzed by SDS-PAGE. Protein visualization and assessment were done on a gel documentation system. For expression of the N-terminal region (NTR) as a His_6-tagged or GST fusion protein, the region corresponding to NTR with additional catalytic domain residues (1–126) of PfPKB was amplified using primers 5′-GAAGTGAATTCGATGATCATATACATG-TAC-3′ and 5′-GGATTCCTCGAGTTTTCCATATGATCCTTC-3′, which possess overhangs for BamHI and XhoI, and was subsequently cloned in pET28 and pGEX4T1 vectors. BL21-RIL cells bearing recombinant plasmids were grown in LB medium containing either kanamycin (25 μg/ml) or ampicillin (100 μg/ml) and chloramphenicol (50 μg/ml). Protein expression was induced by treatment of bacterial cultures with 1 mM isopropyl-1-thio-β-D-galactopyranoside at 18 °C for 12 h. Recombinant His_6 NTR protein was extracted in denaturating extraction buffer (50 mM Tris, pH 7.4, 300 mM NaCl, and 8 M urea), and the clarified lysate was incubated with nickel nitrilotriacetic acid-agarose (Qiagen) with end-to-end shaking for 3 h at room temperature. The resin was poured into a column, washed with extraction buffer, and eluted in extraction buffer containing 25–500 mM imidazole. Fractions containing the protein of interest were pooled and dialyzed against buffers containing decreasing amounts of urea (25 mM Tris, pH 7.4, 150 mM NaCl, 1 mM dithiothreitol, 0–6 M urea) to refold the recombinant protein. GST-NTR was purified as described above for other GST fusion proteins. Recombinant proteins were estimated and analyzed by densitometry.

Assay of PfPKB Activity—GST fusion proteins of PfPKB (its deletions or its mutants) or 10 μl of PfPKB immunoprecipitated from parasite lysate (see below) were assayed for catalytic activity in a buffer containing 50 mM Tris, pH 7.5, 10 mM magnesium chloride, 1 mM dithiothreitol, and 100 μM [γ-^{32}P]ATP (6000 Ci/mmol) using histone H1, histone II_{AS}, or a small peptide substrate of PKB, "crosstide" (22), as phosphate-acceptor substrates. Typically, reactions were carried out for 20–60 min at 30 °C and were terminated by boiling the samples in SDS-PAGE sample buffer. Reaction mixtures were electrophoresed on 15% SDS-PAGE gel (for histone II_{AS}) followed by autoradiography to visualize phosphate incorporation in histone II_{AS}. In some experiments, GST-NTR (0.1 μg) and His_6-NTR (0.1 μg) were preincubated with ΔPfPKB (0.4 μg) before the addition of substrate and ATP.

When peptide substrates were used, reactions were stopped by spotting the samples on P81 phosphocellulose paper followed by washing the paper strips with 75 mM orthophosphoric acid. Phosphate incorporation was assessed by scintillation counting of P81 paper. One unit of enzyme activity represents 1 pmol of phosphate transferred to 1 mg of substrate in 1 min. Data representative of at least three independent experiments are illustrated in all figures.

Generation of anti-PfPKB Serum, Immunoblotting, Immunoprecipitation, and Immunofluorescence—Polyclonal anti-PfPKB serum was raised in rabbits using a synthetic peptide designed from the C-terminal sequence (DFNYNYYEFSGQQK). This peptide was conjugated to keyhole limpet hemocyanin via an additional N terminus cysteine residue (Zymed Laboratories Inc., Inc.)

Parasites were released from infected erythrocytes by 0.1% (w/v) saponin treatment. Cell-free protein extracts either from specific parasite stages or asynchronous cultures were prepared by suspending parasite pellets in a buffer containing 10 mM Tris pH 7.5, 100 mM NaCl, 5 mM EDTA, 1% Triton X-100, and 1× Complete Protease inhibitor mixture (Roche Applied Science) using a syringe and a needle. Lysates were cleared by centrifugation at 14,000 × *g* for 30 min. After separation of lysate proteins on SDS-PAGE gels, proteins were transferred to a nitrocellulose membrane. Immunoblotting was performed using the above-described anti-PfPKB antisera and horseradish peroxidase-labeled anti-rabbit IgG. ECL substrate (Pierce) was used to develop the blots following the manufacturer's instructions.

PfPKB was immunoprecipitated from the schizont-enriched parasite lysate using anti-PfPKB antisera. Erythrocyte-free parasite lysates were prepared as described above except phosphatase inhibitors (20 μM sodium fluoride, 20 μM β-glycerophosphate, and 100 μM sodium vanadate) were added to the lysis buffer. 100 μg of lysate were incubated with the anti-sera at 4 °C overnight on an end-to-end shaker. Subsequently, antigen-antibody complexes were incubated with 50 μl of protein A-Sepharose beads for 2 h with end-to-end shaking. Beads were washed with phosphate-buffered saline several times and were finally resuspended in 50 μl of 1× kinase assay buffer containing phosphatase inhibitors.

Immunofluorescence microscopy was performed on thin blood smears of parasite cultures that were fixed with methanol or acetone. Smears were blocked in phosphate-buffered saline containing 0.05% saponin and 5% bovine serum albumin. Subsequently, incubations with anti-PfPKB and/or anti-$MSP1_{1-19}$ anti-sera (1:100–1:200 dilution) were performed for 2 h at room temperature or at 4 °C overnight. Anti-mouse IgG labeled with fluorescein isothiocyanate and anti-rabbit IgG labeled

A)

*MIIYMYHIYAPFFHTFFLLTIFIIFLLN*YRNDVLFYGKGALKEIKKSMFDENKENAFYKDNMANCALNNMD

I II

NKNRMENECLYKYDEKEEIGKKRLRNSMSLSYERKKRIRPESFNYLKVIGEGSYGKVMLVKHVQNKKLYA

III IV V

MKILRKENILSRNQLEHTKVERNILKCVSHPFIVKMYYAFQTKQKLYFILEYCPGGELFFHLSKLREFSEETA

VIa VIb VII VIII

KFYSSEIILALEYLHDLNIIYRDLKPENVLLDELGHIRLTDFGLSKEGITETNLTKSLCGTPEYLAPEIIEQKGH

IX X XI

GKAVDWWSLGIMLYEMLTGELPFNNTNRNVLFESIKYQKLNYPKNLSPKAVDLLTKLFEKNPKKRLGSGG

TDAQEIKKHPFFKNINWNDVLYKKVKPPFKPKLFNQLDLQNFDKQFLNMPLKYSDQHENTNITFFADPKN

FVVQDFNYNYYEFSGQQK

B)

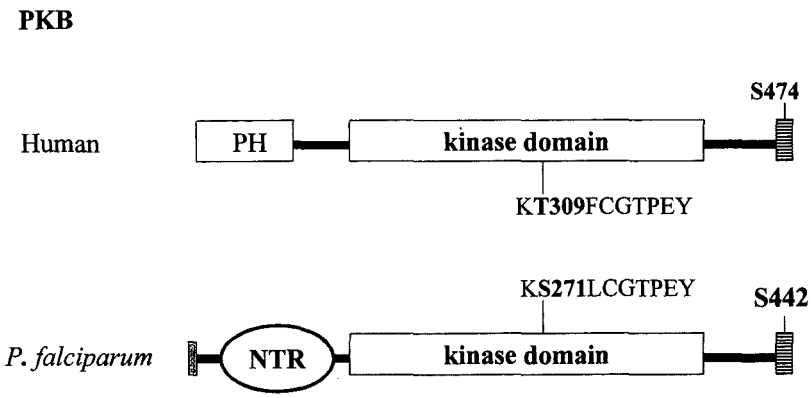

FIG. 1. *A*, amino acid sequence of PfPKB ORF. PfPKB was amplified using PCR primers corresponding to regions indicated by *arrows*. The catalytic domain of PfPKB (starting from the *second arrow*) has all the 11 kinase subdomains conserved. A putative regulatory phosphorylation site (Ser-271) in the activation loop region between subdomains VII and VIII is indicated in *bold*. A hydrophobic patch of amino acids at the C-terminal end is shown in *italics*, and another putative phosphorylation site (Ser-442) in this region is shown in ***bold face***. The putative N-terminal signal sequence is indicated in *italics*. *B*, schematic diagram showing a comparison between human PKB and PfPKB. PfPKB does not possess a PH domain, which is typically present at the N-terminal end of mammalian PKB. It has a putative N-terminal signal sequence (*gray bar*). The activation loop region of PKB contains Thr-309, which is phosphorylated by PDK1. Ser-271 in PfPKB aligns well with Thr-309 of PKB. The C-terminal hydrophobic motif with a putative regulatory phosphorylation site (Ser-442) is also shown.

with Texas Red were used to localize merozoite surface protein 1 (MSP1) and PfPKB, respectively. Parasite nuclei were localized with Hoechst 33342. Stained parasites were visualized using either a NikonTE2000 or a Zeiss confocal microscope. Images were analyzed and merged using Image Proplus or Adobe Photoshop software.

Inhibition of PfPKB Activity and Parasite Growth by Go 6983—Recombinant GST-ΔPfPKB was preincubated for 15 min with varying concentrations of Go 6983 or Go 6976 (Biomol or Calbiochem) prepared in 0.1% Me_2SO or with 0.1% Me_2SO. The enzyme activity was assayed as described above. To monitor the effect of Go 6983 on *P. falciparum* growth, parasites were plated at 1% parasitemia containing mostly rings and were treated either with the indicated concentrations of Go 6983 or 0.1% Me_2SO. At the indicated time points, thin films were prepared and stained with Giemsa reagent, and the number of intra-erythrocytic parasites was counted by using microscopic examination. Parasites were counted from several different fields and also different experiments. The data (Fig. 8) are represented as the ratio of percent of parasite-infected erythrocytes in drug-treated cultures to the ones in the control cultures, which were treated with 0.1% Me_2SO.

RESULTS

Identification and Molecular Cloning of the PfPKB Gene—To identify a PKB homologue in *P. falciparum*, human PKBβ sequence was used to search the *P. falciparum* genome sequence *in silico*. A match on chromosome 12 sequence data base with high sequence homology to the catalytic domain of human PKB (71%) was found. A long and uninterrupted 1.34-kilobase (encoding a polypeptide of 446 amino acids) ORF encompassing this region was designated as PfPKB. PfPKB belongs to the AGC kinase family, which possesses a motif with consensus sequence (S/T)(F/L)CGTP(D/E)Y in its activation loop region (Fig. 1, *A* and *B*). Phosphorylation of S/T (at the first position in this sequence) is pivotal for their activation (19). In addition, PfPKB has a hydrophobic patch of amino acids at its C-terminal end (Fig. 1) that is also present at the C-terminal end of several AGC kinases, although its sequence is only loosely conserved (23). While these studies were in progress, annotation of the *Plasmodium* genome appeared on PlasmoDB (24, 25). BLAST searches of these annotated genes resulted in three major "hits" (Tables I and II). All three protein sequences were related to AGC class kinases. The gene with highest sequence homology was closely related to PfPKB. The other two kinase sequences with around 56% homology to the catalytic domain of PKB have previously been identified as the cAMP-dependent protein kinase (13) and the cGMP-dependent kinase (5) homologues from *P. falciparum*.

PfPKB ORF was amplified using either cDNA or genomic

TABLE I
Summary of the results of a BLAST search of P. falciparum-predicted gene database using human PKBβ sequence as a query

Plasmodium gene	Homology[a]	Experimental identification
	%	
Ch12.glm521	71	*PfPKB* (this work)
Ch9.glm401	56	*PfPKA* (9, 13)
Ch14.glm391	56	*PfPKG* (5)

[a] % Homology represents the percent similarity in amino acids that are identical and belong to a similar chemical class. It is indicated as % similarity in the output of the BLAST program.

TABLE II
Homology between PfPKB and other mammalian AGC kinases

Kinase	Homology[a]
	%
PKB	71
PKCα, -β, -γ	64
cAMP-dependent protein kinase	58
cGMP-dependent protein kinase	53

[a] Results of a BLAST search reflect homology mainly between the catalytic domains of PfPKB and the indicated kinases.

DNA as template, and the amplified PCR products appeared to be identical in size (data not shown). This suggested that PfPKB is at least 1.34 kb in size and introns are absent from this contig, which was confirmed by DNA sequencing. The deduced PfPKB sequence (Fig. 1*A*) shows that it has all kinase subdomains (26) and has a hydrophobic motif at the C terminus present in several AGC class kinases (23). It also has a putative signal sequence at its N-terminal end. Interestingly, PfPKB shares high sequence homology with catalytic domains of PKC isoforms α, β, γ, (~64%, Tables I and II). It should be noted that a PKC homologue has not yet been identified in the *Plasmodium* genome. Our *in silico* analysis suggested that PfPKB may be the closest relative of PKC in *P. falciparum*. Strikingly, PfPKB does not contain a PH domain usually found in PKB of higher eukaryotes. This domain is important for binding to phosphoinositides phosphorylated at 3′-OH (15–17). Because yeast and *Trypanosoma cruzi* homologues of PKB also lack this domain (27–29), it is possible that PKB in these organisms is regulated via different mechanisms other than interactions with 3′-phosphoinositides. During the process of screening for full-length PfPKB, we found clones containing intronic sequences that could result in different-size ORF. This could be a result of alternative splicing or defects in transcripts.

Recombinant PfPKB Catalytic Domain (ΔPfPKB) Is Active—To get insight into the catalytic mechanism of PfPKB, the catalytic domain of this enzyme with the C-terminal extension (ΔPfPKB, indicated in Fig. 1*A*) was expressed as a GST fusion protein in *E. coli* (Fig. 2*A*). Catalytic activity of recombinant ΔPfPKB was assayed using histone II_{AS} and histone H1 as substrates of this enzyme. GST-ΔPfPKB phosphorylated histone II_{AS} (Fig. 2*B*) and H1 (data not shown). It has been observed that AGC protein kinases (PKA, PKC, PKB, PKG) prefer basic residues in the vicinity of the target phosphorylation sites (30). Crosstide, a peptide with sequence GRPRTSSFAEG that has been shown to be a good substrate for PKB (22), was phosphorylated by ΔPfPKB (K_m ~ 20 μM) (Fig. 2*C*). ΔPfPKB also phosphorylated a myelin basic protein-derived peptide (QKRPSQRSKYL) but with 2-fold less efficiency (data not shown here). Because the difference in these peptides was in the location of the basic residues corresponding to the phosphorylatable serine residues, it reflects the preference of PfPKB for basic residues at appropriate position in its substrates.

PfPKB May Be Regulated by Autophosphorylation of Ser-271 and Additional Phosphorylation of Ser-442—PKB is catalytically activated by phosphorylation of activation loop at Thr-309 by PDK1 (18, 23, 31), and deletion of the N-terminal PH domain of PKB results neither in its catalytic activation nor in autophosphorylation; it requires phosphorylation by PDK1 to be active (32). In contrast, catalytic activity of recombinant ΔPfPKB was observed in the absence of any exogenous kinase (Fig. 2, *B* and *C*). Instead, it exhibited autophosphorylation (Fig. 2*D*, *lane 1*). These data suggest that autophosphorylation may be responsible for regulating PfPKB catalytic activity.

Thr-309 phosphorylation in PKB results in conformational changes crucial for its catalysis (15, 23, 31). Because Ser-271 in PfPKB is complementary to Thr-309, it may be in a similar strategic location in the kinase catalytic core (Fig. 1*B*) and may play a role in PfPKB activation. To test this, Ser-271 of PfPKB was replaced by alanine, and the effect on its catalytic activity was assessed. Mutation of this serine to alanine resulted in almost a complete loss of ΔPfPKB activity as the S271A mutant failed to phosphorylate either histone (Fig. 3A) or crosstide (Fig. 3*B*). Moreover, this mutation resulted in a concomitant loss in autophosphorylation of ΔPfPKB (Fig. 3*C*). It has been observed that replacement of Ser/Thr residues by negatively charged aspartate (Asp) or glutamate (Glu) could mimic their phosphorylated state. Replacement of S271A to S271D resulted in a significant recovery of ΔPfPKB activity, which was lost due to the S271A mutation (Fig. 3, *A* and *B*). Collectively, these data suggest that autophosphorylation of Ser-271 is a prerequisite for PfPKB activation. A ΔPfPKB mutant defective in ATP binding was generated by replacing a crucial lysine residue, which is conserved in all protein kinases, to methionine. It neither exhibited detectable autophosphorylation nor kinase activity, confirming that PfPKB autophosphorylation is responsible for its activity (data not shown).

PKB and other mammalian AGC family protein kinases share several other functional similarities such as dependence on additional phosphorylation of their C-terminal end to achieve maximal activity (17). This phosphorylation site (Ser-474 in PKB) is usually part of a loosely conserved hydrophobic motif with the sequence FXF(S/T)Y (23). PKA has a negatively charged residue (Asp or Glu) at this position, which complements the function of phosphorylated Ser or Thr (23). PfPKB contains a hydrophobic motif (YYEFSG) at its C terminus (Fig. 1). Ser-442 in this region was replaced by aspartic acid in addition to the above-described S271D mutation to mimic phosphorylation at this position. The double mutant (S271D, S442D) exhibited catalytic activity even higher than that of single mutant, S271D (Fig. 4). These data suggest that acidic environment provided by phosphorylation at this site may be important for maximal activation of PfPKB, an observation consistent with mammalian PKB.

NTR of PfPKB Negatively Regulates Its Activity—A BLAST search using the NTR amino acid sequence did not show any significant sequence homology with proteins in the nonredundant protein data base. To study the effect of N-terminal region (NTR) on the activity of PfPKB, full-length PfPKB (containing both the N-terminal region and the catalytic domain) was expressed, and its catalytic activity was compared with that of ΔPfPKB. PfPKB exhibited only marginal catalytic activity in comparison to its NTR deleted version, ΔPfPKB (Fig. 5, *A* and *B*). In addition, PfPKB also lacked detectable autophosphorylation activity (Fig. 5*C*). Collectively, these observations suggest that NTR may modulate PfPKB activity by preventing its autophosphorylation, thus preventing its catalytic activation. To determine if NTR directly causes PfPKB inhibition, it was expressed as a GST fusion or a His_6-tagged protein. When recombinant NTR was incubated in a kinase assay mix with ΔPfPKB, its activity (Fig. 5*D*) as well as its autophosphoryla-

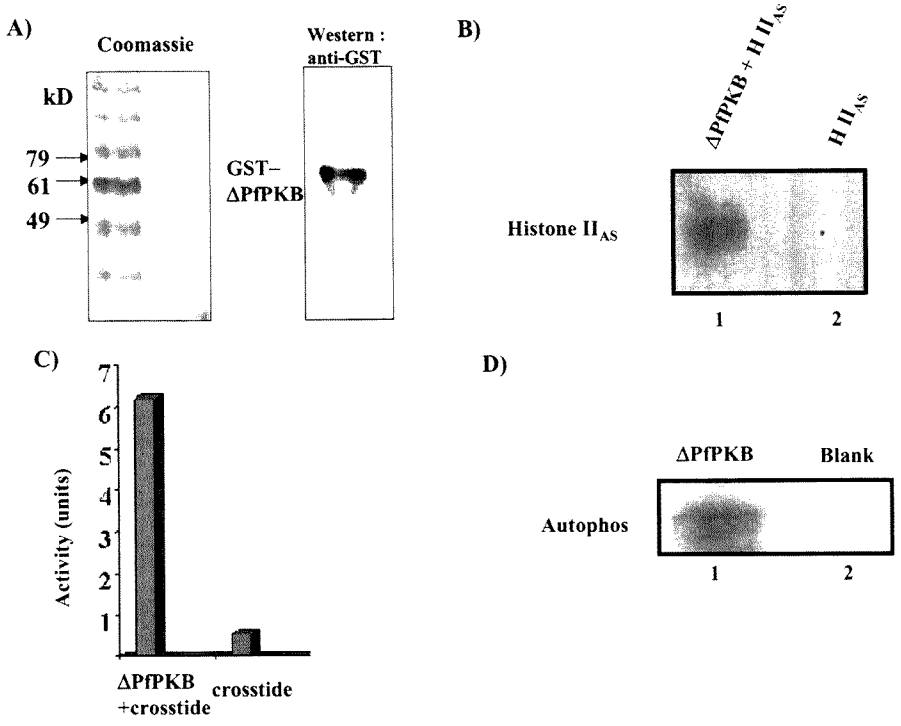

FIG. 2. **Expression of PfPKB catalytic domain and its catalytic activity.** *A*, purified GST-ΔPFPKB, the recombinant PfPKB catalytic domain expressed as a GST fusion protein in *E. coli*, was confirmed by Western blot using anti-GST antibody. *B*, GST-ΔPfPKB phosphorylated histone II$_{AS}$. *C*, a small peptide, crosstide. *D*, GST-ΔPfPKB was incubated in a kinase assay mix without any substrate to assess its autophosphorylation. Phosphate incorporation was monitored by autoradiography (*B* and *D*) or by scintillation counting (*C*).

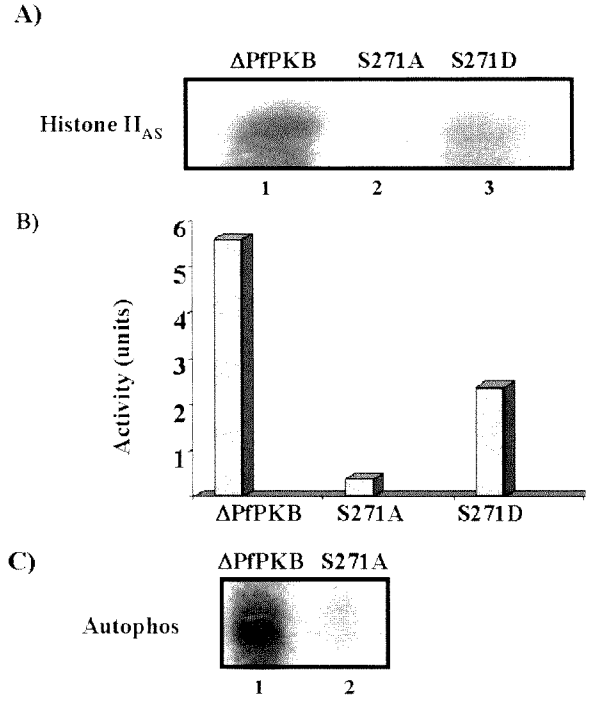

FIG. 3. **PfPKB activity is regulated by autophosphorylation of Ser-271.** The putative phosphorylation site, Ser-271, was either mutated to alanine (S271A) or to aspartate (S271D) in the ΔPfPKB expression plasmid to produce specific recombinant proteins. ΔPfPKB (*lane 1*), S271A (*lane 2*), and S271D (*lane 3*) recombinant proteins were incubated with either histone II$_{AS}$ (*A*) or crosstide (*B*) in a kinase assay mix. In some experiments no exogenous substrate was added to compare autophosphorylation level of ΔPfPKB and S271A (*C*).

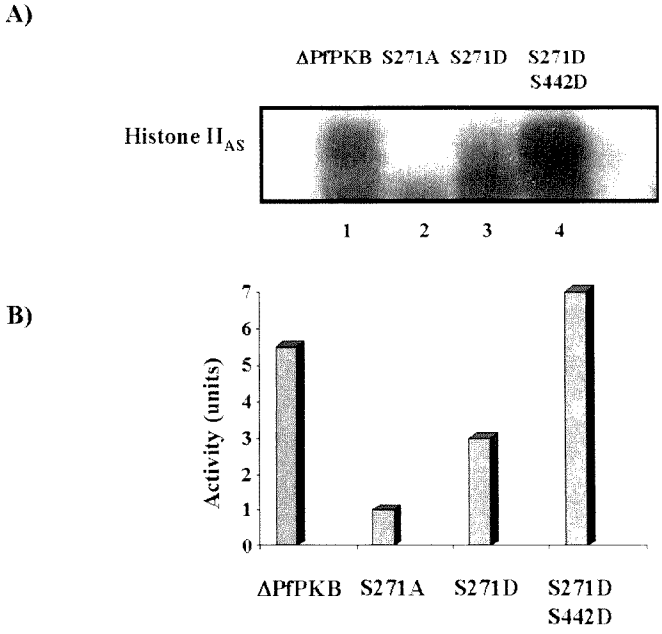

FIG. 4. **Additional phosphorylation of Ser-442 could result in enhancement of PfPKB activity.** Ser-442 was replaced by Asp (in addition to the S271D mutation) to generate a double mutant (S271D,S442D) of ΔPfPKB. The indicated recombinant proteins were used to phosphorylate histone II$_{AS}$ (*A*) or crosstide (*B*), and the phosphorylation state of these substrates was monitored as described above

tion (Fig. 5*E*) was inhibited dramatically. Interaction of NTR with the catalytic region of PfPKB may either cause conformational changes unfavorable for catalysis and/or it may restrict entry of the peptide substrate in the catalytic cleft of the enzyme, resulting in its inability to perform efficient catalysis.

Because the data illustrated in Fig. 3 indicate that phosphorylation of Ser-271 (or its mutation to D) activates ΔPfPKB, it was worth testing the effect of S271D mutation on activation of full-length PfPKB. S271D mutant exhibited catalytic activity higher than that of PfPKB (Fig. 5*F*), suggesting that conformational changes due to phosphorylation-mimicking mutation of Ser-271 to Asp could result in an increase in activity of full length PfPKB. Collectively, the results described above indicate that NTR may prevent the activation of PfPKB by inhibiting its ability to autophosphorylate.

PfPKB Is Expressed in Schizonts and Merozoites—Western blotting, immunofluorescence, and reverse transcription-PCR techniques were used to examine the expression pattern of PfPKB during *P. falciparum* blood stage development. For this purpose, polyclonal antisera were raised against a synthetic

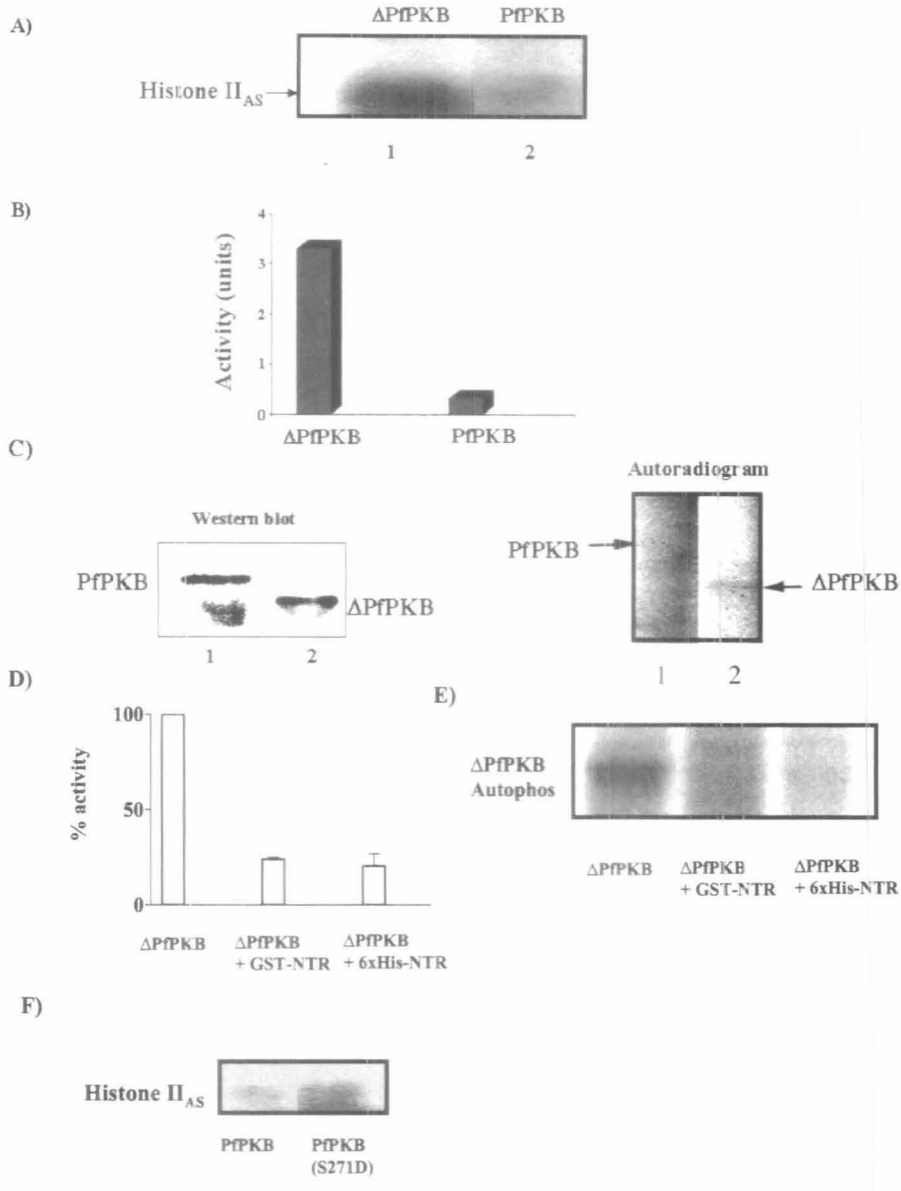

FIG. 5. **N-terminal region of PfPKB hinders its catalytic activity**. PfPKB or its catalytic domain (ΔPfPKB) was assayed for kinase activity using histone II$_{AS}$ (*A*) or crosstide (*B*) as substrates. In some experiments, exogenous substrates were not included, and autophosphorylation levels of GST-PfPKB (*lane 1*) or GST-ΔPfPKB (*lane 2*) were assessed by autoradiography. *C. arrows* indicate the mobility of the GST-PfPKB and GST-ΔPfPKB proteins. Recombinant His$_6$-NTR or GST-NTR was incubated with ΔPfPKB, and its activity was monitored by its ability to phosphorylate crosstide (*D*), or its autophosphorylation was monitored by performing incubations in absence of any substrate (*E*). Catalytic activity of PfPKB was compared with its S271D mutant by performing kinase assays as described above (*F*).

peptide derived from the C terminus of PfPKB (Fig. 6*A*). PfPKB expression was predominantly observed in the schizont stages of the parasite as indicated by a band of ~52 kDa, which is consistent with the predicted molecular mass of 50 kDa (Fig. 6*B*). Reverse transcription-PCR analysis indicated that PfPKB transcripts were mainly present in schizont stages and were observed in the trophozoites at only very low levels (Fig. 6*C*). PfPKB immunoprecipitated from schizont lysates was able to phosphorylate crosstide, indicating PfPKB is active in the schizonts of *P. falciparum* (Fig. 6*D*).

Immunofluorescence studies revealed that PfPKB was present mainly in the mid-late schizont stages of the parasite; other mono-nucleated stages did not show any detectable PfPKB expression (Fig. 6*E*). To probe if PfPKB is localized at the cell surface, co-localization studies were performed using antisera against MSP1, a marker for merozoite surface. PfPKB exhibited a diffused staining pattern in segmented schizonts, indicating its presence in the cytoplasm, and also exhibited some co-localization with MSP1 (Fig. 6*F*). In free merozoites PfPKB seems to be localized at the apical end (Fig. 6*G*), a region that is important for erythrocyte invasion. PfPKB also co-localizes with EBA175, a micronemal protein (data not shown).

Go 6983 Is an Inhibitor of PfPKB Activity and Inhibits Parasite Growth—We were interested in identifying PfPKB inhibitors to help us understand the structure-function relationship of this *Plasmodium* protein kinase and, most importantly, its physiological role in promoting parasite growth and development in the host. Because there are no known or available inhibitors of mammalian PKB, we considered the possibility of inhibitors of other related kinases as putative candidates for PfPKB. For this purpose PKC inhibitors were selected based on following reasons. 1) *In silico* analysis suggested that catalytic domain of PfPKB was most closely related to PKC in comparison to other AGC kinases (Table II); 2) it appears that *P. falciparum* does not have a PKC homologue. Go 6983 and Go 6976 (Fig. 7*A*) are isoform-specific PKC inhibitors that target the ATP binding site (33). Inhibition of any other AGC kinases by these compounds has not yet been reported. The effect of these compounds on *in vitro* recombinant PfPKB activity was tested. Go 6983 inhibited ΔPfPKB activity, as judged by its ability to phosphorylate histone II$_{AS}$ (Fig. 7*B*) and crosstide (Fig. 7*C*), with an IC$_{50}$ of ~1 μM. In contrast, Go 6976 was unable to inhibit the ΔPfPKB activity even at 10 μM concentration (Fig. 7*D*). These data suggested that Go 6983 could be a useful tool for manipulating PfPKB activity in *P. falciparum* for deciphering its role in the life cycle of the parasite. To test this, synchronized *P. falciparum* cultures were incubated with Go 6983, and parasite growth was monitored at different time

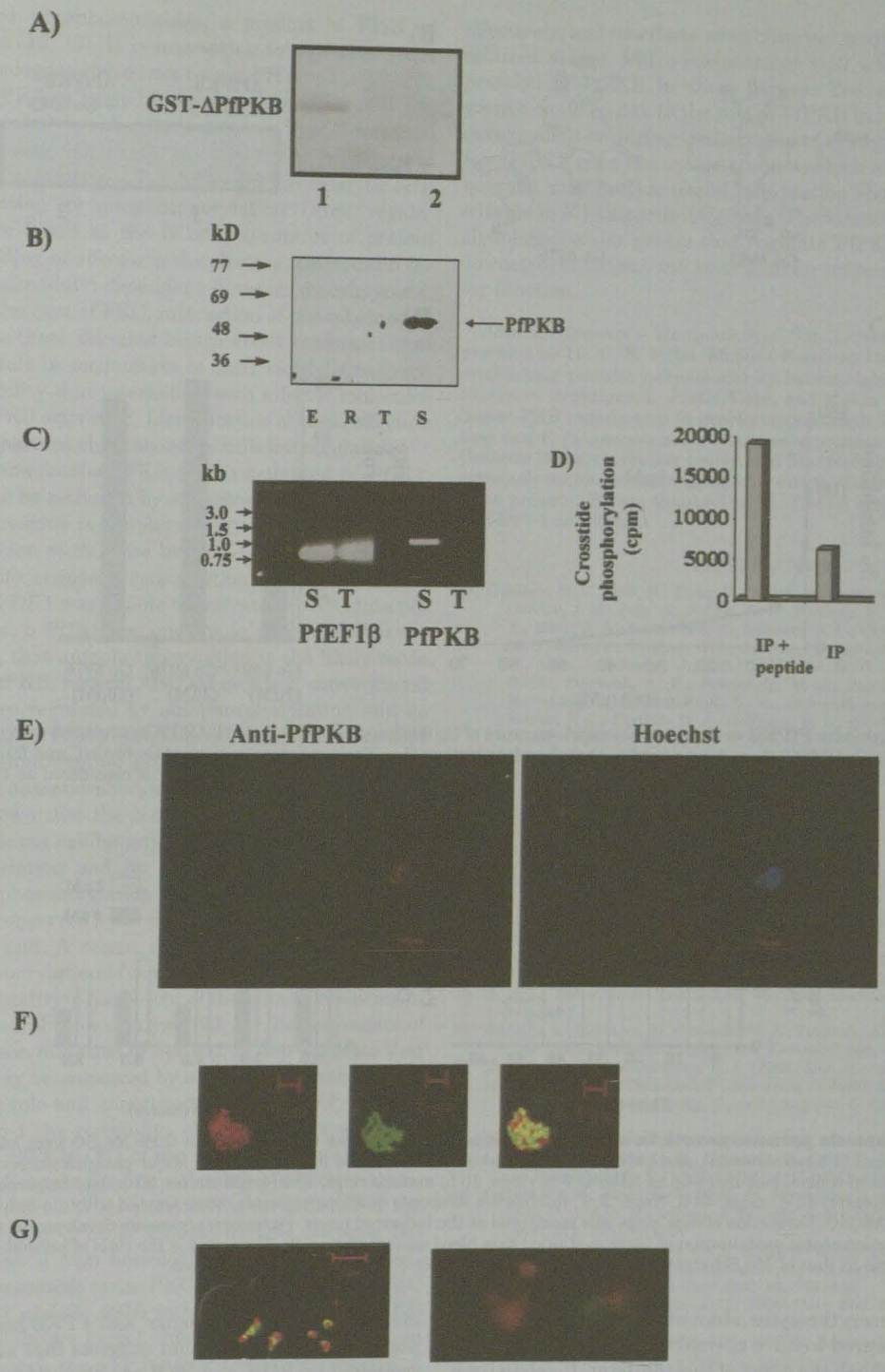

FIG. 6. **PfPKB is expressed mainly in schizont stages of *P. falciparum* life cycle.** Anti-sera raised against a C-terminal peptide of PfPKB recognized the recombinant GST-ΔPfPKB (*A*, *lane 1*) but not the N-terminal region of this kinase, which lacks the C-terminal end (*A*, *lane 2*). *B*, equal amounts of cell lysate prepared from either uninfected erythrocytes (*E*), schizonts (*S*), trophozoites (*T*), or rings (*R*) were used for Western blot analysis with anti-PfPKB antisera. *C*, equal amounts of RNA isolated from either schizont (*S*) or trophozoite (*T*) stages of *P. falciparum* were used for reverse transcription-PCR analysis using primers specific to either *P. falciparum* elongation factor 1β (*PfEF1β*), used as a control (12), or PfPKB. Equal amounts of PCR product were electrophoresed on 1% agarose gel. *D*, PfPKB immunoprecipitate (*IP*) from schizont-rich parasite lysates was used to phosphorylate crosstide. *E*, immunofluorescence studies performed using anti-PfPKB antisera on thin blood smears of *P. falciparum* cultures revealed that only late schizonts but no other asexual stages (Hoechst-stained) were recognized by this anti-sera. Rabbit antisera against PfPKB (*red*) and mouse antisera against MSP1 (*green*) was used to localize these proteins in late/segmented schizonts (*F*) or in free merozoites (*G*). The *right panel* in *G* shows a zoomed image of merozoites stained with MSP1 and PfPKB antisera.

points. There were no apparent effects of this drug until parasites reached the late schizont/segmenter stage (40–44 h). A significant decrease in parasitemia was observed in drug-treated cells subsequent to this point. In Go 6983-treated cells, the number of rings in the following cycle was markedly less compared with the control cultures (Fig. 8*A*). This observation correlates well with the expression profile of PfPKB in the schizont/merozoite stages of the life cycle (Fig. 6). It is reasonable to state that the major effects of Go 6983 were due to its interaction with *Plasmodium* cellular machinery and not a

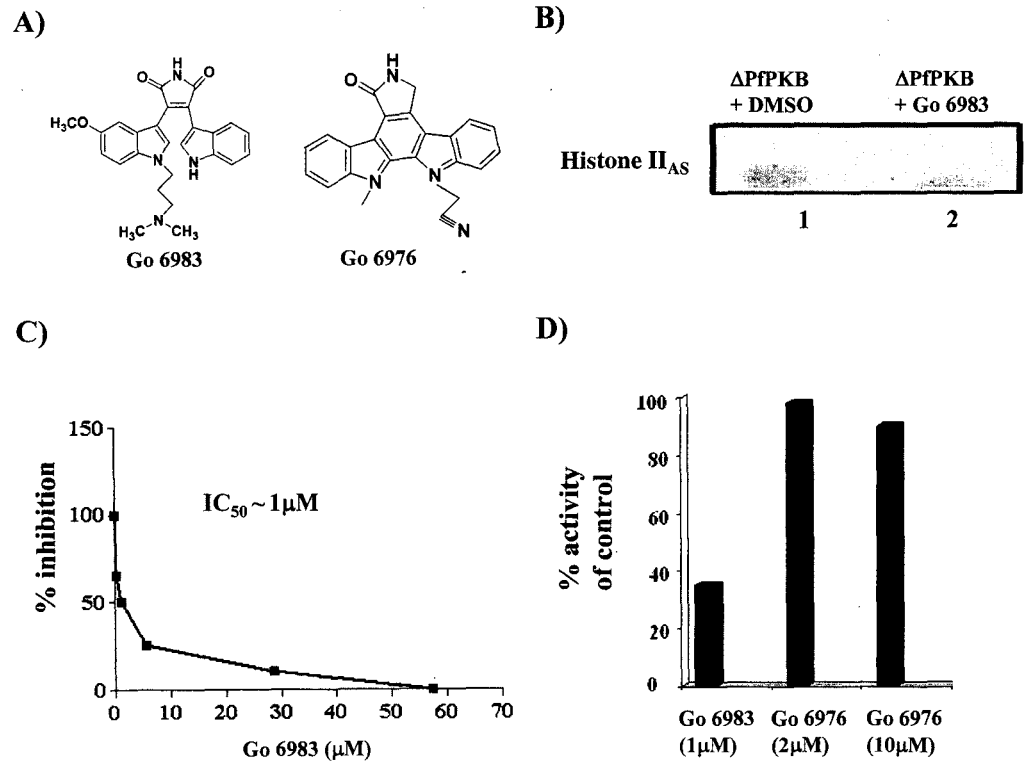

FIG. 7. **Go 6983 inhibits PfPKB activity.** *A*, chemical structure of Go 6983 and Go 6976. *B*, GST-ΔPfPKB incubated with either 1 μM Go 6983 (*lane 2*) or 0.1% Me_2SO (*DMSO*) (*lane 1*) was used to phosphorylate histone II_{AS}. Various concentrations of Go 6983 (*C* and *D*) or Go 6976 (*D*) were used to inhibit peptide substrate phosphorylation by ΔPfPKB. Enzyme activity in the absence of inhibitor is considered as 100%.

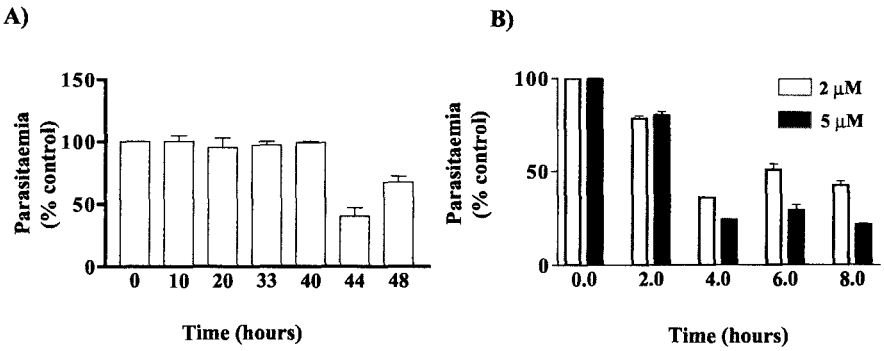

FIG. 8. **Go 6983 arrests parasite growth in a stage-specific manner.** *A*, either 5 μM Go 6983 or 0.1% Me_2SO were added to synchronized *P. falciparum* cultures (1% parasitemia), and parasite growth was monitored at the indicated times. Major parasitic stages (more than 80%) at different time points in control cultures was as follows: 0 h, rings; 10 h, mature rings; 18 h, trophozoites; 33 h, late trophozoites/early schizonts; 40 h, schizonts/segmenter; 44 h, rings; 48 h, rings. *B*, *P. falciparum* schizonts (~3% parasitemia) were treated with the indicated concentrations of Go 6983 or 0.1% Me_2SO. Formation of new rings was monitored at the indicated times. Parasitemia/parasite development was measured at the indicated times by microscopic examination of Giemsa-stained thin blood smears (*A* and *B*). The *y* axis is the ratio of percentage of parasitemia of drug-treated cultures to that of Me_2SO-treated cultures. *Error bars* reflect S.E. from three experiments.

result of effects on erythrocytes, since other parasite stages and erythrocytes appeared to have normal morphology.

To further establish the effect of this inhibitor, *P. falciparum* schizonts were incubated with Go 6983, and development of the parasite was monitored. Although untreated cells formed rings within 4–6 h, Go 6983 treatment resulted in an almost 60% decrease in formation of new rings (Fig. 8*B*). These data suggest that this drug targets directly the late schizont stages or the merozoites, which would prevent invasion of erythrocytes and subsequent formation of fresh rings.

DISCUSSION

Role of signal transduction events in the development of most protozoan parasites is unclear. Especially, information about molecular machinery involved in carrying out these events is lacking. One of our interests is to understand the role of the classical PI3K, PKB pathways in *P. falciparum*. We have identified a PI3K homologue[3] and a PKB homologue (reported here) in *P. falciparum* that suggests that signaling pathways regulated by PI3K and PKB are likely to be conserved in this parasite, although they may not necessarily operate in a manner similar to higher eukaryotes (see the discussion below).

PfPKB shows significant sequence homology to the catalytic domain of protein kinase B in higher eukaryotes. In addition it also shares almost 65% sequence homology with the catalytic domain of protein kinase C, another AGC class Ser/Thr kinase. So far, a PKC homologue has not been identified in *P. falciparum*. Our analysis suggested that PfPKB is closest to, besides PKB, mammalian PKCα, β, γ at the sequence level. PfPKB does not have a PH domain, which plays an important role in subcellular localization and activation of PKB by binding to

[3] P. Sharma, manuscript in preparation.

3′-phosphorylated phosphoinositides, a product of PI3K in mammalian cells (16, 17). It is interesting to note that yeast and *T. cruzi* homologues also do not have a PH domain (27–29), suggesting that PKB in these unicellular eukaryotes may not be directly regulated by phosphoinositides. The N-terminal region of PfPKB does not share any significant homology to proteins in various databases. It inhibits PfPKB catalytic activation by preventing its autophosphorylation. Often, regulatory domains are found at the N or C terminus of protein kinases, and binding of effector molecules (*e.g.* calmodulin interaction with calmodulin-dependent kinases, diacylglycerol, and calcium; in the case of PKC, interaction of phosphoinositides with PKB) to these domains brings about conformational changes that result in modulation of their catalytic activity. There is a possibility that interaction with effector molecules may result in PfPKB activation. Identification of these effectors could provide important clues about its cellular regulation.

In contrast to mammalian PKB that is activated by PDK1, PfPKB appears to be activated by autophosphorylation of Ser-271. This serine residue is complementary to Thr-309 of PKB, and phosphorylation of this site by PDK1 is crucial for PKB activation. Despite sequence conservation in the vicinity of Ser-271, human PDK1 was unable to activate PfPKB (data not shown). Moreover, a PDK1-like enzyme is absent in *Plasmodium*, suggesting that autophosphorylation is the likely mode of activation of PfPKB. Several AGC kinases (*e.g.* conventional PKC isoforms) are regulated by autophosphorylation and do not appear to require PDK1 (34). It is interesting to note that PKB homologue from another protozoan parasite, *T. cruzi*, is also regulated by autophosphorylation (27).

It has been shown that the N-terminal PH domain-deleted versions of PKB do not exhibit any significant catalytic activity or autophosphorylation and its activation is dependent on PDK1-mediated phosphorylation (32). Several AGC kinases possess a loosely conserved hydrophobic patch of amino acids at their C-terminal end. A recent crystal structure of PKB revealed that phosphorylation of Ser-474 in this region promotes conformational stability of the N-lobe of the kinase, resulting in a conformation favorable for catalysis (23, 31). Enhancement of PfPKB activity upon mutation of Ser-442 to Asp suggests that PfPKB activity may be enhanced by a similar mechanism.

To decipher the role and importance of PfPKB to *P. falciparum,* we considered the possibility of using pharmacological inhibitors against PfPKB. One of the major drawbacks in performing these studies was the unavailability of effective mammalian PKB inhibitors. As an alternative, we considered the possibility of inhibitors of other kinases for this purpose. Because PfPKB shares a high homology with protein kinase C isoforms, it was reasonable to use PKC inhibitors. Specific PKC inhibitors Go 6983 and Go 6976 were used to inhibit PfPKB activity. These inhibitors target the ATP binding region on PKC (29). Even though the ATP binding site is well conserved in protein kinases (35), it has been shown that there are subtle differences near this site that can be exploited to design effective and specific inhibitors against these enzymes (36). Several *Plasmodium* kinases have been targeted using inhibitors of their mammalian counterparts (4, 13, 37, 38), and in some cases this information has been used to generate inhibitors specific to the *Plasmodium* enzymes (39–41). Differences in Go 6983 and Go 6976 allow them to distinguish between isoforms of PKC (33); Go 6976 is more effective for conventional PKC isoforms and PKCμ than Go 6983, which is not very effective against PKCμ (33). In case of PfPKB, only Go 6983 and not Go 6976 inhibited its activity. This inhibitor selectivity could be useful as a template for designing more specific and effective inhibitors against PfPKB. Go 6983 inhibited parasite growth effectively, and its effects were observed mainly during or after schizont stages, which corroborates well with the specific expression of PfPKB in these stages. The arrest in parasite growth could be due to the role of PfPKB in late schizont stage development or during the invasion of erythrocytes by merozoites. PfPKB gene disruption studies, which are currently being pursued, may provide useful information about the role of this enzyme in *P. falciparum* life cycle. The identity of the upstream signals/molecular events that regulate PfPKB activity and its downstream targets will be crucial for understanding its cellular function.

Acknowledgments— We thank Prof. Sandip Basu for support. Help provided by Dr. C. R. Pillai, Malaria Research Center, New Delhi in establishing parasite cultures and by Saima Majid, Anindita Bhattacharya, S. Sravanthi, L. Justin Vijay, and Mukta Belwal with recombinant PKB experiments is greatly appreciated. The PlasmoDB data base and *P. falciparum* genome sequence projects (at The Institute of Genomic Research, Sanger center, and Stanford University) have been extremely useful; we acknowledge the efforts of scientists involved with these projects. We are thankful to Dr. Pawan Malhotra for providing anti-MSP1 antibodies.

REFERENCES

1. Gardner, M. J., Hall, N., Fung, E., White, O., Berriman, M., Hyman, R. W., Carlton, J. M., Pain, A., Nelson, K. E., Bowman, S., Paulsen, I. T., James, K., Eisen, J. A., Rutherford, K., Salzberg, S. L., Craig, A., Kyes, S., Chan, M. S., Nene, V., Shallom, S. J., Suh, B., Peterson, J., Angiuoli, S., Pertea, M., Allen, J., Selengut, J., Haft, D., Mather, M. W., Vaidya, A. B., Martin, D. M., Fairlamb, A. H., Fraunholz, M. J., Roos, D. S., Ralph, S. A., McFadden, G. I., Cummings, L. M., Subramanian, G. M., Mungall, C., Venter, J. C., Carucci, D. J., Hoffman, S. L., Newbold, C., Davis, R. W., Fraser, C. M., and Barrell, B. (2002) *Nature* **419,** 498–511
2. Kappes, B., Doerig, C. D., and Graeser, R. (1999) *Parasitol. Today* **15,** 449–454
3. Bhattacharyya, M. K., Hong, Z., Kongkasuriyachai, D., and Kumar, N. (2002) *Int. J. Parasitol.* **32,** 739–747
4. Bracchi-Ricard, V., Barik, S., Delvecchio, C., Doerig, C., Chakrabarti, R., and Chakrabarti, D. (2000) *Biochem. J.* **347,** 255–263
5. Deng, W., and Baker, D. A. (2002) *Mol. Microbiol.* **44,** 1141–1151
6. Doerig, C., Endicott, J., and Chakrabarti, D. (2002) *Int. J. Parasitol.* **32,** 1575–1585
7. Dorin, D., Le Roch, K., Sallicandro, P., Alano, P., Parzy, D., Poullet, P., Meijer, L., and Doerig, C. (2001) *Eur. J. Biochem.* **268,** 2600–2608
8. Dorin, D., Alano, P., Boccaccio, I., Ciceron, L., Doerig, C., Sulpice, R., Parzy, D., and Doerig, C. (1999) *J. Biol. Chem.* **274,** 29912–29920
9. Li, J., and Cox, L. S. (2000) *Mol. Biochem. Parasitol.* **109,** 157–163
10. Li, J. L., Baker, D. A., and Cox, L. S. (2000) *Biochim. Biophys. Acta* **1491,** 341–349
11. Madeira, L., DeMarco, R., Gazarini, M. L., Verjovski-Almeida, S., and Garcia, C. R. (2003) *Biochem. Biophys. Res. Commun.* **306,** 995–1001
12. Mamoun, C. B., and Goldberg, D. E. (2001) *Mol. Microbiol.* **39,** 973–981
13. Syin, C., Parzy, D., Traincard, F., Boccaccio, I., Joshi, M. B., Lin, D. T., Yang, X. M., Assemat, K., Doerig, C., and Langsley, G. (2001) *Eur. J. Biochem.* **268,** 4842–4849
14. Scheid, M. P., and Woodgett, J. R. (2001) *Nat. Rev. Mol. Cell Biol.* **2,** 760–768
15. Alessi, D. R., Andjelkovic, M., Caudwell, B., Cron, P., Morrice, N., Cohen, P., and Hemmings, B. A. (1996) *EMBO J.* **15,** 6541–6551
16. Andjelkovic, M., Alessi, D. R., Meier, R., Fernandez, A., Lamb, N. J., Frech, M., Cron, P., Cohen, P., Lucocq, J. M., and Hemmings, B. A. (1997) *J. Biol. Chem.* **272,** 31515–31524
17. Vanhaesebroeck, B., and Alessi, D. R. (2000) *Biochem. J.* **346,** 561–576
18. Williams, M. R., Arthur, J. S., Balendran, A., van der, K. J., Poli, V., Cohen, P., and Alessi, D. R. (2000) *Curr. Biol.* **10,** 439–448
19. Belham, C., Wu, S., and Avruch, J. (1999) *Curr. Biol.* **9,** 93–96
20. Trager, W., and Jensen, J. B. (1976) *Science* **193,** 673–675
21. Lambros, C., and Vanderberg, J. P. (1979) *J. Parasitol.* **65,** 418–420
22. Cross, D. A., Alessi, D. R., Cohen, P., Andjelkovich, M., and Hemmings, B. A. (1995) *Nature* **378,** 785–789
23. Yang, J., Cron, P., Thompson, V., Good, V. M., Hess, D., Hemmings, B. A., and Barford, D. (2002) *Mol. Cell* **9,** 1227–1240
24. Bahl, A., Brunk, B., Crabtree, J., Fraunholz, M. J., Gajria, B., Grant, G. R., Ginsburg, H., Gupta, D., Kissinger, J. C., Labo, P., Li, L., Mailman, M. D., Milgram, A. J., Pearson, D. S., Roos, D. S., Schug, J., Stoeckert, C. J., Jr., and Whetzel, P. (2003) *Nucleic Acids Res.* **31,** 212–215
25. Kissinger, J. C., Brunk, B. P., Crabtree, J., Fraunholz, M. J., Gajria, B., Milgram, A. J., Pearson, D. S., Schug, J., Bahl, A., Diskin, S. J., Ginsburg, H., Grant, G. R., Gupta, D., Labo, P., Li, L., Mailman, M. D., McWeeney, S. K., Whetzel, P., Stoeckert, C. J., and Roos, D. S. (2002) *Nature* **419,** 490–492
26. Hanks, S. K., and Hunter, T. (1995) *FASEB J.* **9,** 576–596
27. Pascuccelli, V., Labriola, C., Tellez-Inon, M. T., and Parodi, A. J. (1999) *Mol. Biochem. Parasitol.* **102,** 21–33
28. Fujita, M., and Yamamoto, M. (1998) *Curr. Genet.* **33,** 248–254
29. Toda, T., Cameron, S., Sass, P., and Wigler, M. (1988) *Genes Dev.* **2,** 517–527
30. Obata, T., Yaffe, M. B., Leparc, G. G., Piro, E. T., Maegawa, H., Kashiwagi, A., Kikkawa, R., and Cantley, L. C. (2000) *J. Biol. Chem.* **275,** 36108–36115
31. Yang, J., Cron, P., Good, V. M., Thompson, V., Hemmings, B. A., and Barford,

D. (2002) *Nat. Struct. Biol.* **9,** 940–944
32. Biondi, R. M., Kieloch, A., Currie, R. A., Deak, M., and Alessi, D. R. (2001) *EMBO J.* **20,** 4380–4390
33. Gschwendt, M., Dieterich, S., Rennecke, J., Kittstein, W., Mueller, H. J., and Johannes, F. J. (1996) *FEBS Lett.* **392,** 77–80
34. Parekh, D. B., Ziegler, W., and Parker, P. J. (2000) *EMBO J.* **19,** 496–503
35. Manning, G., Whyte, D. B., Martinez, R., Hunter, T., and Sudarsanam, S. (2002) *Science* **298,** 1912–1934
36. Garcia-Echeverria, C., Traxler, P., and Evans, D. B. (2000) *Med. Res. Rev.* **20,** 28–57
37. Silva-Neto, M. A., Atella, G. C., and Shahabuddin, M. (2002) *J. Biol. Chem.* **277,** 14085–14091
38. Le Roch, K., Sestier, C., Dorin, D., Waters, N., Kappes, B., Chakrabarti, D., Meijer, L., and Doerig, C. (2000) *J. Biol. Chem.* **275,** 8952–8958
39. Woodard, C. L., Li, Z., Kathcart, A. K., Terrell, J., Gerena, L., Lopez-Sanchez, M., Kyle, D. E., Bhattacharjee, A. K., Nichols, D. A., Ellis, W., Prigge, S. T., Geyer, J. A., and Waters, N. C. (2003) *J. Med. Chem.* **46,** 3877–3882
40. Xiao, Z., Waters, N. C., Woodard, C. L., Li, Z., and Li, P. K. (2001) *Bioorg. Med. Chem. Lett.* **11,** 2875–2878
41. Knockaert, M., Gray, N., Damiens, E., Chang, Y. T., Grellier, P., Grant, K., Fergusson, D., Mottram, J., Soete, M., Dubremetz, J. F., Le Roch, K., Doerig, C., Schultz, P., and Meijer, L. (2000) *Chem. Biol.* **7,** 411–422

THE JOURNAL OF BIOLOGICAL CHEMISTRY VOL. 281, NO. 37, pp. 27126–27133, September 15, 2006

PfPKB, a Protein Kinase B-like Enzyme from *Plasmodium falciparum*

II. IDENTIFICATION OF CALCIUM/CALMODULIN AS ITS UPSTREAM ACTIVATOR AND DISSECTION OF A NOVEL SIGNALING PATHWAY*

Received for publication, February 28, 2006, and in revised form, June 29, 2006 Published, JBC Papers in Press, June 29, 2006, DOI 10.1074/jbc.M601914200

Ankush Vaid[1] **and Pushkar Sharma**[2]

From the Eukaryotic Gene Expression Laboratory, National Institute of Immunology, New Delhi 110067, India

Intracellular cell signaling cascades of protozoan parasite *Plasmodium falciparum* are not clearly understood. We have reported previously (Kumar, A., Vaid, A., Syin, C., and Sharma, P. (2004) *J. Biol. Chem.* 279, 24255–24264) the identification and characterization of a protein kinase B-like enzyme in *P. falciparum* (PfPKB). PfPKB lacks the phosphoinositide-interacting pleckstrin homology domain present in mammalian protein kinase B. Therefore, the mechanism of PfPKB regulation was expected to be different from that of the host and had remained unknown. We have identified calmodulin (CaM) as the regulator of PfPKB activity. A CaM binding domain was mapped in the N-terminal region of PfPKB. CaM, in a calcium-dependent manner, interacts with this domain and activates PfPKB. CaM associates with PfPKB in the parasite and regulates its activity. Furthermore phospholipase C acts as an upstream regulator of this cascade as it facilitates the release of calcium from intracellular stores. This is one of the first multicomponent signaling pathways to be dissected in the malaria parasite.

Plasmodium falciparum is responsible for most cases of human malaria worldwide. This parasite invades both hepatocytes as well as erythrocytes in human host, but it is the erythrocytic phase of its life cycle that causes severe pathogenesis of malaria. After invading erythrocytes, the parasite undergoes well defined developmental changes inside the erythrocyte host. The parasite adopts a ringlike morphology and acquires necessary nutrients from the host during the trophozoite stages. Subsequently nuclear division gives rise to multinucleated schizont containing ~24 merozoites. These merozoites when released after schizont rupture invade fresh erythrocytes to start another cycle of asexual development. Although it is known that *Plasmodium* can utilize host G-protein signaling (2) and alters phosphorylation of erythrocyte cytoskeletal proteins during infection (3), parasite signaling pathways have remained largely uncharacterized. Given the importance of cell signaling cascades in proliferation and differentiation of eukaryotic cells, dissection of signal transduction mechanisms may provide useful insights about the development of this protozoan parasite. *Plasmodium* genome analysis revealed that there are close to 65 protein kinases, major mediators of cell signaling, in *P. falciparum* (4, 5). Apart from a few of these kinases (6–10), the function and mechanism of regulation and identity of cellular targets of most of these enzymes is largely unknown.

We recently identified a protein kinase B-like enzyme in *P. falciparum* (PfPKB)[3]. Despite sharing significant sequence homology (~70%) with the catalytic domain of PKB, PfPKB lacks a pleckstrin homology (PH) domain present at the N terminus of the mammalian enzyme. The N-terminal region (NTR) of PfPKB is inhibitory as its deletion results in PfPKB catalytic activation (1). The NTR does not exhibit similarity with any other protein in the non-redundant protein data base. PKB binds phosphoinositides via the PH domain, which is crucial for its membrane translocation and catalytic activation. Whereas PKB is activated by phosphoinositide-dependent kinase 1-mediated phosphorylation at Thr-308 in its activation loop (11), autophosphorylation of PfPKB at its analogous Ser-271 residue results in its activation (1). PfPKB is expressed mainly in the schizont/merozoite stages of *P. falciparum*. Using a pharmacological inhibitor, we had proposed a role of PfPKB during schizont-to-ring transition of the parasite (1). Despite this information, it had remained unknown how PfPKB is regulated in *P. falciparum*. In the present study we identified calmodulin as the upstream regulator of PfPKB activity *in vitro* and *in vivo*. These findings resulted in identification of a novel signaling pathway in the malaria parasite.

EXPERIMENTAL PROCEDURES

Reagents—pGEX4T1-PfPKB and pET-NTR plasmids used for protein expression and anti-PfPKB rabbit antisera used in these studies have been described earlier (1). Site-directed mutagenesis was carried out using the QuikChange site-di-

* This work was supported in part by a senior research fellowship (to P. S.) from The Wellcome Trust, UK and by intramural funding from the Department of Biotechnology, New Delhi to National Institute of Immunology. Paper I in this series is Ref. 1. The costs of publication of this article were defrayed in part by the payment of page charges. This article must therefore be hereby marked "*advertisement*" in accordance with 18 U.S.C. Section 1734 solely to indicate this fact.

[1] A junior research fellow of Council of Scientific and Industrial Research, New Delhi.

[2] To whom correspondence should be addressed. Tel.: 91-11-26717123 (ext. 791); Fax: 91-11-26162125; E-mail: pushkar@nii.res.in.

[3] The abbreviations used are: PfPKB, protein kinase B-like enzyme in *P. falciparum*; CaM, calmodulin; ΔPfPKB, deletion of PfPKB lacking the NTR; CBD, calmodulin binding domain; NTR, N-terminal region; PKB, mammalian protein kinase B; PLC, phospholipase C; PfPKB-IP, PfPKB immunoprecipitate; PI3K, phosphatidylinositol 3-kinase; scr, scrambled; PH, pleckstrin homology; GST, glutathione *S*-transferase; BAPTA-AM, 1,2-bis(2-amino-phenoxy)ethane-*N*,*N*,*N*′,*N*′-tetraacetic acid tetrakis(acetoxymethyl) ester.

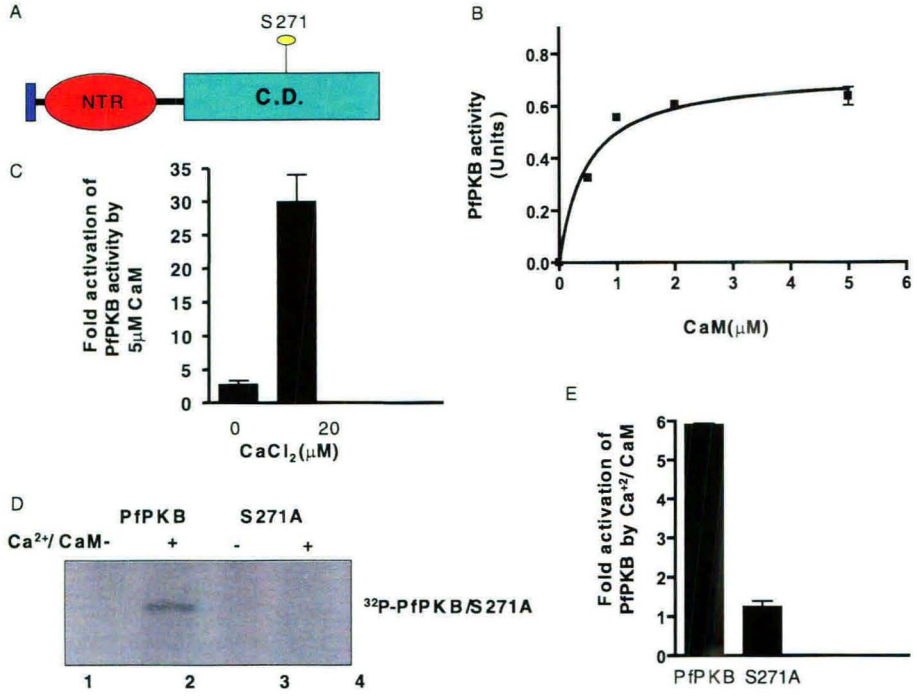

FIGURE 1. **CaM activates PfPKB in a calcium-dependent manner.** *A*, schematic representation of PfPKB domain architecture. Autophosphorylation of Ser-271 in PfPKB catalytic domain (*C.D.*) can result in its activation, whereas its NTR (*red*) prevents its autophosphorylation as well as catalytic activation (1). The *blue bar* indicates the presence of a putative N-terminal signal peptide in PfPKB. *B*, Ca^{2+}/CaM activates PfPKB *in vitro*. Recombinant GST-PfPKB (1.4 μM) was preincubated with various concentrations of CaM and 100 μM $CaCl_2$, and kinase assays were performed using a small peptide, crosstide, as substrate. *C*, CaM regulates PfPKB activity in a calcium-dependent manner. GST-PfPKB was incubated in the presence or absence of 5 μM CaM in a buffer containing either 20 μM $CaCl_2$ or 1 mM EGTA (0 mM $CaCl_2$), and PfPKB activity was assayed as described in *B*. *D* and *E*, CaM promotes autophosphorylation of PfPKB, which is responsible for its activation. Equal amounts of GST-PfPKB or its S271A mutant were incubated with (*lanes 2* and *4*) or without (*lanes 1* and *3*) 5 μM CaM and 100 μM $CaCl_2$ in the absence (*D*) or presence of crosstide (*E*), and kinase assays were performed as described above. The phosphorimage shows that PfPKB (*lane 2*) and not S271A (*lane 4*) was autophosphorylated in the presence of Ca^{2+}/CaM. Unlike PfPKB, S271A mutant failed to exhibit CaM-mediated activation (*E*). -Fold activation was calculated by comparing the ability of PfPKB or S271A to phosphorylate crosstide in the presence or absence of CaM (see "Experimental Procedures"). *Error bars* reflect S.E. from more than three experimental determinations.

rected mutagenesis kit (Stratagene). The peptides crosstide (GRPRTSSFAEG), calmodulin (CaM) binding domain (CBD) peptide (IGKKRLRNSMSLSYERKKRIR), and scrambled (scr) peptide (MKLSGKRYRNSRLKEIRSRIK) were custom synthesized by Peptron. scr peptide has an amino acid composition similar to CBD, but their arrangement has been scrambled. U73322, U73122, and W7 were purchased from Calbiochem. Anti-CaM monoclonal antibody against *Dictyostelium discoideum* CaM and purified bovine CaM were also obtained from Calbiochem. Unless indicated, all other fine chemicals were purchased from Sigma.

Parasite Culture—P. falciparum strain 3D7 was cultured at 37 °C in RPMI 1640 medium using either 10% AB^+ human serum or 0.5% Albumax II (Invitrogen) (complete medium). Cultures were gassed with 7% CO_2, 5% O_2, and 88% N_2, and synchronization of the parasites in culture was achieved by sorbitol treatment (1, 12). Sorbitol synchronization yielded parasites purely in ring form; these rings matured to trophozoites 30–36 h later. After nuclear division schizonts containing merozoites were observed. Ruptured schizonts with emerging merozoites were seen after ~44 h; this was followed by formation of fresh rings as a result of red blood cell invasion. Typically pharmacological inhibitors were incubated with schizonts for 15–60 min (~3% parasitemia) at 5% hematocrit.

Site-directed Mutagenesis and Recombinant Protein Expression—For expression of PfPKB as a GST fusion protein, pGEX4T1-PfPKB plasmid construct was used (1). Deletion mutant ΔCBD and S271A mutants were generated by using the above mentioned PfPKB construct and the QuikChange site-directed mutagenesis kit (Stratagene). Recombinant proteins were expressed and purified as described earlier (1). Protein concentration was estimated by performing densitometry of SDS-PAGE gels using NIH Image software.

Immunoblotting and Immunoprecipitation—Parasites were released from infected erythrocytes by 0.05% (w/v) saponin treatment. Cell-free protein extracts from specific parasite stages were prepared by suspending parasite pellets in a buffer containing 10 mM Tris, pH 7.5, 100 mM NaCl, 5 mM EDTA, 1% Triton X-100, 20 μM sodium fluoride, 20 μM β-glycerophosphate, 100 μM sodium orthovanadate, and 1× Complete protease inhibitor mixture (Roche Applied Science) using a syringe and a needle. In most experiments 1 mM $CaCl_2$ was also included in the buffer, and 1 mM EGTA was added to perform experiments in calcium-free buffer. Lysates were cleared by centrifugation at 14,000 × *g* for 30 min. PfPKB was immunoprecipitated from the schizont or the merozoite lysates using anti-PfPKB antisera (1). 50–100 μg of lysate were incubated with the antisera at 4 °C overnight on an end-to-end shaker. Subsequently antigen-antibody complexes were incubated with 50 μl of protein A/G-Sepharose for 6 h with shaking at 4 °C. Resin was washed with the lysis buffer several times and was finally resuspended in 50 μl of 1× kinase assay buffer. After separation of parasite lysates or PfPKB-IP on SDS-PAGE gels, Western blotting was performed as described previously (1).

Assay of Kinase Activity—GST fusion proteins of PfPKB (or its variants) or 10 μl of immunoprecipitated PfPKB were assayed in a buffer containing 50 mM Tris, pH 7.5), 10 mM magnesium chloride, 1 mM dithiothreitol, and 100 μM [γ-^{32}P]ATP (6000 Ci/mmol) using a small peptide substrate ("crosstide") or histone II_{AS} as the phosphate acceptor substrate. Reactions were terminated by spotting the reaction mixture on P81 phosphocellulose paper (Whatmann), and phosphate incorporation was measured by scintillation counting of the P81 paper. When histone was used as the substrate, reactions were stopped by boiling the reaction mixture in SDS-PAGE loading buffer. After electrophoresis, phosphate incorporation in histone was visualized by using a Fuji FLA5000 phos-

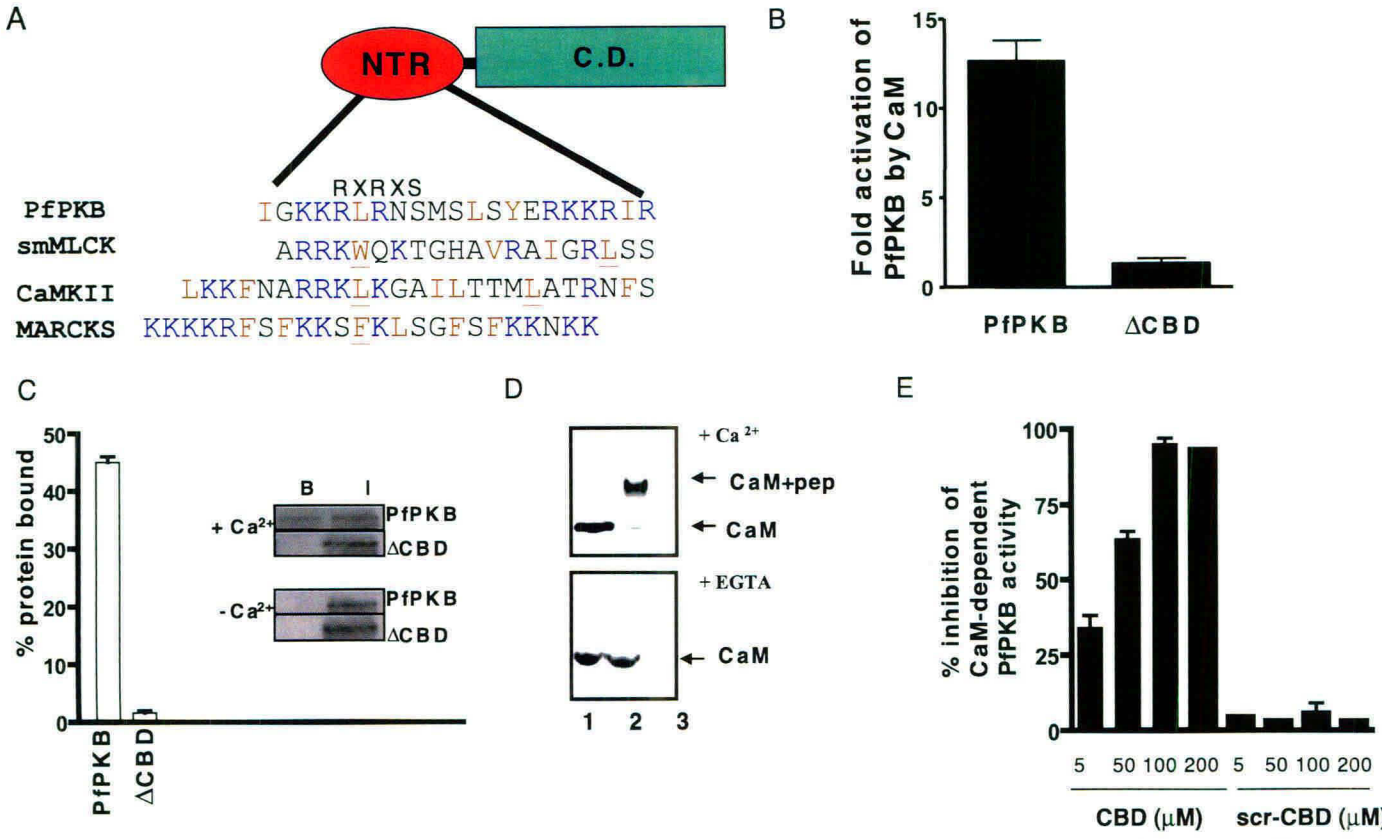

FIGURE 2. **CaM interacts with a CBD in the NTR of PfPKB.** *A*, presence of a putative CBD in the N-terminal region of PfPKB, which has several basic (*blue*) and hydrophobic (*brown*) residues. Shown is a sequence comparison of PfPKB CBD with the CaM binding regions of smooth muscle light chain kinase (*smMLCK*), CaM-dependent kinase II (*CamKII*), and myristoylated alanine-rich C kinase substrate (*MARCKS*). Key hydrophobic residues involved in CaM anchoring are *underlined* (16, 27). An *RXRXS* type pseudosubstrate motif embedded in CBD of PfPKB is also indicated. *B*, deletion of CBD impairs activation of PfPKB by Ca^{2+}/CaM. Equal amounts of GST-PfPKB or its CBD-deleted version, GST-ΔCBD, were incubated with or without 5 μM CaM and 100 μM $CaCl_2$. Kinase assays were performed as described for Fig. 1. *C*, 2.5 μg of GST-PfPKB or GST-ΔCBD were incubated with CaM-agarose resin in a buffer containing 1 mM $CaCl_2$ (*inset, top panel*) or 1 mM EGTA (*inset, bottom panel*). Proteins bound to CaM were eluted with 5 mM EGTA and were detected by performing immunoblotting using anti-GST antibody. Quantitation of protein bands from the blots was done by densitometry, and data are presented as percentage of total input protein that was bound to Ca^{2+}/CaM. The *inset* shows a representative immunoblot with eluted protein (*B*) and the input protein (*I*). No detectable binding of PfPKB or ΔCBD was observed in the absence of calcium. *D*, 10 μM CaM was incubated with 10 μM CBD peptide (*lane 2*) or alone (*lane 1*) in a buffer containing 1 mM $CaCl_2$ (*top panel*) or 1 mM EGTA (*bottom panel*). *Lane 3* represents a control experiment in which the CBD peptide alone was incubated with the buffer. The mixture was separated by native PAGE. The Coomassie-stained gel shows slower mobility of CaM-CBD complex only in the presence of calcium. *E*, CBD peptide prevents activation of PfPKB by CaM. GST-PfPKB was incubated with 5 μM CaM, which had been preincubated with the indicated concentration of CBD, scr-CBD peptides, water, and kinase assays were performed using 1 mM crosstide as substrate as described under "Experimental Procedures." Activity of CaM-PfPKB in the absence of CBD peptides was considered as 100%. Data are presented as mean ± S.E. of three independent experiments. *C.D.*, catalytic domain.

phorimaging system. For typical CaM activation experiments, recombinant proteins were incubated with purified bovine CaM in the presence or absence of $CaCl_2$ 15 min prior to addition of the phosphoacceptor substrate (100 μM crosstide or 5 μg of histone) and ATP. Unless indicated, the concentration of CaM and $CaCl_2$ used in kinase assays was 5 and 100 μM, respectively. For experiments described in Fig. 1*B*, Ca^{2+}/CaM was preincubated with GST-PfPKB 1 h and ATP prior to the addition of crosstide. 1 unit of PfPKB activity is equivalent to 1 μmol of phosphate/min/mg. All experiments were done at least three times.

CaM-Peptide Interaction—CaM-peptide interaction experiments (Fig. 2*D*) were performed as described earlier (13) with a few modifications. Briefly CaM and peptides were incubated in a buffer containing 25 mM Tris·HCl, pH 7.4, 192 mM glycine for 1 h at room temperature in the presence (1 mM $CaCl_2$) or absence (2 mM EGTA) of calcium. The mixture was resolved by 15% native PAGE at constant current of 25 mA.

RESULTS

Calmodulin Activates PfPKB Activity in a Calcium-dependent Manner—We have previously reported that PfPKB shares significant homology with the catalytic domain of PKB. However, it lacks the N-terminal PH domain present in PKB (Fig. 1*A*). When NTR of PfPKB is deleted it results in its catalytic activation, which is strictly dependent on autophosphorylation of Ser-271 in its activation loop (1). Based on these observations, it was reasonable to assume that PfPKB may be activated by interaction of regulatory molecules with the inhibitory NTR.

Preliminary experiments performed in our laboratory suggested that the activity of recombinant PfPKB can be regulated by factors present in parasite protein lysates in a calcium-dependent manner. Because the activity of recombinant PfPKB was not directly modulated by calcium, it was reasonable to speculate that calcium may control PfPKB activity with the aid of one of its effector molecules (data not shown). CaM is a

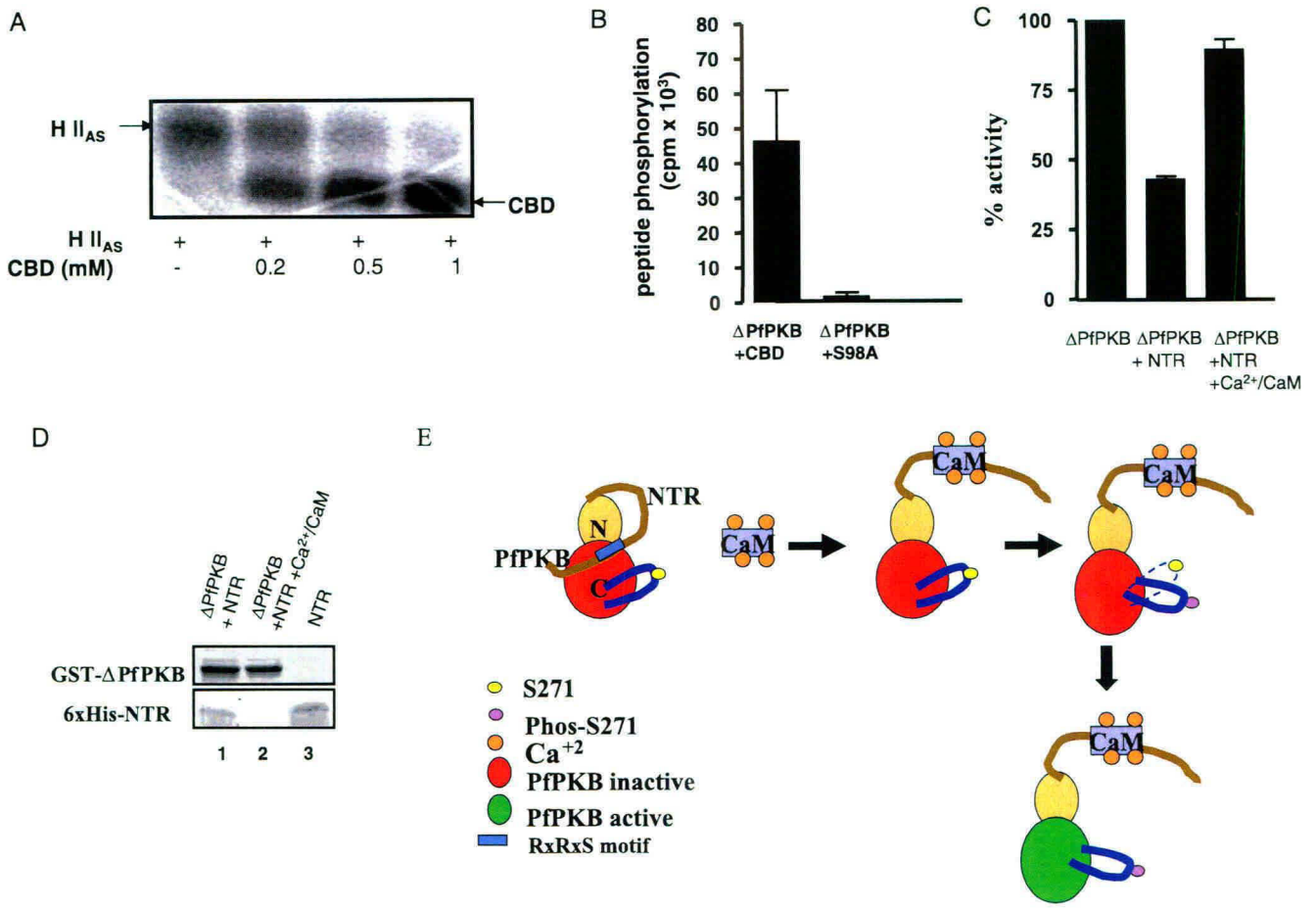

FIGURE 3. **A pseudosubstrate motif is present in the CBD.** *A*, ΔPfPKB, an N terminus-deleted version of PfPKB lacking the first 98 residues that is active independently of CaM, was incubated in a kinase assay mixture with or without CBD peptide. Histone was used as the phosphate acceptor substrate. Inhibition of histone phosphorylation was accompanied by a simultaneous increase in CBD peptide phosphorylation. *B*, ΔPfPKB was incubated in a kinase assay mixture, and 50 μM CBD or CBD-S98A peptide was used as phosphoacceptor substrate. The phosphorylation of these peptides was measured as described for crosstide in Fig. 1. The average from two determinations done at the same time is shown, and *error bars* indicate S.E. *C*, 4 μM His_6-NTR (*6xHis-NTR*) was preincubated with buffer alone or with 4 μM CaM and 100 μM $CaCl_2$ before addition to the kinase assay mixture containing ΔPfPKB. Kinase activity was determined as described above, and the activity in the absence of NTR was considered as 100%. *D*, 2.5 μM His_6-NTR was either preincubated with buffer alone (*lane 1*) or with 100 μM $CaCl_2$ and 2.5 μM CaM (*lane 2*) before addition of 2.5 μM GST-ΔPfPKB. Glutathione-Sepharose beads were used to pull down the complex of GST-ΔPfPKB and His_6-NTR. After washing, the proteins bound to the beads were analyzed by SDS-PAGE. Coomassie staining of the gels revealed the presence of NTR bound to PfPKB only in the absence of CaM (*lane 1*). In the presence of Ca^{2+}/CaM, no NTR-PfPKB interaction was observed (*lane 2*). *Lane 3* is the input His_6-NTR used for the experiment. *E*, a model for PfPKB activation by Ca^{2+}/CaM. PfPKB is locked in an inactive state as a pseudosubstrate region in the NTR occupies its catalytic cleft. Ca^{2+}/CaM binding to CBD, which spans the pseudosubstrate motif, causes a conformational change resulting in the dissociation of NTR from the catalytic cleft thereby facilitating the autophosphorylation of Ser-271 of the activation loop. These events result in the catalytic activation of PfPKB. *Phos-S271*, phosphorylated Ser-271.

major calcium-binding protein ubiquitously expressed in almost all eukaryotes including *Plasmodium* and is well conserved across species. *P. falciparum* homologue of CaM (GenBank™ accession number X56950) shares ~97% homology with CaM from other eukaryotes (14). Incubation of CaM with recombinant PfPKB resulted in a dose-dependent increase in its activity as judged by its ability to phosphorylate a small peptide, crosstide, a well established PKB substrate (15) (Fig. 1*B*). The maximal activation of 1.4 μM PfPKB was achieved at ~2 μM CaM with a K_{CaM} of ~0.5 μM. Importantly PfPKB activation by CaM was dependent on calcium (Fig. 1*C*). Because it has been shown previously that PfPKB activation is dependent on autophosphorylation of Ser-271 in its activation loop (1), it was worth exploring the role of phosphorylation of this site in CaM-mediated PfPKB activation. Calcium/CaM catalyzed autophosphorylation of PfPKB (Fig. 1*D*), and mutation of its Ser-271 to Ala (S271A) resulted in almost complete loss of its autophosphorylation and concomitant attenuation of its catalytic activity (Fig. 1*E*). Collectively these data suggest that Ca^{2+}/CaM activates PfPKB by promoting its autophosphorylation at Ser-271 (Fig. 1, *B–E*).

Identification of a CBD in PfPKB—CaM interacts with segments of proteins that form amphipathic α-helices and are rich in basic and hydrophobic amino acids (16). On examination of NTR of PfPKB, a 21-amino acid motif possessing a putative CBD was identified (Fig. 2*A*). To test whether this motif is the CBD of PfPKB, a deletion mutant of PfPKB lacking these 21 amino acids (ΔCBD) was created. Unlike PfPKB, CaM failed to activate this mutant (Fig. 2*B*). Direct binding of PfPKB and ΔCBD was tested by using CaM immobilized on agarose. Whereas PfPKB exhibited significant binding to CaM-agarose, ΔCBD mutant failed to interact with CaM (Fig. 2*C*), suggesting that this 21-amino acid stretch is the only CaM binding site in PfPKB. As expected PfPKB did not show binding to CaM in the absence of calcium (Fig. 2*C*, *inset*). CaM-CBD interaction was further validated by using a synthetic peptide corresponding to

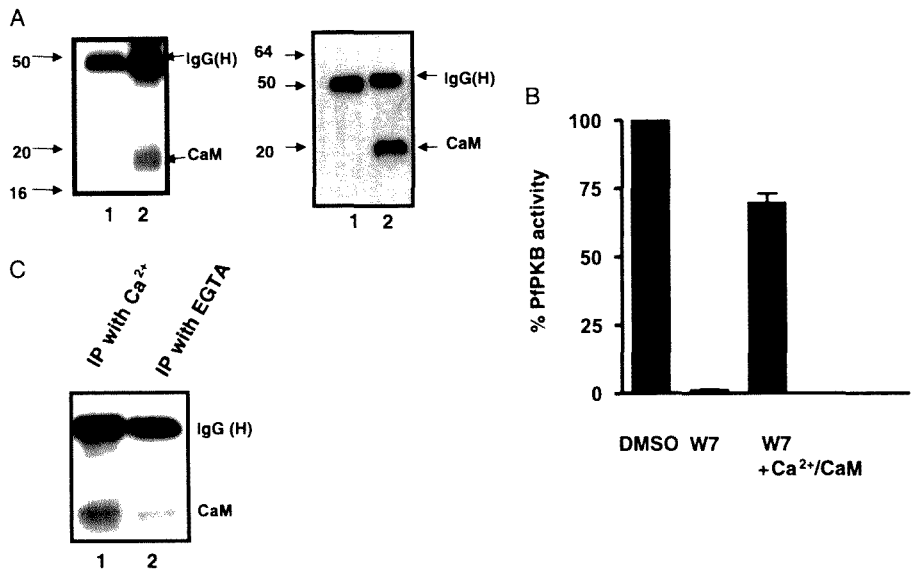

FIGURE 4. **CaM regulates PfPKB activity in *P. falciparum* cultures.** *A*, PfPKB and CaM associate in *P. falciparum*. PfPKB was immunoprecipitated from schizont (*both panels*) or red blood cell (*right panel*) lysates, and immunoprecipitate (*IP*) was electrophoresed on an SDS-PAGE gel followed by Western blot analysis using anti-CaM antibody. Detection of CaM in the immunoprecipitate of PfPKB suggested that these proteins interact in the parasite (*lane 2, both panels*). Mock immunoprecipitation experiments were performed by using preimmune antisera (*left panel, lane 1*) or red blood cell lysate (*right panel, lane 1*). *B*, CaM inhibitor W7 inhibits PfPKB activation in *P. falciparum* cultures. Schizont-rich *P. falciparum* cultures were treated with 50 μM W7. Subsequently PfPKB was immunoprecipitated from parasite protein lysates, and PfPKB-IP-associated activity was assayed. Significant loss in PfPKB activity was observed upon W7 treatment. Addition of 0.1 mM $CaCl_2$ and 5 μM CaM to PfPKB-IP from W7-treated parasites resulted in a significant recovery of PfPKB activity. The results are presented as mean ± S.E. of three independent experiments; the activity of PfPKB in Me_2SO (*DMSO*)-treated parasites was considered as 100%. *C*, PfPKB was immunoprecipitated from schizonts in a buffer containing either 1 mM $CaCl_2$ or EGTA, and immunoblotting was performed to detect the associated CaM. A representative of three independent experiments is shown in the figure. *H*, heavy.

the CBD sequence. CBD peptide exhibited CaM binding as it caused a mobility shift of CaM on a native PAGE gel in the presence of calcium. When calcium was excluded from the reaction mixture CBD did not interact with CaM as it failed to exhibit a shift in its electrophoretic mobility (Fig. 2*D*). CBD peptide prevented PfPKB activation in a dose-dependent manner when incubated with CaM (Fig. 2*E*) indicating that this peptide competes with the CBD of PfPKB for CaM.

Data presented in Fig. 1 and our previous studies (1) indicate that the NTR is inhibitory for PfPKB in the absence of CaM binding. It is possible that the NTR either keeps PfPKB in an inactive state either by masking its catalytic cleft and/or by physically interacting with its active site. To investigate this, ΔPfPKB, a deletion mutant of PfPKB that lacks most of the NTR and first nine residues of CBD and is constitutively active (1), was used. Incubation of ΔPfPKB with CBD peptide inhibited its ability to phosphorylate histone. Interestingly this was accompanied by simultaneous phosphorylation of the CBD peptide (Fig. 3*A*). These observations indicated that the CBD peptide can also interact with PfPKB active site. A similar inhibition in phosphorylation of crosstide by ΔPfPKB was observed (data not shown). Upon close examination of CBD sequence, an R*X*R*X*S type motif was found embedded in the CBD (Fig. 2*A*) that closely resembles a putative substrate motif for AGC family kinases like PfPKB (17) and is not present in ΔPfPKB. It is possible that this motif may act as a pseudosubstrate and thus have affinity for PfPKB active site. Replacement of the Ser (Ser-98 of PfPKB) in the R*X*R*X*S motif to Ala resulted in a loss of phosphorylation of CBD peptide, indicating that this motif can indeed interact with PfPKB catalytic site (Fig. 3*B*). As expected, a control peptide with an amino acid composition similar to CBD but in scrambled order (scr-CBD) did not show any phosphorylation of scr-CBD (data not shown). Because there was no evidence of Ser-98 phosphorylation in intact PfPKB, we termed this as the "pseudosubstrate" motif.

Consistent with our previous observations (1), NTR when added to ΔPfPKB inhibited its activity. Ca^{2+}/CaM attenuated this inhibition significantly suggesting that NTR interaction with CaM could prevent PfPKB inhibition (Fig. 3*C*). Furthermore direct interaction between ΔPfPKB and NTR could be demonstrated. When NTR was incubated with Ca^{2+}/CaM, it did not interact with ΔPfPKB suggesting that Ca^{2+}/CaM can prevent binding of the NTR (Fig. 3*D*).

Based on the results presented in Figs. 1–3 we propose the following model for PfPKB regulation: PfPKB is most likely held in an inactive conformation by CBD/NTR as the R*X*R*X*S pseudosubstrate motif present in this domain occupies the catalytic cleft of the kinase. Ca^{2+}/CaM binding to CBD induces a conformational change that causes the release of NTR from the catalytic site resulting in PfPKB autophosphorylation and its catalytic activation (Fig. 3*E*).

Regulation of PfPKB by CaM in P. falciparum—Whereas PfPKB is specifically expressed in schizonts/merozoites (1), CaM is present in all intraerythrocytic stages (18). To determine whether PfPKB interacts with CaM in the parasite, PfPKB was immunoprecipitated from schizonts followed by Western blotting for CaM. CaM was co-immunoprecipitated with PfPKB indicating that these proteins associate in the parasite. In contrast, mock immunoprecipitation experiments performed with either preimmune antisera or red blood cell lysates did not show the presence of CaM (Fig. 4*A*). The ability of CaM to activate PfPKB in *P. falciparum* was tested by using W7, a specific CaM inhibitor, which has been used previously to demonstrate its role in erythrocyte invasion (19, 20). Incubation of either schizonts or free merozoites (data not shown) with W7 resulted in a significant loss of PfPKB activity indicating that CaM is a PfPKB regulator *in vivo*. This was further established when addition of purified CaM to the PfPKB-IP from W7-treated parasites led to a significant recovery of PfPKB activity (Fig. 4*B*). Collectively these observations establish that CaM is a regulator of PfPKB in *P. falciparum*. Moreover when PfPKB was immunoprecipitated in the absence of calcium, a significant loss of CaM binding resulted (Fig. 4*C*), suggesting

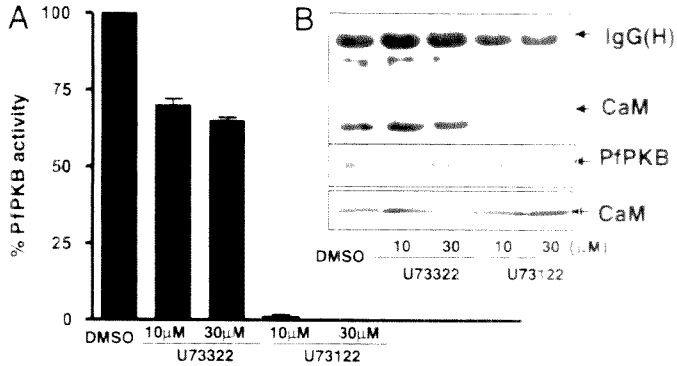

FIGURE 5. **Phospholipase C is an upstream regulator of PfPKB signaling pathway.** *A*, *P. falciparum* schizonts were incubated with the indicated concentrations of either phospholipase C inhibitor U73122 or its analogue U73322 for 30 min, and PfPKB-IP activity was determined. U73122 treatment caused a significant decrease in PfPKB activity. The results are presented as mean ± S.E. of three independent experiments, and the activity of PfPKB in Me$_2$SO (*DMSO*)-treated parasites was considered as 100%. *B*, PfPKB (*top panel*) or whole cell lysates (*bottom panel*) were subjected to Western blotting for CaM and PfPKB. A significant decrease in the amount of CaM co-precipitated with PfPKB was observed only in U73122-treated parasites without altering levels of PfPKB and CaM in whole parasite lysates (*bottom panel*). A representative of three independent experiments is shown.

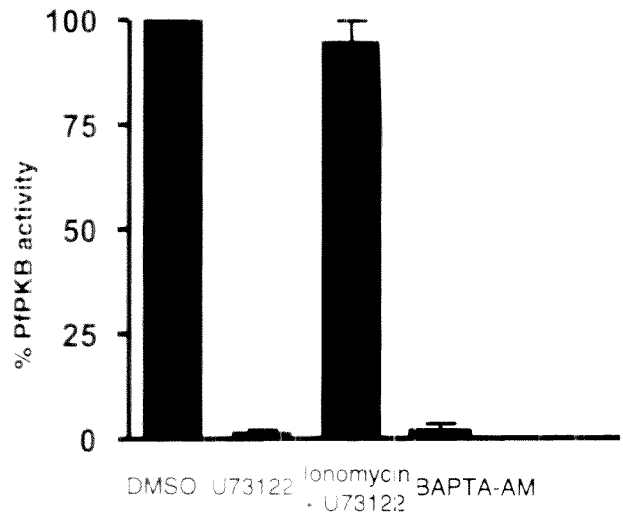

FIGURE 6. **PLC-mediated calcium release controls PfPKB activity.** Schizont stage parasites were treated with U73122 (30 μM) or BAPTA-AM (100 μM) alone or with a combination of U73122 (30 μM) and ionomycin (10 μM), and PfPKB IP-associated activity was measured using crosstide as substrate as described above. The results are presented as mean ± S.E. of three independent experiments relative to the activity of PfPKB in Me$_2$SO (*DMSO*)-treated parasites (100%).

that calcium is necessary for CaM-PfPKB interaction in the parasite.

Phospholipase C-mediated Calcium Release Regulates CaM-PfPKB Interaction—Because experiments described above (Figs. 1 and 4*C*) suggest that the activation of PfPKB by CaM is dependent on calcium, it was important to investigate the mechanism via which parasitic calcium regulates PfPKB. Intracellular calcium levels of the parasite are tightly regulated in *Plasmodium*, and inhibitors of phospholipase C (PLC) (22), which block inositol 1,4,5-trisphosphate formation, prevent release of free calcium from intracellular parasite stores (22, 23). To investigate the role of PLC in PfPKB activation, schizonts were incubated with either U73122, a specific inhibitor of PLC, or its less potent analogue U73322. U73122 treatment resulted in a significant attenuation of PfPKB activity. In contrast, U73322 only caused a marginal effect (Fig. 5*A*). The loss of PfPKB activity was accompanied by a reduction in amount of CaM associated with PfPKB in PLC inhibitor-treated parasites (Fig. 5*B*). Similar inhibition of PfPKB activity was obtained when merozoites were treated with PLC inhibitors[4] (data not shown).

It was important to determine whether PLC-mediated regulation of PfPKB was due to its ability to control intracellular calcium levels. To probe this, parasites were treated with U73122 in the presence of ionomycin, a calcium ionophore that can mobilize calcium. Recovery of PfPKB activity, which was lost due to PLC inhibition (Fig. 6), was observed suggesting that PLC controls PfPKB activity by regulating calcium levels inside the parasite. A cell-permeable intracellular calcium chelator, BAPTA-AM, attenuated PfPKB activity, providing direct evidence that PfPKB is regulated by intracellular calcium (Fig. 6). It is important to indicate that *P. falciparum* has a PLC homologue that shares significant similarity with the catalytic domain of mammalian PLC.[5] In summary, we identified a novel signaling pathway in the malarial parasite that involves activation of PfPKB by CaM and PLC serves as an upstream activator of this pathway as it provides the release of calcium necessary for PfPKB activation.

DISCUSSION

Based on the sequence homologies we had identified PfPKB as a PKB-like kinase in *P. falciparum*. The PI3K-PKB pathway is a major player in a wide variety of cellular processes in mammalian cells (24, 25). *Plasmodium* possesses only one PI3K homologue[5] and PfPKB, a protein kinase B-like enzyme in *P. falciparum* (1). PfPKB shares several common features with the catalytic domain of PKB such as the regulatory motif in the T-loop that has a regulatory Ser-277, which is in a location similar to Thr-308 of PKB-1.

PKB is regulated by interaction of 3′-phosphorylated phosphoinositides with its N-terminal PH domain (26) and phosphorylation of PKB at Thr-308 by phosphoinositide-dependent kinase-1. In contrast, PfPKB is activated by autophosphorylation of Ser-277. The NTR of PfPKB does not have a PH or any other modular domain but it prevents PfPKB activation (1). Because NTR failed to exhibit any similarity with proteins in the non-redundant data base, it was difficult to postulate its mode of regulation. Biochemical studies performed with PfPKB indicated that its directly regulated by Ca^{2+}-CaM. Whereas PfPKB is expressed mainly in the schizont merozoite stages, our recent findings suggest that PI3K homologue in *P. falciparum* may be present mainly during merozoite stages[6]; this also fits in well with a phosphoinositide-independent mechanism of PfPKB regulation.

CaM interacts with segments of proteins that are rich in basic and hydrophobic residues and have the propensity of forming α-helices. Typically, hydrophobic residues in CBDs of target proteins are critical for anchoring them to hydrophobic

[4] P. Sharma, unpublished results.

[5] S. Kumar and P. Sharma, unpublished information.

[6] S. Kumar and P. Sharma, unpublished results.

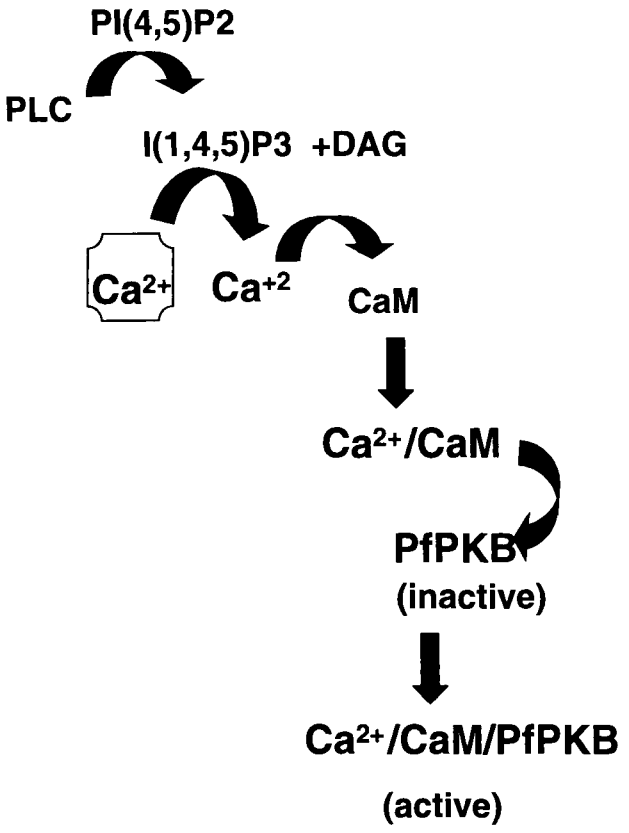

FIGURE 7. **A novel signaling pathway in *P. falciparum*.** Studies described in this report suggest that CaM activates PfPKB in a calcium-dependent manner by interacting with a CBD in its N terminus (Figs. 1 and 2). Phospholipase C, the enzyme involved in generation of inositol 1,4,5-trisphosphate (*I(1,4,5)P3*), acts as an upstream regulator of this pathway (Fig. 5) as inositol 1,4,5-trisphosphate may facilitate the release of calcium needed for PfPKB activation. *PI(4,5)P2*, phosphatidylinositol 4,5-bisphosphate; *DAG*, diacylglycerol.

pockets present in CaM. These residues may be separated by 10, 14, or 16 residues as shown in examples illustrated in Fig. 2*A* (16, 27). The number of CBDs that do not strictly follow these rules has grown; moreover there are CBDs that use only one of these residues for interaction (27, 28). These studies reflect the diversity in interaction of CaM with its targets. The CBD of PfPKB has a Leu-6 and Ile-20 that are spaced by 15 residues and may anchor binding to CaM; this is a minor diversion from standard examples shown in Fig. 2*A*.

Mapping of the CBD led to identification of an *RXRXS* pseudosubstrate motif in the NTR and facilitated the elucidation of the mechanism of PfPKB activation by CaM. These studies could potentially be utilized to devise tools for intervening with PfPKB activation.

Free calcium levels in the parasite are controlled by PLC as it generates inositol 1,4,5-trisphosphate, which releases calcium from the intracellular stores (21). PLC inhibitor U73122 has been successively used in *Plasmodium* to block calcium release (22). Using this inhibitor we were able to demonstrate that PLC is the upstream regulator of PfPKB as it mediates calcium release crucial for PfPKB activation. These data provide a direct link between PfPKB and PLC-mediated calcium signaling (Fig. 7).

In silico analyses suggest that *Plasmodium* may lack typical CaM-dependent protein kinases, and more strikingly a protein kinase C-like enzyme seems to be absent (4). Given its versatility in eukaryotic signaling, lack of a protein kinase C-like enzyme in *Plasmodium* was indeed surprising. Protein kinase C belongs to the same AGC class of kinases as cAMP-dependent protein kinase and PKB, which share significant homology in their catalytic domain region. For instance, PKB and protein kinase C have ~67% similarity in their catalytic domains. In addition to the similarity between PfPKB and PKB, it is important to note that PfPKB also shares reasonable homology (~64%) with mammalian protein kinase C (1). We used this information to identify a protein kinase C inhibitor, Go6983, as an inhibitor of PfPKB. When added to schizont stage cultures, this inhibitor blocked ring formation suggesting that PfPKB may be involved in schizont-to-ring transition (1); no other parasitic stage was affected by this compound. Schizont/merozoite-specific expression (1) may allow PfPKB to play a role in early/late stages of parasite life cycle.

Release of intracellular calcium is critical for various parasitic functions (29). Importantly it appears to be indispensable for successful erythrocyte invasion (30, 31). CaM is known to localize at strategic locations in merozoites and control invasion (19, 20). However, the lack of identity of Ca^{2+}/CaM targets leaves a gap in understanding their role in the parasite life cycle. We have shown that CaM interacts and regulates PfPKB in response to upstream events in the schizont. Therefore, it is possible that PfPKB may be one of the major targets via which CaM may control important parasitic processes like invasion. Identification of downstream targets of PfPKB will help further in unraveling the function of this pathway.

Acknowledgment—We thank Dr. Pillai from Malaria Research Center for initial help with parasite cultures.

REFERENCES

1. Kumar, A., Vaid, A., Syin, C., and Sharma, P. (2004) *J. Biol. Chem.* **279,** 24255–24264
2. Harrison, T., Samuel, B. U., Akompong, T., Hamm, H., Mohandas, N., Lomasney, J. W., and Haldar, K. (2003) *Science* **301,** 1734–1736
3. Ward, G. E., Fujioka, H., Aikawa, M., and Miller, L. H. (1994) *Exp. Parasitol.* **79,** 480–487
4. Ward, P., Equinet, L., Packer, J., and Doerig, C. (2004) *BMC Genomics* **5,** 79
5. Gardner, M. J., Hall, N., Fung, E., White, O., Berriman, M., Hyman, R. W., Carlton, J. M., Pain, A., Nelson, K. E., Bowman, S., Paulsen, I. T., James, K., Eisen, J. A., Rutherford, K., Salzberg, S. L., Craig, A., Kyes, S., Chan, M. S., Nene, V., Shallom, S. J., Suh, B., Peterson, J., Angiuoli, S., Pertea, M., Allen, J., Selengut, J., Haft, D., Mather, M. W., Vaidya, A. B., Martin, D. M., Fairlamb, A. H., Fraunholz, M. J., Roos, D. S., Ralph, S. A., McFadden, G. I., Cummings, L. M., Subramanian, G. M., Mungall, C., Venter, J. C., Carucci, D. J., Hoffman, S. L., Newbold, C., Davis, R. W., Fraser, C. M., and Barrell, B. (2002) *Nature* **419,** 498–511
6. Billker, O., Dechamps, S., Tewari, R., Wenig, G., Franke-Fayard, B., and Brinkmann, V. (2004) *Cell* **117,** 503–514
7. Merckx, A., Le, R. K., Nivez, M. P., Dorin, D., Alano, P., Gutierrez, G. J., Nebreda, A. R., Goldring, D., Whittle, C., Patterson, S., Chakrabarti, D., and Doerig, C. (2003) *J. Biol. Chem.* **278,** 39839–39850
8. Khan, S. M., Franke-Fayard, B., Mair, G. R., Lasonder, E., Janse, C. J., Mann, M., and Waters, A. P. (2005) *Cell* **121,** 675–687
9. Reininger, L., Billker, O., Tewari, R., Mukhopadhyay, A., Fennell, C., Dorin-Semblat, D., Doerig, C., Goldring, D., Harmse, L., Ranford-Cartwright, L., Packer, J., and Doerig, C. (2005) *J. Biol. Chem.* **280,**

31957–31964
10. Tewari, R., Dorin, D., Moon, R., Doerig, C., and Billker, O. (2005) *Mol. Microbiol.* **58,** 1253–1263
11. Alessi, D. R., Andjelkovic, M., Caudwell, B., Cron, P., Morrice, N., Cohen, P., and Hemmings, B. A. (1996) *EMBO J.* **15,** 6541–6551
12. Trager, W., and Jensen, J. B. (1976) *Science* **193,** 673–675
13. Sun, X. T., Li, B., Zhou, G. M., Tang, W. Q., Bai, L., Sun, D. Y., and Zhou, R. G. (2000) *Plant Cell Physiol.* **41,** 804–810
14. Robson, K. J., Gamble, Y., and Acharya, K. R. (1993) *Philos. Trans. R. Soc. Lond. B Biol. Sci.* **340,** 39–53
15. Cross, D. A., Alessi, D. R., Cohen, P., Andjelkovich, M., and Hemmings, B. A. (1995) *Nature* **378,** 785–789
16. Hoeflich, K. P. and Ikura, M. (2002) *Cell* **108,** 739–742
17. Obata, T., Yaffe, M. B., Leparc, G. G., Piro, E. T., Maegawa, H., Kashiwagi, A., Kikkawa, R., and Cantley, L. C. (2000) *J. Biol. Chem.* **275,** 36108–36115
18. Cowman, A. F., and Galatis, D. (1991) *Exp. Parasitol.* **73,** 269–275
19. Matsumoto, Y., Perry, G., Scheibel, L. W., and Aikawa, M. (1987) *Eur. J. Cell Biol.* **45,** 36–43
20. Scheibel, L. W., Colombani, P. M., Hess, A. D., Aikawa, M., Atkinson, C. T., and Milhous, W. K. (1987) *Proc. Natl. Acad. Sci. U. S. A.* **84,** 7310–7314
21. Garcia, C. R. (1999) *Parasitol. Today* **15,** 488–491
22. Hotta, C. T., Markus, R. P., and Garcia, C. R. (2003) *Braz. J. Med. Biol. Res.* **36,** 1583–1587
23. Gazarini, M. L., Thomas, A. P., Pozzan, T., and Garcia, C. R. (2003) *J. Cell Biol.* **161,** 103–113
24. Scheid, M. P., and Woodgett, J. R. (2001) *Nat. Rev. Mol. Cell. Biol.* **2,** 760–768
25. Vanhaesebroeck, B., and Alessi, D. R. (2000) *Biochem. J.* **346,** 561–576
26. Alessi, D. R., and Cohen, P. (1998) *Curr. Opin. Genet. Dev.* **8,** 55–62
27. Yamauchi, E., Nakatsu, F., Matsubara, M., Kato, H., and Taniguchi, H. (2003) *Nat. Struct. Biol.* **10,** 226–231
28. Rhoads, A. R., and Friedberg, F. (1997) *FASEB J.* **11,** 331–340
29. Biagini, G. A., Bray, P. G., Spiller, D. G., White, M. R., and Ward, S. A. (2003) *J. Biol. Chem.* **278,** 27910–27915
30. Garcia, C. R., Dluzewski, A. R., Catalani, L. H., Burting, R., Hoyland, J., and Mason, W. T. (1996) *Eur. J. Cell Biol.* **71,** 409–413
31. McCallum-Deighton, N., and Holder, A. A. (1992) *Mol. Biochem. Parasitol.* **50,** 317–323

THE JOURNAL OF BIOLOGICAL CHEMISTRY VOL. 282, NO. 15, pp. 11499–11508, April 13, 2007

Traffic to the Malaria Parasite Food Vacuole

*A NOVEL PATHWAY INVOLVING A PHOSPHATIDYLINOSITOL 3-PHOSPHATE-BINDING PROTEIN**[S]

Received for publication, November 29, 2006, and in revised form, January 29, 2007 Published, JBC Papers in Press, February 8, 2007, DOI 10.1074/jbc.M610974200

Michael T. McIntosh[‡1,2], **Ankush Vaid**[§1,3], **H. Dean Hosgood**[‡], **Justin Vijay**[§], **Anindita Bhattacharya**[§], **Mayurbhai H. Sahani**[§], **Pavlina Baevova**[‡], **Keith A. Joiner**[‡4], **and Pushkar Sharma**[§5]

From the [‡]*Department of Medicine, Yale University School of Medicine, New Haven, Connecticut 06520 and* [§]*Eukaryotic Gene Expression Laboratory, National Institute of Immunology, New Delhi 110067, India*

Phosphatidylinositol 3-phosphate (PI3P) is a key ligand for recruitment of endosomal regulatory proteins in higher eukaryotes. Subsets of these endosomal proteins possess a highly selective PI3P binding zinc finger motif belonging to the FYVE domain family. We have identified a single FYVE domain-containing protein in *Plasmodium falciparum* which we term FCP. Expression and mutagenesis studies demonstrate that key residues are involved in specific binding to PI3P. In contrast to FYVE proteins in other organisms, endogenous FCP localizes to a lysosomal compartment, the malaria parasite food vacuole (FV), rather than to cytoplasmic endocytic organelles. Transfections of deletion mutants further indicate that FCP is essential for trophozoite and FV maturation and that it traffics to the FV via a novel constitutive cytoplasmic to vacuole targeting pathway. This newly discovered pathway excludes the secretory pathway and is directed by a C-terminal 44-amino acid peptide domain. We conclude that an FYVE protein that might be expected to participate in vesicle targeting in the parasite cytosol instead has a vital and functional role in the malaria parasite FV.

Malaria parasites inflict a tremendous global burden on the health and productivity of human kind. Among the species predominantly infective to humans, *Plasmodium falciparum* stands out as responsible for more than half of all infections and for causing the most severe forms of the disease resulting in the death of more than 1.5 million people annually (1). Malaria parasites circulate in the human host by repeated invasion and development within the human erythrocyte. During the 48-h cycle of development, parasites endocytose 80–90% of the host cell cytosol and hemoglobin. Specialized proteases are believed to traffic to vesicles containing hemoglobin to initiate the digestion of hemoglobin on route to its final destination, the lysosomal compartment, or parasite food vacuole (FV)[6] (2). Although the endocytic process is characterized by morphologically distinct parasite structures including specialized structures for the uptake of hemoglobin (cytostomes), hemoglobin-containing vesicles, and a single FV (3), the contribution of protein components to the endocytic pathway required for membrane trafficking, molecular signaling, effector protein recruitment, and formation of these structures remains unknown.

Phosphatidylinositol 3-phosphate (PI3P) plays a fundamental regulatory role in endocytic systems of higher eukaryotes (4–6). Rab5, a universally conserved component of early endosomes, recruits the type III PI 3-kinase in mammals and yeast. Hence, the product of this kinase, PI3P, is found in the early endosomes of mammals and is likewise restricted to the endocytic pathway in yeast (6–8). Various other endosomal regulatory proteins bind PI3P and thereby localize to endocytic compartments in yeast and mammals (9). Many among these including the early endosomal autoantigen-1 (EEA1) contain a highly selective PI3P binding zinc finger motif belonging to the FYVE domain family (conserved in Fab1, YOTB, Vac1, and EEA1) (9).

Although *P. falciparum* appears limited with regard to Rab5 effectors and other endocytic machinery, it does possess a phosphatidylinositol biosynthetic pathway (10). We, therefore, asked if *P. falciparum* possesses functional FYVE domain proteins. Using a bioinformatics approach we identified a single FYVE domain-containing protein encoded in the parasite genome. Surprisingly, this protein did not localize to endocytic structures as would be predicted for an FYVE domain family protein but, rather, localized discreetly to the lumen of the FV, a lysosomal compartment characterized by the presence of hemozoin (a crystallized heme byproduct of hemoglobin digestion). By identifying the domain responsible for targeting to the FV, we not only explain this unexpected result but identify a new direct trafficking pathway between the parasite cytosol and the parasite FV.

* This work was supported by a senior research fellowship of The Wellcome Trust (to P. S.) and grants from the Ellison Foundation and the Burroughs Wellcome Fund New Initiatives in Malaria Research (to K. A. J.). The costs of publication of this article were defrayed in part by the payment of page charges. This article must therefore be hereby marked "*advertisement*" in accordance with 18 U.S.C. Section 1734 solely to indicate this fact.

[S] The on-line version of this article (available at http://www.jbc.org) contains supplemental Fig. S1.

[1] These authors made equal contributions.

[2] To whom correspondence may be addressed: Yale University School of Epidemiology and Public Health, 60 College St., New Haven, CT 06520. Tel.: 203-785-3458; E-mail: michael.mcintosh@yale.edu.

[3] Recipient of a Junior Research Fellowship from the Center for Scientific and Industrial Research, India.

[4] Current address: Office of the Dean, College of Medicine, University of Arizona, Tucson AZ 85724-5017.

[5] To whom correspondence may be addressed. Tel.: 91-11-26717123 (ext. 791); Fax: 91-11-26162125; E-mail: pushkar@nii.res.in.

[6] The abbreviations used are: FV, food vacuole; EEA1, early endosomal autoantigen-1; AD, activation domain; BD, DNA binding domain; ER, endoplasmic reticulum; BFA, brefeldin A; Cvt, cytoplasmic to vacuole trafficking; TGN, trans-Golgi network; HRPII, histidine-rich protein II; PI3P, phosphatidylinositol (PI) 3-phosphate; GFP, green fluorescent protein.

EXPERIMENTAL PROCEDURES

In Vitro Cultivation of P. falciparum—*P. falciparum* strain 3D7 (obtained from MR4) was employed in experiments contributing to Figs. 4 and 5, whereas strain FCR3 (a gift from Dr. Kasturi Haldar) was used to obtain Figs. 6–9. Parasites were maintained in 5% CO_2 (for FCR3) or 90% N2, 5% CO_2, and 5% O_2 for (3D7) in leukocyte-free erythrocytes of blood group A+ (American Red Cross) at 5% hematocrit and cultured in RPMI 1640 medium (Invitrogen) supplemented with 25 mM HEPES, sodium bicarbonate (2 g·liter^{-1}), gentamicin (1 μg·ml^{-1}), 92 μM hypoxanthine and contained 10% human serum, type AB as described (11). Parasite synchronization was achieved by isolation of late stage trophozoites on Percoll sorbitol gradients as described (12) followed by reintroduction into culture with fresh red blood cells. Four hours after the first detection of ring stage parasites, cultures were treated with 5% sorbitol (13) to lyse all remaining late stage parasites. This yielded highly synchronous cultures.

Cloning of FCP and Plasmid Constructs—Using open reading frame-specific primers with appropriate 5′ end restriction sites, FCP cDNA was reverse transcription-PCR amplified from total asexual stage *P. falciparum* RNA using RT-Superscript II (Invitrogen) and Kod hot start DNA polymerase (Novagen Inc.). For yeast 2-hybrid analysis, FCP cDNA was appropriately digested and ligated into yeast two-hybrid vectors pACT-2 and pGBT-9 (Invitrogen) between the BamHI and XhoI sites of pACT-2 and EcoRI and BamHI sites of pGBT-9. Ligations were made in-frame and downstream of the GAL4 activation domain (AD) or DNA binding domain (BD) to obtain pAD-FCP and pBD-FCP. The cDNA sequence of cloned FCP was identical to that of the putative gene (Pf14_0574) represented in the 3D7 *P. falciparum* genome data base.

For GFP expression studies in *Plasmodium*, the eGFP gene of pEGFP-C2 (Invitrogen) was replaced with the GFP-M2 gene of pHDGFP (14). This yielded the plasmid pGFP-M2-C2. Subsequently FCP was subcloned from the yeast expression vector pBD-FCP into the EcoRI and SalI sites of pGFP-M2-C2 such that the gene fusion was in-frame and downstream of GFP-M2. Domain deletions were constructed from pBD-FCP and converted to GFP-M2 gene fusions by ligation between the EcoRI and SalI sites of pGFP-M2-C2. FCP-Δ-c-coil was obtained by digestion of pBD-FCP with BglII and BamHI followed by blunt ending and self-ligation. This removed the entire C terminus including the complete coiled-coil domain. FCP-Δ-FYVE was obtained by digestion of pBD-FCP with KpnI and BglII followed by blunt ending and self-ligation. This deleted only the FYVE domain and kept the N terminus and remainder of FCP in-frame. FCP-Δ-c44 was obtained by digestion of pBD-FCP with StyI and BamHI followed by blunt ending and self-ligation. This removed the C-terminal conserved domain encoding the final 44 amino acids of FCP. Transfer to pGFP-M2-C2 yielded the following plasmid constructs: pGFP-F-Δ-c-coil, pGFP-F-Δ-FYVE, and pGFP-F-Δ-c44. To explore the function of the C-terminal 44 amino acids, pGFP-44aa was constructed by PCR amplification of the C-terminal 132 bp encoding the 44-amino acid peptide using forward and reverse primers bearing EcoRI and SalI sites, respectively, and cloning into the EcoR1 and SalI sites of pGFP-M2-C2. Primers (GFPM2-ATTB1, 5′-GGGGACAAGTTTGTACAAAAAAGCAGGCTAAAAATGAGTAAAGGAGAAGAACTTTTC-3′, and GFP-ATTB2, 5′-GGGGACCACTTTGTACAAGAAAGCTGGGTTGATCAGTTATCTAGATCCGG-3′) flanking the GFP gene fusion cassettes in the above plasmids, which contained 5′ attB1 and attB2 recombination sites, respectively, were used to PCR amplify all GFP-gene fusions such that they were suitable for cloning into pDONR-21 (Invitrogen) using the BP reaction and Gateway™ recombination cloning system (Invitrogen). Subsequent LR reactions (Invitrogen) with the *Plasmodium* Gateway™ destination vector pHH1-DR0 28-DEST (15) (a kind gift from Prof. Tina Skinner-Adams, Queensland Institute of Medical Research, Australia) resulted in the following *Plasmodium* GFP expression vectors: EXP- GFPM2, EXP-GFP-FCP, EXP-GFP-FCPΔ-c-coil, EXP-GFP-FCPΔ-c44, EXP-GFP-FCPΔ-FYVE, EXP-GFP-44aa. These expression vectors all utilize the *Plasmodium* HSP86 5′-untranslated region as a constitutive promoter for the expression of the GFP gene fusions

For protein expression studies, FCP cDNA was cloned in PQE-UA vector (Qiagen) to facilitate its expression as an N-terminal His_6-tagged protein. Site-directed mutagenesis was performed by using the QuikChange kit (Stratagene).

Recombinant Protein Expression in E. coli and Anti-FCP Antiserum Production—BL21-RIL *E. coli* (Stratagene) was transformed with PQE-FCP plasmid or its variants. Cultures were grown in LB media containing 100 μg/ml ampicillin and 25 μg/ml chloramphenicol. Recombinant protein was induced at mid-logarithmic phase (A_{600} value of 0.6) by the addition of 1 mM isopropyl 1-thio-β-D-galactopyranoside either at 37 °C for 4 h or at 18 °C for 14 h. Bacterial cells were harvested by centrifugation at 4000 × *g* for 30 min and suspended in buffer A (50 mM Tris, pH 7.4, 6 M urea, 500 mM NaCl) followed by sonication. Cell lysates were clarified by centrifugation at 20,000 × *g* for 30 min at 4 °C. Subsequently, supernatant was incubated with nickel-nitrilotriacetic acid-agarose (Qiagen) for 12 h at 4 °C. After washes in buffer A, recombinant His_6-tagged proteins were eluted in 50 mM Tris, pH 8.0, containing 500 mM NaCl, 300 mM imidazole, 1 mM dithiothreitol, and 6 M urea. Eluted proteins were renatured by dialysis against buffer containing reduced amounts (4 to 0 M) of urea. Refolded recombinant proteins were analyzed by gel filtration and SDS-PAGE, and a protein band of the expected molecular mass of 37 kDa was detected by Coomassie staining. To confirm the identity of the recombinant protein, the 37-kDa protein band was excised and subjected to tryptic digest and mass spectrometric analysis by the Institute of Molecular Medicine, The Chatterjee Group, New Delhi (supplemental Fig. S1). To raise anti-sera against FCP, 100 μg of recombinant FCP was emulsified with complete Freund's adjuvant and used to raise antisera in mice and rabbits.

Dot-blot Phosphoinositide Binding Assays—Dot-blot assays were performed as described previously (16). Briefly, various phosphoinositides were serially diluted and spotted on nitrocellulose membrane and air-dried for 2 h. Subsequently, the membrane was blocked with 3% bovine serum albumin in buffer A (50 mM Tris-HCl, pH 7.4, 150 mM sodium chloride, 0.1% Tween 20) for 3 h. The membrane was incubated with recombinant His_6-FCP (0.5 μg/ml) or its variants diluted in

blocking buffer for 12 h at 4 °C. The membrane was washed 5 times with buffer A before 3 h of incubation with anti-His_6 antibody (BD Biosciences). Subsequently, the membrane was incubated with horseradish peroxidase-labeled anti-mouse IgG, and phosphatidylinositol-bound protein was detected by chemiluminescence.

Yeast Two-hybrid Growth Assays—Yeast two-hybrid liquid culture growth assays were performed as previously described (17). Yeast were transformed with all possible paired plasmid combinations as well as with individual plasmids as controls, and protein-protein interactions were determined based on growth in His-dropout medium. Stringency was further assessed in increasing concentrations of 3-amino-1,2,4-trizol.

Immunoblotting and Immunolocalization—For immunoblot experiments described in Fig. 5, parasite material was separated from erythrocytes and parasitophorous vacuole-derived material by lysis in 0.1% saponin analogous to a previously published procedure (33). An equal number of parasites fractionated into a pellet or concentrated supernatant was denatured by boiling in 2% SDS, applied to SDS-PAGE, and subsequently transferred to nitrocellulose. Immunoblotting was performed using rabbit anti-FCP and horseradish peroxidase-labeled goat anti-rabbit IgG. Blots were developed using a WestDura ECL kit (Pierce).

For immunofluorescence, parasitized red blood cells were spread on slides and fixed in methanol for 10 min. Subsequently, slides were blocked with 3% bovine serum albumin for 12 h at 4 °C and incubated with a 1:50 dilution of mouse anti-FCP antisera. After washing with phosphate-buffered saline, slides were stained with goat anti-mouse IgG conjugated to Texas Red. Cells were visualized on a Zeiss LSM510 confocal microscope equipped with a CCD camera. Control experiments were performed using preimmune bleeds.

For immunoelectron microscopy, parasites were fixed in 4% paraformaldehyde (EM Polysciences Inc.), 0.1% glutaraldehyde (EM Polysciences Inc.), and 0.25 M HEPES, pH 7.4, embedded in 1× phosphate-buffered saline containing 10% bovine skin gelatin (Sigma) and incubated at 4 °C in cryo-protectant containing 10% polyvinylpyrolidone and 2.7 M sucrose. Subsequently, parasite blocks were applied to pins, snap-frozen in liquid nitrogen, and subjected to ultra thin sectioning in a liquid nitrogen-cooled cryo-ultramicrotome. Sections were applied to nickel-coated grids, incubated with a 1:1000 dilution of affinity-purified rabbit anti-FCP IgG at 25 °C, and stained with gold-conjugated goat anti-rabbit IgG. Electron micrographs were obtained digitally by a CCD camera using a Philips Techni Bio-Twin electron microscope.

Parasite Transfection, Localization, and Dominant Negative Effects—Transient transfections of malaria parasites with EXP-GFP vectors (see above details) were performed by a modification of the previously described preloading technique (18). 200 μl of packed red blood cells were washed once in incomplete cytomix (19) (containing 120 mM KCl, 0.15 mM $CaCl_2$, 2 mM EGTA, 5 mM $MgCl_2$, 10 mM K_2HPO_4/KH_2PO_4, and 25 mM Hepes, pH 7.6) and then resuspended to 400 μl in ice-cold incomplete cytomix. Red blood cells were then preloaded with 50 μg of plasmid DNA by electroporation in a ECM630 Electro Cellular Manipulator™ (BTX) at settings of 310 V, 25 ohms, and 950 microfarads. To ensure synchronous transfections and facilitate morphological interpretation of potential dominant negative effects, cultures were synchronized as described above. Subsequently, late stage parasites were once again purified by Percoll sorbitol gradient as described above and then added to preloaded red blood cells and cultured for 40–46 h before microscopic analysis for GFP expression and morphological detail. Microscopy was performed at 1000× magnification using a Nikon Optiphot II microscope equipped with epifluorescence and Nomarski optics or at 1000× using a Zeiss Axioscope with epifluorescence. FV localization was verified by photography of cells under simultaneous fluorescence and bright field phase contrast at low light levels. Images were collected by CCD camera, labeled in Adobe PhotoShop 6.0 (Adobe), and arranged in Adobe Illustrator 10 (Adobe).

RESULTS

Plasmodium Encodes a Single FYVE Domain Protein—Sequence alignment of FYVE domains yielded the consensus sequence R(R/K)HHCR, which was used to search the *P. falciparum* genome data base. This revealed only a single FYVE domain-containing protein (Pf14_0574). Analysis by SOCKET (20) indicated the presence of a coiled-coil domain (residues 163–266) downstream of the FYVE zinc finger domain (residues 42–92). Thus, we named the protein FCP for FYVE and coiled-coil domain-containing protein. An additional gene (PF13_0055), annotated as encoding a potential FYVE domain, more closely resembled a RING domain and, hence, was not investigated further.

Sequencing of *FCP* cDNA confirmed a lack of introns, and comparison of the amino acid sequence with other orthologous counterparts indicated that *FCP* was highly conserved with 70–80% amino acid identity within the malaria parasite genus *Plasmodium* (Fig. 1*A*). Additional searches indicated that at least two potential FYVE domain-containing proteins exist in the related parasite *Toxoplasma gondii*. TBLASTN searches excluding the FYVE domains of other family members including EEA1, Hrs, YOT1, Fab1, and Vac1 failed to identify genes encoding proteins of significant homology in *P. falciparum*. This provided the first indication that FCP might not function in the same fashion as the endosomal FYVE proteins of higher eukaryotes.

X-ray crystal structures for *Saccharomyces cerevisiae* Vps27p, *Drosophila melanogaster* Hrs, and human EEA1 have further defined the secondary and tertiary structure of the FYVE domain as containing a core fold similar to that of the RING domain (21). *FCP* encodes all of the conserved residues and attributes known to be required for PI3P binding by other FYVE domain proteins. Among these are eight invariant zinc-coordinating cysteine residues arranged in four *CXXC* motifs, an upstream *WXXD* motif, and a downstream RVC motif, each intimately involved in PI3P binding (Fig. 1*B*). In addition, the glycine residue immediately adjacent to the second pair (*CXXC*) of zinc-coordinating cysteines is invariant among all known FYVE domain proteins and is believed to provide flexibility required for formation of the core fold of the domain (Fig. 1*B*). The R(R/K)HHCR consensus sequence is known to be the principal site of PI3P binding (Fig. 1*B*).

FCP Specifically Interacts with PI3P—To better understand phosphoinositide interactions with FCP, we performed lipid

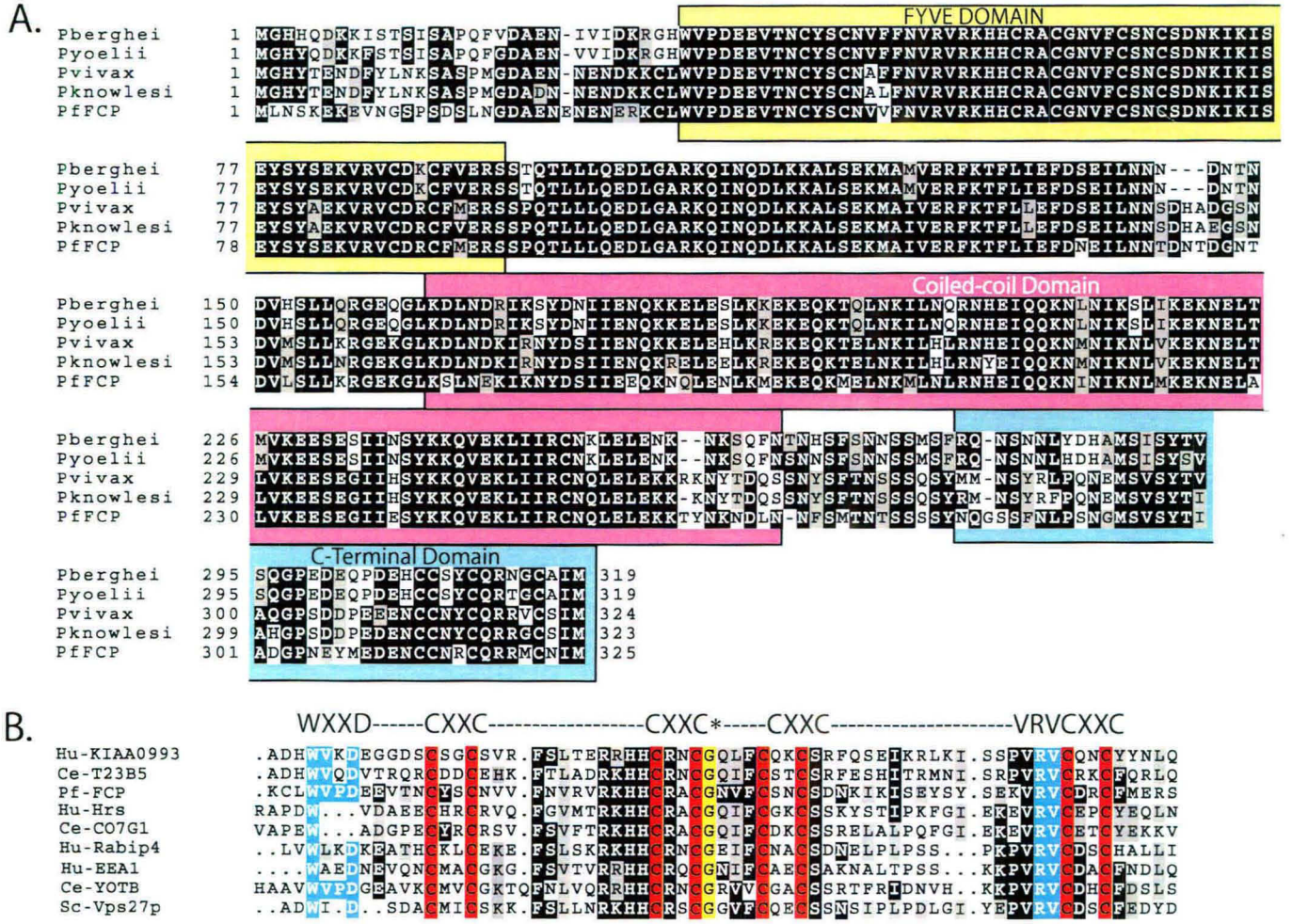

FIGURE 1. **Alignments of malaria parasite FCP proteins and FYVE domains.** *A*, the sequence of *P. falciparum* FCP was aligned with its orthologous counterparts from rodent malaria species *Plasmodium berghei* and *Plasmodium yoelii*, and primate malaria species *Plasmodium vivax* and *Plasmodium knowlesi*. A high level of conservation is shared among the FYVE domains (*yellow*), coiled-coil domains (*magenta*), and C termini (*blue*). *B*, the FYVE domain of FCP was aligned with the FYVE domains of other proteins found in *S. cerevisiae* (*Sc*), *Homo sapiens* (*Hu*), and *Caenorhabditis elegans* (*Ce*). *Pf*, *P. falciparum*. Conserved motifs include W*XX*D (*blue*), eight zinc coordinating cysteine residues arranged in four *CXXC* clusters (*red*), the PI3P binding site R(R/K)HHCR with an adjacent flexible glycine residue (*yellow*), and the RVC motif (*blue*).

dot-blot assays using recombinant wild type and site-directed mutants of FCP. Wild type FCP bound specifically to PI3P (Fig. 2*B*). Deletion of the FYVE domain (data not shown) resulted in a complete loss of phosphoinositide binding as did a site-directed substitution K55A (Fig. 2*B*), which resides within the conserved motif R(R/K)HHCR (Figs. 1*B* and 2*A*). The crystal structure of the EEA1 FYVE domain bound to inositol 1,3-diphosphate has revealed that amino acid residues form a coordination network with the 1′ and 3′ phosphates of PI3P, and it has been hypothesized that these residues may lend specificity to FYVE-PI3P interaction (22). To test this we replaced all flanking arginines (Arg-52, Arg-54, and Arg-59) with neutral alanine residues. This three-amino acid substitution resulted in a loss in specificity for PI3P as indicated by increased binding to phosphoinositides, PI 3,4,5-triphosphate and PI 4,5-diphosphate. This loss in PI3P binding specificity demonstrated that indeed a critical interaction does exist between these basic residues and the 1′ and 3′ phosphates of PI3P (Figs. 2, *A* and *B*).

FCP Self-associates—Several FYVE proteins have been shown to dimerize by virtue of a coiled-coil domain, thereby increasing their avidity for PI3P (23, 24). For example, EEA1

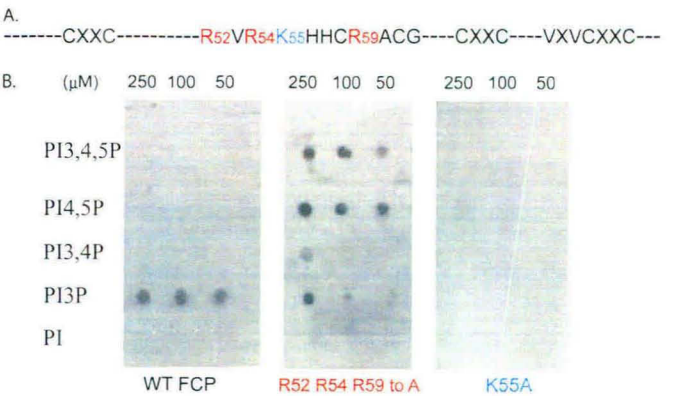

FIGURE 2. **FCP binds PI3P specifically.** *A*, a schematic of the FYVE domain is shown. Basic residues mutated to test functional binding to phosphoinositides included K55 (*blue*) changed to alanine or three arginine residues Arg-52, Arg-54, and Arg-59 (*red*) simultaneously changed to alanine. *B*, binding of recombinant wild type FCP or its mutants (*K55A*) or (*R52 R54 R59 to A*) to varying concentrations of phospho (*P*)-inositides were assayed. WT, wild type.

dimerizes when bound by Rab5 and then simultaneously binds two PI3P molecules in the early endosome (25). In this way EEA1 is believed to participate in tethering of opposing vesicu-

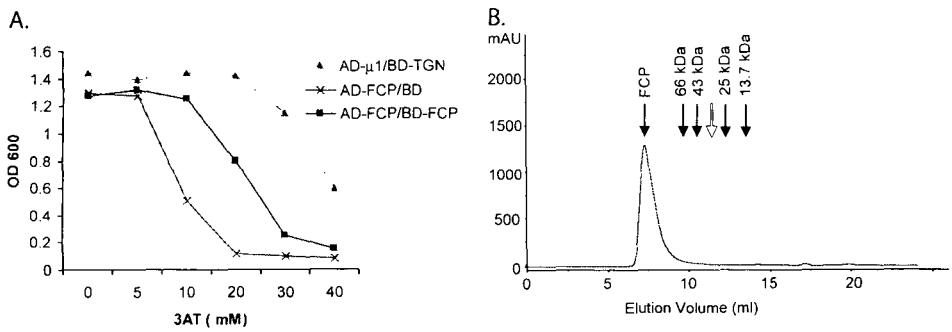

FIGURE 3. **Self-association of FCP.** *A*, a liquid yeast two-hybrid growth assay (17) was used to assess the ability of FCP to self-interact. Separate gene fusions of FCP were constructed by fusing cDNAs to the C terminus of either the GAL4 *AD* or GAL4 DNA *BD* and expressed in yeast. Growth (expressed as optical density of culture at 600 nm) in HIS− medium containing increasing concentrations of the promoter inhibitor 3-amino-1,2,4-trizol (*3AT*) was indicative of a interaction between proteins. An interaction was evident between AD-FCP and BD-FCP. The positive control for protein-protein interaction consisted of the human μ1 chain fused to the AD and a triplicate SDYQRL motif of the TGN38 protein known to bind the μ chain (47). Shown are the positive control, AD-human μ1 paired with BD-TGN, negative control, AD-FCP paired with pGBT-9, and experimental sample AD-FCP paired with BD-FCP. *B*, affinity-purified His_6-FCP was subjected to gel filtration chromatography on a 24-ml Superdex-75 column using an Akta Prime system (Amersham Biosciences). The column was precalibrated using bovine serum albumin (66 kDa, eluting at 9.5 ml), ovalbumin (43 kDa, eluting at 10.8 ml), chymotrypsinogen A (25 kDa, eluting at 12.8 ml), and ribonuclease A (13.7 kDa, eluting at 13.8 ml) as standards. FCP protein was not found to elute at the expected monomeric size of 37 kDa (*white arrow*). Instead, elution of FCP at 7.5 ml was close to the expected void volume of the column, suggesting that it may predominate as a dimer.

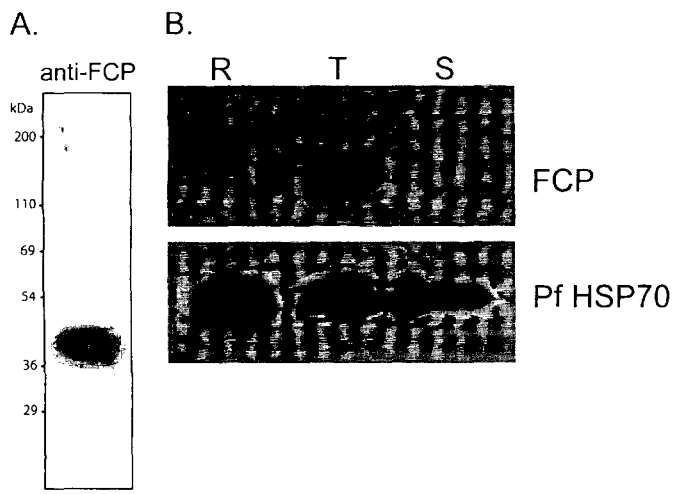

FIGURE 4. **Stage-specific expression of FCP in *P. falciparum*.** *A*, a single band at 37–40 kDa was detected by Western blot using *anti-FCP* antisera raised in mice. *B*, stage-specific Western blots revealed FCP expression during the trophozoite stage (*T*) and a lack of FCP expression in ring (*R*) and schizont (*S*) stages. The loading control *PfHSP70* was found to be equally expressed throughout all stages. Equal quantities of total protein, 20 μg, were loaded per lane.

lar and target membranes during the homotypic fusion of early endosomes (26). To test this hypothesis we employed a yeast two-hybrid growth assay (17). Yeast expression plasmids were constructed by fusing the yeast GAL4 AD or GAL4 DNA BD to the N terminus of FCP.

Persistent growth of yeast in HIS− medium in increasing concentrations of 3-amino-1,2,4-trizol indicates an interaction between bait and target proteins, each fused to AD or BD, respectively. A representative plot (Fig. 3*A*) shows inhibited growth of yeast expressing a negative control pair, AD-FCP and BD vector only, enhanced growth demonstrating a modest interaction between AD-FCP and BD-FCP and a robust growth curve from yeast expressing a positive control interaction between AD-human μ1 and BD-trans Golgi network-binding protein (BD- TGN) (17). Results from this analysis suggested an interaction between AD-FCP and BD-FCP. When recombinant FCP was chromatographed on a Superdex-75 gel filtration column, it too exhibited dimerization or self-association (Fig. 3*B*). The strong tendency of FCP to dimerize was also indicated by the presence of a 74-kDa dimeric species on an incomplete denaturing SDS-PAGE gel, which was confirmed by Western blot and mass spectrometric analyses to be FCP (supplemental Fig. S1). We, therefore, conclude that FCP, like other FYVE domain proteins, can undergo a self-association. Given the involvement of coiled-coil domains in the oligomerization of other proteins, it is likely that dimerization of FCP is mediated by the coiled-coil domain of FCP. This dimerization event is likely to increase the avidity of the protein-lipid interaction by coordinating the presentation of two FYVE domains in tandem to two available PI3P ligands instead of one (27).

FCP Traffics to the Lumen of the FV in Late Trophozoites—Western blot analyses of stage-specific *P. falciparum* revealed that expression of FCP occurs during the late trophozoite stage of the parasite intra-erythrocytic life cycle (Figs. 4, *A* and *B*). Although this stage is known to be the most active stage for consumption of host cell hemoglobin and metabolism, FCP was remarkably not found to be localized to cytoplasmic endocytic vesicles or hemoglobin uptake structures but rather to the parasite FV, a lysosomal compartment characterized by the presence of hemozoin crystals (Fig. 5*A*).

To determine whether FCP traffics to the outer surface, inner surface or lumen of the FV, cryo-immunoelectron microscopy using rabbit anti-FCP was employed. As shown in Figs. 6, *A* and *B*, immunogold particles specifically stained the more electron lucent lumen of the FV. Fig. 6*A* shows a close-up of a cross-section through a folded FV with immunogold staining for FCP most abundant in the electron lucent lumen and to a lesser extent in association with hemozoin. Less than 1% of background staining was observed outside of the FV, evident in Fig. 6*B*, which shows the cross-section of a host cell, parasite, and its FV. Likewise, no significant immunogold staining was observed on other host cell or parasite structures. as evidenced in Fig. 6*C*, which shows three well defined parasites, each lacking a cross-section through a FV. These observations indicate that FCP traffics and translocates to the lumen of the parasite FV in late trophozoites and not merely to the surface.

FCP Traffics via a Mechanism That Excludes the Classical and Alternate Secretory Pathways—Sorting mechanisms for targeting proteins to the lysosomes of higher eukaryotes principally begin with entry of the proteins into the secretory pathway. Lysosomal proteins are synthesized and enter the rough ER and proceed to the Golgi where they are directed by recep-

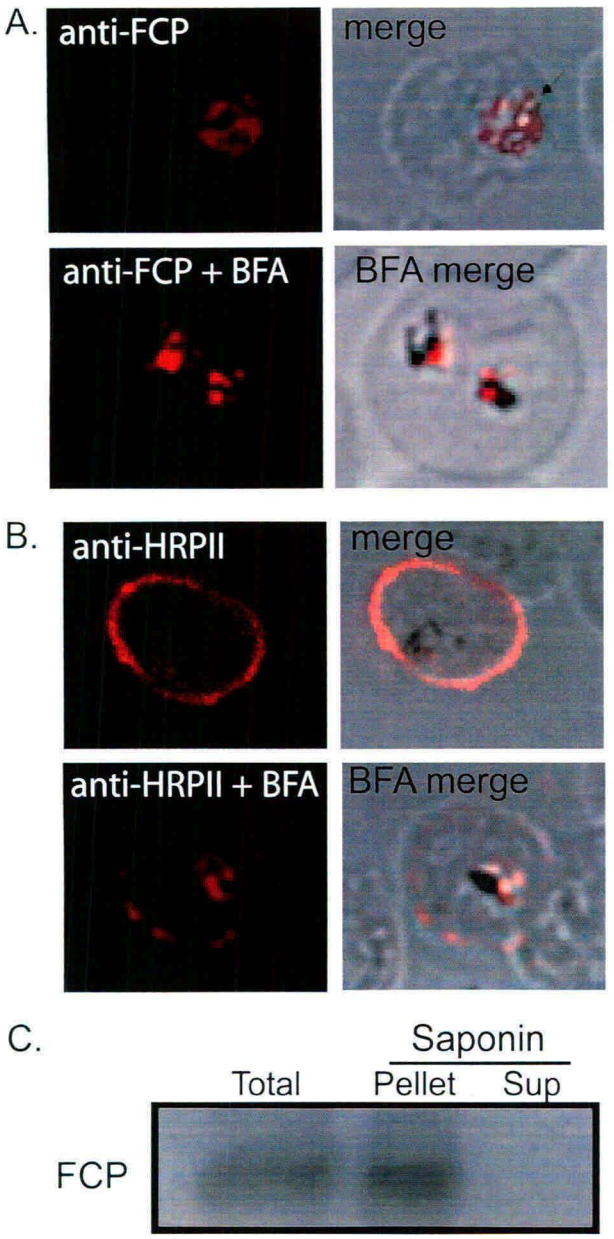

FIGURE 5. **FCP localizes to the FV but does not traffic via the classical or alternate secretory pathways.** *A*, immunofluorescence using anti-FCP revealed a discrete localization to the parasite FV. Ring stage parasites were treated either with 5 $\mu g \cdot ml^{-1}$ BFA (*anti-FCP + BFA*) or solvent as control (anti-FCP) for 12 h before immunofluorescence microscopy. BFA treatment did not alter FV localization of FCP. *B*, as a control experiment, parasites treated with BFA (*anti-HRPII + BFA*) or without BFA (*anti-HRPII*) were stained using antisera against a known secreted protein, HRPII. HRPII was localized predominantly to the cytoplasm of the host infected erythrocyte (*anti-HRPII*). BFA treatment resulted in a significant loss in erythrocyte localization of HRPII and a concomitant increase in the parasite cytoplasm (*anti-HRPII + BFA*). *C*, trophozoite-infected erythrocytes were treated with saponin to separate the erythrocyte and parasitophorous vacuole contents (*Sup*) from the parasite material (*Pellet*), and immunoblotting was performed for FCP. FCP was found in the pellet fraction rather than the concentrated supernatant fraction.

tor-mediated vesicular transport initiated in the trans-Golgi. These secretory vesicles are then redirected to the endocytic system so that they may be targeted to the lysosome.

To explore the mechanism of FCP trafficking, parasites were treated with brefeldin A (BFA) (Fig. 5*B*). This compound is known to block protein secretion by disruption of transport vesicle budding from the Golgi and concomitant inhibition of anterograde transport of proteins from the ER to the cis-Golgi (28). In *Plasmodium* BFA blocks not only the classical secretory pathway but also an alternate secretory pathway typically used by proteins destined for the host cell (29, 30). Hence, BFA treatment results in protein accumulation in the ER by blocking the classical secretory pathway and accumulation in yet another compartment or subcompartment by blocking the alternate secretory pathway (31). After treatment with BFA, FCP was still found localized to the FV, indicating that it does not utilize either the classical or alternate secretory pathways found in *P. falciparum* (Fig. 5*A*). In a control experiment secretion of the histidine-rich protein II (HRPII) to the erythrocyte cytosol, as has been previously described (32), was significantly blocked by BFA treatment (Fig. 5*B*).

As a protease, plasmepsin II has been shown to be secreted before endocytosis and trafficking to the FV (2); we needed to further confirm that a transient or rapid secretion event to either the parasitophorous vacuole or red blood cell cytoplasm did not occur. To address this possibility, parasitized red blood cells were treated with 0.1% saponin (33). This treatment is known to permeabilize both erythrocyte and parasitophorous vacuole membranes (13, 33). FCP was not found in the concentrated supernatant fraction but remained in the pellet or parasite soma fraction (Fig. 5*C*), indicating its absence from the secretory pathway. This further suggests that FCP may circumvent the secretory pathways and instead indicates that a novel trafficking pathway is at work.

The FYVE Domain Does Not Affect Trafficking of FCP but Is Functionally Critical to the Parasite—As seen for the endogenous protein (Figs. 5 and 6), transient transfection and expression of GFP-FCP in *P. falciparum* revealed a discrete localization of the tagged protein to the FV (Fig. 7*A*). To further delineate functional attributes of the conserved domains of FCP and to identify the domains responsible for the targeting, we transfected parasites with plasmid constructs containing various domain deletions of FCP fused to the C terminus of GFP (Fig. 7*B*). Transient transfection and live cell fluorescence were employed throughout the transfection studies to avoid artifacts due to selection of clonal transfectant populations or fixation artifacts that may alter morphology and fluorescence patterns. Transfectants expressing a deletion of the FYVE domain (GFP-FCP-ΔFYVE) displayed a discrete spot of fluorescence (Fig. 7*C*) that we later show coincides with the parasite FV (see Fig. 9*A*). This pattern indicated that PI3P binding is not involved in the targeting event. Of note, the dwarfed morphologies of the GFP-FCP-ΔFYVE transfectants appeared to be the result of a dominant negative growth defect. Parasites failed to attain the same size as normal 30–36-h trophozoites and also failed to develop large hemozoin crystals or FVs with wild type dimensions. A more detailed investigation of this mutant is discussed below (see Fig. 9).

Deletion of the C terminus including deletion of the coiled-coil domain (GFP-FCP-Δ-c-coil), while retaining the FYVE domain, ablated trafficking of GFP to the FV as seen by the cytoplasmic fluorescence pattern (Fig. 7*C*). This, once again demonstrated that the PI3P binding domain is not involved in targeting FCP to the FV. From the above findings we concluded

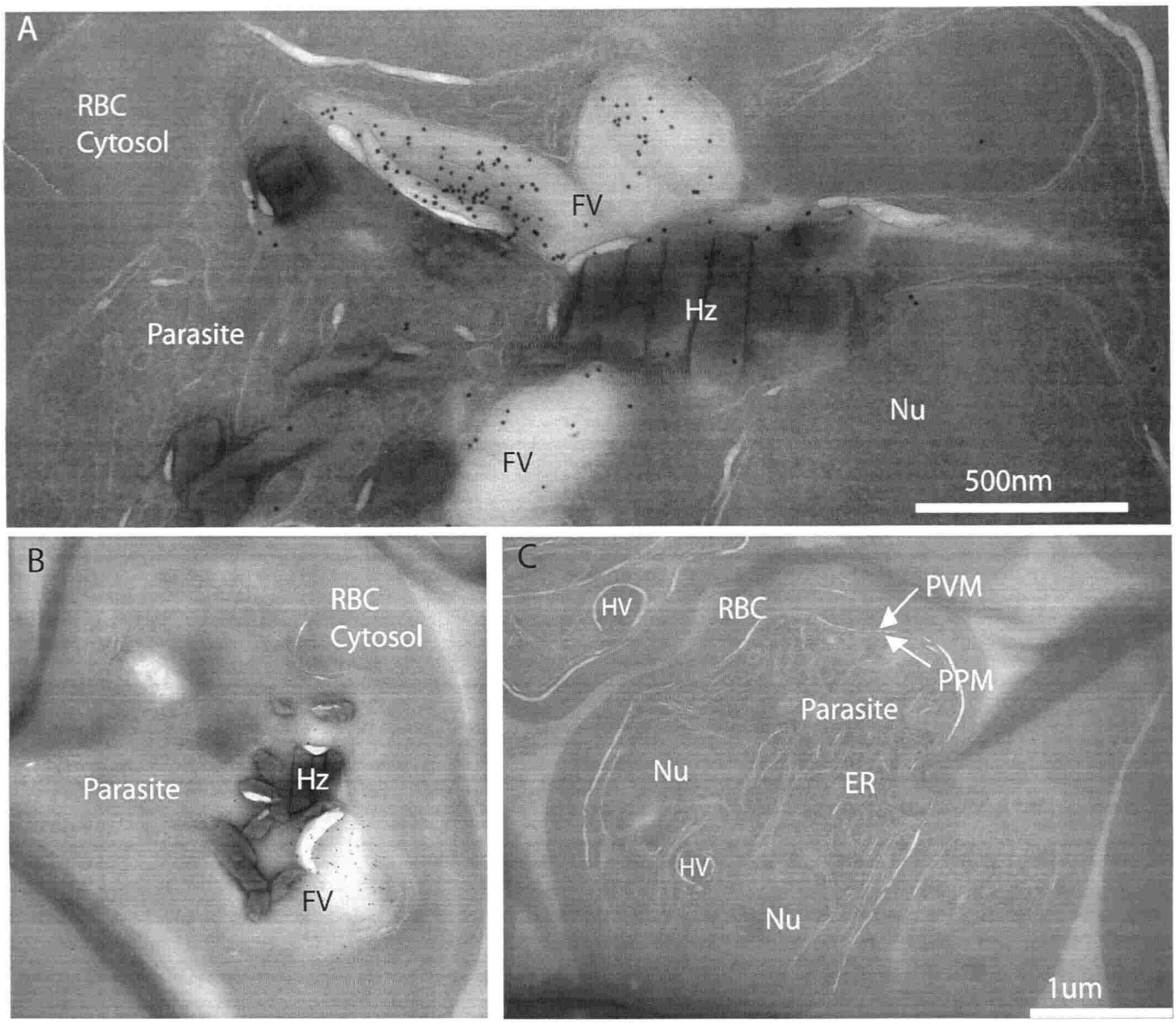

FIGURE 6. **FCP localizes to the lumen of the FV.** *A*, cryo-immunoelectron micrograph showing a close-up of a folded FV with immunogold-stained FCP in the lumen of the parasite FV in a late trophozoite. Various structures are indicated as host red blood cell cytosol (*RBC Cytosol*), parasite body (*parasite*), parasite nucleus (*Nu*), FV, and hemozoin (*Hz*). *B* shows a more complete parasite with a cross-section through the FV indicating a lack of immunogold staining outside the FV. *C*, three parasites from a different region of the same ultrathin section that was immunogold-stained for anti-FCP in *A* and *B*. Note the lack of concentrated gold particles on all visible parasite structures including ER, parasite plasma membrane (*PPM*), parasitophorous vacuolar membrane (*PVM*), and hemoglobin containing vesicles (*HV*). As apparent from *A* and *C*, less than 1% of immunogold appeared outside of the parasite FV.

that deletion of the FYVE domain generates a dominant negative phenotype, which likely impairs hemoglobin processing and/or uptake but not trafficking.

The C-terminal 44-Amino Acid Domain of FCP Is Necessary and Sufficient to Target FCP to the FV—To further delineate which regions in the C terminus mediate targeting, we deleted the conserved C-terminal 44 amino acids (GFP-FCP-Δc44) downstream of the coiled-coil domain. As can be seen from the cytoplasmic fluorescence pattern (Fig. 7*C*), targeting to the FV was once again ablated, indicating that this C-terminal peptide is indeed required for trafficking GFP to the FV (Fig. 7*C*).

To determine whether the C-terminal 44 amino acids are sufficient for targeting to the FV, we tagged the C terminus of GFP with the 44-amino acid peptide, thus eliminating all of the other potentially confounding components of FCP. Indeed, transfection of GFP-44aa resulted in trafficking of GFP to the FV (Fig. 8*A*), whereas transfection with GFP control vector alone resulted in a cytoplasmic fluorescence that notably excluded the FV (Fig. 8*B*). It is, thus, evident that the 44-amino acid peptide, notably conserved between diverse rodent and primate species of *Plasmodium*, functions as a direct cytoplasmic to vacuole trafficking (Cvt) signal.

Dominant Negative Effects of the FYVE Deletion Mutant—As mentioned above, deletion of the FYVE domain revealed a dominant negative growth or developmental defect but did not appear to alter localization to the FV (Fig. 7*C*). The GFP-FCP-ΔFYVE-expressing parasites failed to mature morphologically into normal trophozoites. Given their small size and diminutive FVs, morphologies of mutant parasites were poor, making clear localization of signal to the FV difficult.

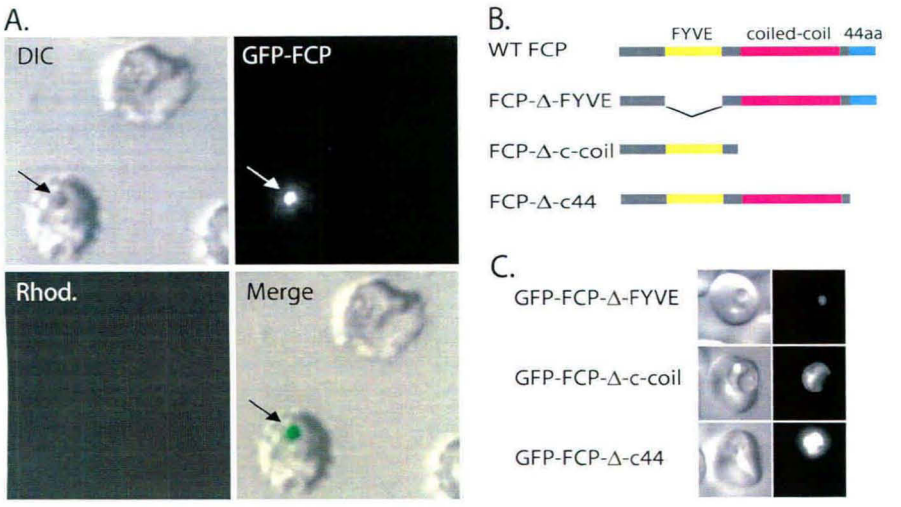

FIGURE 7. **Localization of GFP-FCP and domain deletion mutants in *P. falciparum*.** *A*, stage synchronous *P. falciparum* was transfected with either GFP-wild type FCP (*WT-FCP*) yielding a discrete localization to the FV characterized by the presence of hemozoin crystals (*arrow*). *B*, a schematic diagram shows the various GFP gene fusions and deletion constructs employed. *aa*, amino acids. *C*, various domain deletions of FCP as indicated in *B* were transfected into *P. falciparum*. Deletion of the FYVE domain (*GFP-FCP-ΔFYVE*) produced morphologically stunted parasites but did not appear to alter localization of the protein. In contrast, C-terminal deletion including deletion of the coiled-coil domain (*GFP-FCP-Δ-c-coil*) or deletion of the C-terminal 44-amino acid domain alone (*GFP-FCP-Δc44*) each displayed altered localization to the cytoplasm. *DIC*, differential interference contrast.

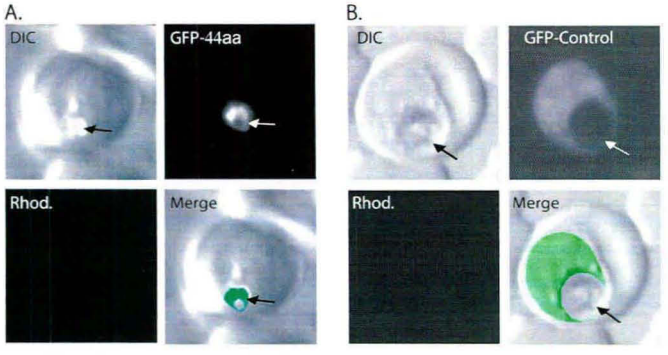

FIGURE 8. **C-terminal peptide directs traffic to the FV.** *A*, differential interference contrast (*DIC*) and fluorescence images of *P. falciparum* transfected with an expression plasmid encoding GFP with a C-terminal fusion of the 44 amino acid peptide (*GFP-44aa*) deemed necessary for trafficking of GFP-FCP to the FV. In trophozoite stage parasites fluorescence appeared localized only to the FV (*arrow*), indicating this peptide is sufficient for trafficking to the FV. *B*, control studies with the GFP expression vector lacking the targeting peptide (*GFP-Control*) demonstrated a cytoplasmic fluorescence pattern that excluded the FV (*arrow*). In the composite image, brightness and contrast of individual image layers were adjusted. Pseudo *green* color was applied to the fluorescence layer and superimposed onto the DIC image using Adobe Photoshop 6.0.

Regardless of the altered morphologies, expression of GFP-FCP-ΔFYVE yielded a GFP fluorescence pattern that coincided with visible, albeit diminutive FVs within stunted parasites (Fig. 9*A*) as compared with untransfected parasites in the same culture (data not shown) and 36-h parasites expressing a GFP control vector (Fig. 9*B*).

For *P. falciparum*, ring stage parasites represent the first 24 h of development within the red blood cells. Trophozoites represent the next 16 h of development, and finally, schizonts, characterized by 8–32 distinct nuclei, represent the last 8 h of development within red blood cells. Because trophozoites are morphologically characterized by the presence of a visible FV-containing hemozoin, the 36-h GFP-FCP-ΔFYVE-expressing parasites we observed (Fig. 9*A*) were representative of morphologically stunted trophozoites with one or more defects in hemoglobin uptake or metabolism.

To further confirm that GFP-FCP-ΔFYVEs were not developmentally arrested rings but rather stunted or defective trophozoites, we harvested parasites at 36 h post-transfection by centrifugation through Percoll-sorbitol gradients as described previously (12). This method is based on density differences triggered by parasite-induced new permeation pathways that result in the increased solute permeability of host red blood cells infected with later stage parasites (trophozoites and schizonts) as compared with early stage parasites (rings) (12). Because the GFP-FCP-ΔFYVE-expressing parasites were isolated in the trophozoite fraction of Percoll-sorbitol gradients (data not shown), we believe that they were developmentally mature enough to display new permeation pathways.

DISCUSSION

A variety of signal sequence topologies are defined in *P. falciparum* that mediate targeting to membranes or organelles inside or outside of the parasite. Conserved conventions such as N-terminal mitochondrial targeting signals are known to be functional in *Plasmodium* (34, 35). In addition, the presence of a chloroplast remnant organelle termed the apicoplast adds additional complexity to the trafficking of proteins in malaria. Trafficking to the apicoplast has been found to use an N-terminal pre-sequence (36, 37). This bipartite sorting signal consists of an N-terminal signal peptide for entry into the secretory pathway via the ER followed by an apicoplast membrane transit peptide that permits transit across the membranes of the apicoplast (37). Similarly for secretion, a tripartite sorting signal consisting of an N-terminal signal sequence followed by two transit peptides directs secretion of proteins from the parasite across the parasite plasma membrane and surrounding parasitophorous vacuolar membrane for delivery into the host red blood cell (29, 30, 38). A limited number of secreted proteins with a conventional N-terminal signal sequence are targeted to the parasitophorous vacuolar membrane or other membranes (*e.g.* EXP-1). The aspartic proteases plasmepsin I and II are type II integral membrane proteins with internal signal sequences and are thought to be delivered to the parasite FV initially via the secretory pathway, which later converges with the parasite endocytic pathway (2). In a similar fashion the principal sorting mechanisms for targeting proteases and hydrolases to the lysosomes of mammals and yeast include entry into the ER and secretory pathway followed by receptor-mediated vesicular transport initiated in the trans-Golgi, which redirects secretory

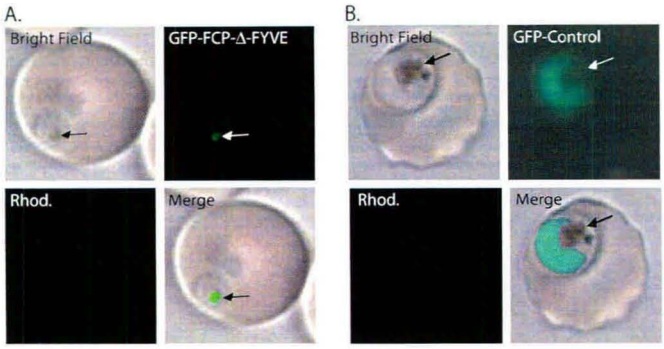

FIGURE 9. **Morphology of the ΔFYVE mutant.** Transfection of parasites with *GFP-FCP-ΔFYVE* revealed a profound dominant negative effect. *A*, bright field and fluorescence images of a late stage trophozoite expressing *GFP-FCP-ΔFYVE*. Note the stunted size of the parasite, nominal FV, and negligible amount of hemozoin as compared with the control GFP-transfected late stage trophozoite in *panel B*. *B*, control studies with the GFP expression vector lacking FCP (*GFP-Control*) demonstrated a cytoplasmic fluorescence pattern that excluded the FV (*arrow*).

vesicles to the endocytic system. Herein, however, we have identified a signal-sequence-independent mechanism for targeting to the FV, an organelle on the secretory and endocytic pathways.

In contrast to these previously defined protein sorting pathways, the Cvt pathway directed by the C-terminal peptide of FCP appears distinct in that it does not utilize the secretory pathway. Principally, FCP and GFP both lack recognizable N-terminal signal sequences typically required for entry into the secretory pathway, and neither contains a transmembrane span. In addition and as seen above in Fig. 5, treatment with BFA, known to block both the classical and alternate secretory pathways in *Plasmodium*, fails to alter trafficking of FCP to the FV. Hence, our data suggests that a non-secretory Cvt pathway exists perhaps for FV proteins that lack N-terminal or internal signal sequences.

Precedents for a Cvt pathway, also known as a constitutive autophagy pathway, have emerged from studies on *S. cerevisiae*, reviewed in Huang and Klionsky (39). This less traveled path of direct receptor-mediated transport to the digestive vacuole of yeast has been proposed for two soluble proteins, the pro-form of the hydrolase API (40, 41) and the α-mannosidase I precursor (Ams1p) (42, 43). Like FCP, these examples lack N-terminal signal sequences, do not enter the secretory pathway, and have peptide signals that are necessary for directed targeting to the yeast digestive vacuole. Indeed, the extreme C terminus of Ams1p has also been fused to the normally secreted protein, invertase, resulting in redirection of the chimeric invertase from the secretory pathway to the yeast vacuole (42). Disruption of these trafficking signals results in a redistribution of the hydrolases to the cytosol instead of the lysosome as we have observed for GFP-FCP variants lacking the C-terminal trafficking signal (41, 42). As with these examples in yeast, at present there is no obvious primary sequence similarity shared between the FCP trafficking peptide and other known FV proteins found in *Plasmodium*.

A link to PI3P functions in Cvt as well as in endocytosis has emerged in a study of Etf1, another PI3P-binding protein from yeast. ETf1 was identified as an effector of the yeast PI 3-kinase (Vps34), and deletion of ETf1 or mutation of its PI3P binding domain causes a severe defect only in Cvt/constitutive autophagy, not in endocytosis (44). In this regard Vps34 and its product PI3P are known to be involved in endocytosis, classical sorting of hydrolases such as CPY to the lysosome, starvation induced macroautophagy, and Cvt. By contrast, ETf1 appears only to be involved in the Cvt pathway (44).

Our domain analysis identifies and reveals that different functional attributes (PI3P binding, oligomerization, and FV trafficking) exist in modular domains of FCP. Conservation of FCP throughout the genus *Plasmodium* and an apparent lack of other FYVE domain-containing proteins in *Plasmodium* argue in favor of a vital non-redundant function for FCP in malaria parasites. The dominant negative effects of the FYVE domain deletion construct further argue for a vital function. In particular, the negligible amount of hemozoin in the ΔFYVE mutant parasites suggests a functional contribution by FCP either directly or indirectly to the metabolism of hemoglobin, general function of the FV, or polymerization of heme. Indeed, the FV provides vital functions to the parasite (45), and several antimalarial compounds are thought to act by inhibition of heme polymerization (46). A better understanding of protein and lipid trafficking mechanisms and characterization of FV resident proteins such as FCP should aid in the development of strategies to combat malaria.

Acknowledgments—We gratefully thank the members of Joiner and Sharma laboratories for helpful discussions during the course of this work. We are grateful to Dr. Tina Skinner-Adams (Queensland Institute of Medical Research, Royal Brisbane Hospital, Queensland Australia) for gifts of Plasmodium Gateway expression vectors, Dr. Kasturi Haldar (Northwestern University, Chicago, IL) for the gift of parasites, Dr. Nancy Ruddle and Dr. Liangbiao Zheng (both at Yale University) for use of laboratory facilities and equipment, and to Drs. Marc Pypaert (Yale University) and S. Parshuraman (National Institute of Immunology, New Delhi, India) for expert assistance in cryo-immunoelectron microscopy and confocal microscopy, respectively.

REFERENCES

1. Danis, M., and Gentilini, M. (1998) *Rev. Prat.* **48,** 254–257
2. Klemba, M., Beatty, W., Gluzman, I., and Goldberg, D. E. (2004) *J. Cell Biol.* **164,** 47–56
3. Atkinson, C. T., and Aikawa, M. (1990) *Blood Cells* **16,** 351–368
4. Pfeffer, S. (2003) *Cell* **112,** 507–517
5. Schu, P. V., Takegawa, K., Fry, M. J., Stack, J. H., Waterfield, M. D., and Emr, S. D. (1993) *Science* **260,** 88–91
6. Gillooly, D. J., Raiborg, C., and Stenmark, H. (2003) *Histochem. Cell Biol.* **120,** 445–453
7. Gillooly, D. J., Morrow, I. C., Lindsay, M., Gould, R., Bryant, N. J., Gaullier, J. M., Parton, R. G., and Stenmark, H. (2000) *EMBO J.* **19,** 4577–4588
8. Christoforidis, S., Miaczynska, M., Ashman, K., Wilm, M., Zhao, L., Yip, S. C., Waterfield, M. D., Backer, J. M., and Zerial, M. (1999) *Nat. Cell Biol.* **1,** 249–252
9. Birkeland, H. C., and Stenmark, H. (2004) *Curr. Top. Microbiol. Immunol.* **282,** 89–115
10. Elabbadi, N., Ancelin, M. L., and Vial, H. J. (1994) *Mol. Biochem. Parasitol.* **63,** 179–192
11. Trager, W., and Jensen, J. B. (1976) *Science* **193,** 673–675
12. Kutner, S., Breuer, W. V., Ginsburg, H., Aley, S. B., and Cabantchik, Z. I. (1985) *J. Cell. Physiol.* **125,** 521–527
13. Lambros, C., and Vanderberg, J. P. (1979) *J. Parasitol.* **65,** 418–420

14. Kadekoppala, M., Kline, K., Akompong, T., and Haldar, K. (2000) *Infect. Immun.* **68,** 2328–2332
15. Skinner-Adams, T. S., Hawthorne, P. L., Trenholme, K. R., and Gardiner, D. L. (2003) *Trends Parasitol.* **19,** 17–18
16. Jensen, R. B., La Cour, T., Albrethsen, J., Nielsen, M., and Skriver, K. (2001) *Biochem. J.* **359,** 165–173
17. Hoppe, H. C., Ngo, H. M., Yang, M., and Joiner, K. A. (2000) *Nat. Cell Biol.* **2,** 449–456
18. Deitsch, K., Driskill, C., and Wellems, T. (2001) *Nucleic Acids Res.* **29,** 850–853
19. van den Hoff, M. J., Moorman, A. F., and Lamers, W. H. (1992) *Nucleic Acids Res.* **20,** 2902
20. Walshaw, J., and Woolfson, D. N. (2001) *J. Mol. Biol.* **307,** 1427–1450
21. Misra, S., and Hurley, J. H. (1999) *Cell* **97,** 657–666
22. Dumas, J. J., Merithew, E., Sudharshan, E., Rajamani, D., Hayes, S., Lawe, D., Corvera, S., and Lambright, D. G. (2001) *Mol. Cell* **8,** 947–958
23. Hayakawa, A., Hayes, S. J., Lawe, D. C., Sudharshan, E., Tuft, R., Fogarty, K., Lambright, D., and Corvera, S. (2004) *J. Biol. Chem.* **279,** 5958–5966
24. Stenmark, H., Aasland, R., and Driscoll, P. C. (2002) *FEBS Lett.* **513,** 77–84
25. Simonsen, A., Lippe, R., Christoforidis, S., Gaullier, J. M., Brech, A., Callaghan, J., Toh, B. H., Murphy, C., Zerial, M., and Stenmark, H. (1998) *Nature* **394,** 494–498
26. Woodman, P. G. (2000) *Traffic* **1,** 695–701
27. Mao, Y., Nickitenko, A., Duan, X., Lloyd, T. E., Wu, M. N., Bellen, H., and Quiocho, F. A. (2000) *Cell* **100,** 447–456
28. Hendricks, L. C., McClanahan, S. L., Palade, G. E., and Farquhar, M. G. (1992) *Proc. Natl. Acad. Sci. U. S. A.* **89,** 7242–7246
29. Marti, M., Good, R. T., Rug, M., Knuepfer, E., and Cowman, A. F. (2004) *Science* **306,** 1930–1933
30. Hiller, N. L., Bhattacharjee, S., van Ooij, C., Liolios, K., Harrison, T., Lopez-Estrano, C., and Haldar, K. (2004) *Science* **306,** 1934–1937
31. Nacer, A., Berry, L., Slomianny, C., and Mattei, D. (2001) *Int. J. Parasitol.* **31,** 1371–1379
32. Akompong, T., Kadekoppala, M., Harrison, T., Oksman, A., Goldberg, D. E., Fujioka, H., Samuel, B. U., Sullivan, D., and Haldar, K. (2002) *J. Biol. Chem.* **277,** 28923–28933
33. Klemba, M., Gluzman, I., and Goldberg, D. E. (2004) *J. Biol. Chem.* **279,** 43000–43007
34. Bhaduri-McIntosh, S., and Vaidya, A. B. (1998) *Exp. Parasitol.* **88,** 252–254
35. Sato, S., Rangachari, K., and Wilson, R. J. (2003) *Mol. Biochem. Parasitol.* **130,** 155–158
36. Foth, B. J., and McFadden, G. I. (2003) *Int. Rev. Cytol.* **224,** 57–110
37. Waller, R. F., Reed, M. B., Cowman, A. F., and McFadden, G. I. (2000) *EMBO J.* **19,** 1794–1802
38. Lopez-Estrano, C., Bhattacharjee, S., Harrison, T., and Haldar, K. (2003) *Proc. Natl. Acad. Sci. U. S. A.* **100,** 12402–12407
39. Huang, W. P., and Klionsky, D. J. (2002) *Cell Struct. Funct.* **27,** 409–420
40. Klionsky, D. J., Cueva, R., and Yaver, D. S. (1992) *J. Cell Biol.* **119,** 287–299
41. Oda, M. N., Scott, S. V., Hefner-Gravink, A., Caffarelli, A. D., and Klionsky, D. J. (1996) *J. Cell Biol.* **132,** 999–1010
42. Yoshihisa, T., and Anraku, Y. (1990) *J. Biol. Chem.* **265,** 22418–22425
43. Yoshihisa, T., and Anraku, Y. (1989) *Biochem. Biophys. Res. Commun.* **163,** 908–915
44. Wurmser, A. E., and Emr, S. D. (2002) *J. Cell Biol.* **158,** 761–772
45. Francis, S. E., Sullivan, D. J., Jr., and Goldberg, D. E. (1997) *Annu. Rev. Microbiol.* **51,** 97–123
46. Ziegler, J., Linck, R., and Wright, D. W. (2001) *Curr. Med. Chem.* **8,** 171–189
47. Ohno, H., Fournier, M. C., Poy, G., and Bonifacino, J. S. (1996) *J. Biol. Chem.* **271,** 29009–29015